IAEA TECDOC SERIES

IAEA-TECDOC-2055

IAEA-TECDOC-2055

Neutron Activation Analysis Using Short Half-life Radionuclides

IAEA
International Atomic Energy Agency

NEUTRON ACTIVATION ANALYSIS USING SHORT HALF-LIFE RADIONUCLIDES

The following States are Members of the International Atomic Energy Agency:

AFGHANISTAN
ALBANIA
ALGERIA
ANGOLA
ANTIGUA AND BARBUDA
ARGENTINA
ARMENIA
AUSTRALIA
AUSTRIA
AZERBAIJAN
BAHAMAS
BAHRAIN
BANGLADESH
BARBADOS
BELARUS
BELGIUM
BELIZE
BENIN
BOLIVIA, PLURINATIONAL STATE OF
BOSNIA AND HERZEGOVINA
BOTSWANA
BRAZIL
BRUNEI DARUSSALAM
BULGARIA
BURKINA FASO
BURUNDI
CABO VERDE
CAMBODIA
CAMEROON
CANADA
CENTRAL AFRICAN REPUBLIC
CHAD
CHILE
CHINA
COLOMBIA
COMOROS
CONGO
COSTA RICA
CÔTE D'IVOIRE
CROATIA
CUBA
CYPRUS
CZECH REPUBLIC
DEMOCRATIC REPUBLIC OF THE CONGO
DENMARK
DJIBOUTI
DOMINICA
DOMINICAN REPUBLIC
ECUADOR
EGYPT
EL SALVADOR
ERITREA
ESTONIA
ESWATINI
ETHIOPIA
FIJI
FINLAND
FRANCE
GABON
GAMBIA
GEORGIA
GERMANY
GHANA
GREECE
GRENADA
GUATEMALA
GUINEA
GUYANA
HAITI
HOLY SEE
HONDURAS
HUNGARY
ICELAND
INDIA
INDONESIA
IRAN, ISLAMIC REPUBLIC OF
IRAQ
IRELAND
ISRAEL
ITALY
JAMAICA
JAPAN
JORDAN
KAZAKHSTAN
KENYA
KOREA, REPUBLIC OF
KUWAIT
KYRGYZSTAN
LAO PEOPLE'S DEMOCRATIC REPUBLIC
LATVIA
LEBANON
LESOTHO
LIBERIA
LIBYA
LIECHTENSTEIN
LITHUANIA
LUXEMBOURG
MADAGASCAR
MALAWI
MALAYSIA
MALI
MALTA
MARSHALL ISLANDS
MAURITANIA
MAURITIUS
MEXICO
MONACO
MONGOLIA
MONTENEGRO
MOROCCO
MOZAMBIQUE
MYANMAR
NAMIBIA
NEPAL
NETHERLANDS, KINGDOM OF THE
NEW ZEALAND
NICARAGUA
NIGER
NIGERIA
NORTH MACEDONIA
NORWAY
OMAN
PAKISTAN
PALAU
PANAMA
PAPUA NEW GUINEA
PARAGUAY
PERU
PHILIPPINES
POLAND
PORTUGAL
QATAR
REPUBLIC OF MOLDOVA
ROMANIA
RUSSIAN FEDERATION
RWANDA
SAINT KITTS AND NEVIS
SAINT LUCIA
SAINT VINCENT AND THE GRENADINES
SAMOA
SAN MARINO
SAUDI ARABIA
SENEGAL
SERBIA
SEYCHELLES
SIERRA LEONE
SINGAPORE
SLOVAKIA
SLOVENIA
SOUTH AFRICA
SPAIN
SRI LANKA
SUDAN
SWEDEN
SWITZERLAND
SYRIAN ARAB REPUBLIC
TAJIKISTAN
THAILAND
TOGO
TONGA
TRINIDAD AND TOBAGO
TUNISIA
TÜRKİYE
TURKMENISTAN
UGANDA
UKRAINE
UNITED ARAB EMIRATES
UNITED KINGDOM OF GREAT BRITAIN AND NORTHERN IRELAND
UNITED REPUBLIC OF TANZANIA
UNITED STATES OF AMERICA
URUGUAY
UZBEKISTAN
VANUATU
VENEZUELA, BOLIVARIAN REPUBLIC OF
VIET NAM
YEMEN
ZAMBIA
ZIMBABWE

The Agency's Statute was approved on 23 October 1956 by the Conference on the Statute of the IAEA held at United Nations Headquarters, New York; it entered into force on 29 July 1957. The Headquarters of the Agency are situated in Vienna. Its principal objective is "to accelerate and enlarge the contribution of atomic energy to peace, health and prosperity throughout the world''.

IAEA-TECDOC-2055

NEUTRON ACTIVATION ANALYSIS USING SHORT HALF-LIFE RADIONUCLIDES

INTERNATIONAL ATOMIC ENERGY AGENCY
VIENNA, 2024

COPYRIGHT NOTICE

For further information on this publication, please contact:

Physics Section
International Atomic Energy Agency
Vienna International Centre
PO Box 100
1400 Vienna, Austria
Email: Official.Mail@iaea.org

Printed by the IAEA in Austria
May 2024

IAEA Library Cataloguing in Publication Data

Names: International Atomic Energy Agency.
Title: Neutron activation analysis using short half-life radionuclides / International Atomic Energy Agency.
Description: Vienna : International Atomic Energy Agency, 2024. | Series: IAEA TECDOC series, ISSN 1011-4289 ; no. 2055 | Includes bibliographical references.
Identifiers: IAEAL 24-01684 | ISBN 978-92-0-119024-6 (paperback : alk. paper) | ISBN 978-92-0-119124-3 (pdf)
Subjects: LCSH: Nuclear activation analysis. | Radioisotopes. | Nuclear reactors. | Irradiation.

FOREWORD

Neutron activation analysis (NAA) is the technique most widely used in research reactors worldwide. Six decades of experience in NAA has resulted in commonly applied analytical protocols, with measurements at about two to seven days and at three weeks after neutron irradiation. This approach can be implemented at most research reactors and other neutron sources and may result in information on as many as 30–40 chemical elements. The associated turnaround time of at least one week (and often several weeks) is, however, one of the reasons for the declining interest of third parties in using NAA as a commercial service, with competing multielement analysis techniques being favoured.

NAA with short half-life radionuclides enables an analysis turnaround time of one working day in principle. It also enables the detection of many important elements that cannot otherwise be measured with NAA based on longer half-lives. NAA with short half-life radionuclides has been applied at research reactors, neutron generators and isotopic neutron sources ever since the development of NAA, and it may provide competitive and, in some cases, even unique opportunities for an NAA facility. NAA measurements with durations of minutes or even seconds allow for the possibility of reporting results very quickly, even on the same day of the analysis, considerably increasing analytical throughput and therefore the competitiveness of the technique. This opportunity has not been fully seized by NAA laboratories however, particularly in research reactors, because of the technical and analytical difficulties involved. Overcoming these issues and implementing NAA with short half-life radionuclides can provide analytical laboratories with new opportunities and improve their position in the market for multielement non-destructive analytical techniques.

Implementing and/or optimizing NAA with short half-life radionuclides necessitates the evaluation and possible modification of the various components needed for analysis, in particular the irradiation facility, the counting equipment and the calibration approach. The objective of this publication is to provide information in these fields to users of short half-life radionuclides in NAA and to newcomers in the field. This publication addresses all aspects of the implementation and optimization of NAA with short half-life radionuclides at research reactors, neutron generators and isotopic neutron sources. The majority of the experimental details however, in particular on sensitivity, relate to research reactor based NAA.

The IAEA acknowledges the experts who contributed to this publication, in particular P. Bode (Kingdom of the Netherlands) and P. Vermaercke (Belgium). The IAEA officer responsible for this publication was N. Pessoa Barradas of the Division of Physical and Chemical Sciences.

EDITORIAL NOTE

This publication has been prepared from the original material as submitted by the contributors and has not been edited by the editorial staff of the IAEA. The views expressed remain the responsibility of the contributors and do not necessarily represent the views of the IAEA or its Member States.

Guidance and recommendations provided here in relation to identified good practices represent expert opinion but are not made on the basis of a consensus of all Member States.

Neither the IAEA nor its Member States assume any responsibility for consequences which may arise from the use of this publication. This publication does not address questions of responsibility, legal or otherwise, for acts or omissions on the part of any person.

The use of particular designations of countries or territories does not imply any judgement by the publisher, the IAEA, as to the legal status of such countries or territories, of their authorities and institutions or of the delimitation of their boundaries.

The mention of names of specific companies or products (whether or not indicated as registered) does not imply any intention to infringe proprietary rights, nor should it be construed as an endorsement or recommendation on the part of the IAEA.

The authors are responsible for having obtained the necessary permission for the IAEA to reproduce, translate or use material from sources already protected by copyrights.

The IAEA has no responsibility for the persistence or accuracy of URLs for external or third party Internet web sites referred to in this publication and does not guarantee that any content on such web sites is, or will remain, accurate or appropriate.

CONTENTS

1. INTRODUCTION

1.1 BACKGROUND

Neutron activation analysis (NAA) is defined by the IUPAC as “a measurement principle for measuring elemental or isotopic contents in a specified amount of a material, in which the activity of radionuclides formed directly or indirectly by nuclear reactions of neutrons, or the absorption of electromagnetic radiation by stable nuclides, is measured” [1].

In practice, neutron-induced activation results in a mixture of radioactive nuclei, which can be measured for their individual contributions by two approaches:

— The resulting radioactive sample is kept intact, and the elements are determined by taking advantage of the differences in decay rates of the radionuclides via measurements at different decay intervals using appropriate instruments: This is usually called non-destructive or Instrumental NAA (INAA);
— The resulting radioactive sample is decomposed, and through chemical separations it is divided into fractions with a few elements (and their activation products) each: This is usually called destructive or Radiochemical NAA (RNAA).

Over eighty years of experience in INAA have resulted in commonly applied analytical protocols for many applications, with measurements at about two to seven days and at three weeks after neutron irradiation. This approach can be implemented at most research reactors and other neutron sources without significant difficulties, and may result in information on about 30 to 40 chemical elements. However, the associated turnaround of at least one week — and often several weeks — is one of the main reasons for the declining interest of third parties in the opportunities of NAA as a service provider, with multi-element analysis techniques like inductively coupled plasma mass spectrometry (and other related mass spectrometry techniques) providing similar information within a much shorter timeframe.

The radionuclides produced by neutron irradiation may have half-lives varying from a fraction of a second to days, or even years. There is no formal convention for the classification of radionuclides on the basis of the length of their half-lives. Commonly, radionuclides with half-lives varying from approximately a few seconds to approximately two hours are, within the NAA community, considered to be the 'short half-life' radionuclides (or ‘short-lived’, in NAA jargon); radionuclides with half-lives shorter than about one minute are sometimes classified as ‘ultra shorts’. There is no common annotation for the group of radionuclides with half-lives up to approximately two days. These are referred to as ‘medium half-life radionuclides in this publication, whereas radionuclides with longer half-lives are considered to be ‘long half-life’ radionuclides.

NAA with short half-life radionuclides enables analysis turnaround time of, in principle, one working day. It has been applied at research reactors, neutron generators and isotopic neutron sources ever since the development of NAA. The first indications of the use of short half-life radionuclides in NAA for measuring elements are reported in the early 1950s by Albert and his co-workers who measured, using reactor activation, ^{64}Cu and ^{56}Mn as impurities in Fe after chemical separations [2, 3]. More opportunities came upon the introduction of the scintillation counter, which can be derived from a 1956 review paper [4], although many still used fast radiochemical separations. As an example, Brooksbank et.al. used radiochemical separation for measurement of, amongst others, ^{38}Cl and ^{52}V in titanium [5]. Atchinson et.al. demonstrated, with neutrons generated using a Van de Graaff generator, how NAA can be used for measuring

the halogens ^{20}F, ^{38}Cl, ^{80}Br and ^{129}I in various compounds [6] and elaborated on the interfering $^{23}Na(n,a)^{20}F$ reaction. In 1955, Lévêque et al. also published the measurement of ^{20}F and ^{179m}Hf in zirconium [7]. Turner [8] showed that rapid analysis is possible for measuring Si and Al using fast neutrons from a 14 MeV neutron generator. From the 1960s onwards, non-destructive NAA started to replace the radiochemical separations with the availability of the Ge(Li) detector and later on the high purity germanium (HPGe) detector and associated spectrometers. The technique contributed to a rapid growth in applications of NAA in which short half-life radionuclides were used.

Amiel et al. pioneered the measurement of neutrons emitted by short half-life radionuclides, firstly for determining Li and O [9, 10] via neutron emission by ^{17}N and later on for measuring short half-life fission products of uranium [11]. This approach has become a separate branch of NAA, currently known as delayed neutron counting or delayed NAA (DNAA). At the 3rd International conference on Modern Trends in Activation Analysis (MTAA-3) in 1968, Givens et al. presented the concept of cyclic activation analysis [12], along with an example of its use in 14 MeV NAA for improving the detection limit for oxygen determination. A few years later, Egan et al. [13] applied cyclic activation analysis to reactor-based NAA of ^{77m}Se in biological material. Cyclic activation analysis has also been combined with delayed neutron counting [14]. The pioneering work into the development of methods and electronics for dead time correction in the 1960s–1970s [15–19], has contributed significantly to improving the accuracy of NAA results. Commercially available gamma-ray spectrometers are now available with a 'loss free counting' (LFC) function or 'zero dead time (ZDT) function. These technologies widened the field of applications by measuring short half-life radionuclides and, with it, increased the opportunity to NAA laboratories for providing reliable services with a very short turnaround.

Determination of elements such as Al, Mg, Mn, Ti, V and Ca by their short half-life radionuclides has become common for applications in many disciplines such as (but not limited to) geosciences, archaeology, environmental sciences, food and nutritional studies and biology. The IAEA published in 1987 'Applications of short-lived activation products in NAA of bio-environmental specimens' [20] in which the advantages and limitations are discussed, examples are given of rapid analysis conditions and a bibliographic overview is presented.

It can be concluded that there is ample evidence that measuring the activity of short half-life radionuclides, of neutron-activated chemical elements, may provide competitive and maybe even unique opportunities for an NAA facility. NAA measurements with durations of minutes, or even seconds, allow for the possibility of reporting results very quickly, even on the same day of the analysis.

This high throughput considerably increases the competitiveness of NAA, but the opportunity is not fully seized by NAA laboratories, particularly in research reactors, because of the technical and analytical difficulties involved. Overcoming these issues and implementing NAA with short half-life radionuclides can provide laboratories with new opportunities and improve their position in the market for multi-elemental non-destructive analytical techniques.

1.2 OBJECTIVE

Implementing and/or optimizing NAA with short half-life radionuclides requires the evaluation, and possible modification, of the various components needed for analysis. In particular, these components include the irradiation facility, the counting equipment and the calibration approach. The objective of this publication is to provide guidance in these fields to users of short half-life radionuclides in NAA and newcomers in the area.

1.3 SCOPE

This publication addresses all aspects of the implementation and optimization of NAA with short half-life radionuclides at research reactors, neutron generators and isotopic neutron sources. The majority of the experimental details, in particular on sensitivity, relates to research reactor based INAA. The processing of short half-life radionuclides in RNAA is not addressed in this publication.

1.4 STRUCTURE

This publication is structured in this introduction, followed by eight technical sections and the conclusions.

Five unique characteristics of NAA using short half-life radionuclides are described in Section 2. The publication is further structured following these five characteristics. ‘Singleness’ is outlined in Section 3 by an overview of the elements that can only be measured in NAA by their short half-life neutron activation products. ‘Speed’ of analysis is discussed in Section 4 and typical analytical protocols are given. ‘Sensitivity’ is addressed in detail for reactor-based NAA in Section 5 with indications of the achievable minimum detectable amounts if elements are measured by either their short half-life radionuclides or their medium and/or long half-life radionuclides. ‘Selectivity’, the aspects of interferences by competitive nuclear reactions and/or during gamma ray spectrometry is discussed in Section 6 ‘Safety’ issues of measuring short half-life radionuclides and of the operation of the irradiation facility are discussed in Section 7.

Then, Section 8 addresses specific requirements and design features of irradiation facilities and Section 9 addresses counting systems with special attention to measuring rapidly decaying activities. Conclusions are given in Section 10.

2. CHARACTERISTICS OF NAA USING SHORT HALF-LIFE RADIONUCLIDES

Measurement of neutron activation produced short half-life radionuclides is less universally practiced at reactors, mostly because the irradiation facilities are not available, are not fast enough or because it is not possible to quickly separate the sample vial from the irradiation container and transfer it to the counting system. This is an unfortunate limitation since short half-life radionuclides have the following interesting features for both scientific research projects and for providing third party services:

(1) Singleness: Some chemical elements can only be measured in NAA by radionuclides with short half-lives (further referred to as SHL), such as: Al, Ar, B, Be, Cl, F, I, Li, Mg, Mn, Nb, O, Pb, Rh, S, Si, Ti and V. Their associated half-lives vary from less than 1 second (e.g., ^{207m}Pb, 0.8 s), to minutes (e.g., ^{28}Al, 2.3 min) or a few hours (e.g., ^{56}Mn, 2.6 h). This is further detailed in Section 3. The ability to measure the halogens F, Cl and I offers an especially unique opportunity for NAA, as other common analytical techniques often have issues with the trueness of the total amount of these elements caused by their volatility. Likewise, the measurement of oxygen in metals using fast neutron activation has been a well established procedure for many years in facilities using fast neutron generators.

(2) Speed: Elements that can be measured by their short half-life radionuclides can be reported more quickly than if measured on their longer half-life activation products, since the time needed for the individual steps in the analysis (irradiation, decay, counting) is in the order of seconds and minutes rather than in hours and days. This fast turnaround may, however, sometimes be at the cost of a lower sensitivity. As an example, the determination of selenium can be completed within 1 minute on the basis of the ^{77m}Se nuclide ($t_{1/2}$ = 17.5 s), e.g., by a 10 s irradiation, 20 s decay (including removal of sample from irradiation container and transfer to counting system) and 20 s count, whereas on the basis of the ^{75}Se nuclide ($t_{1/2}$ = 120 d) it would require a few days up to a few weeks by an irradiation of 1–4 h, 5 or 20 days decay time and several hours counting. NAA using short half-life radionuclides therefore provides an opportunity to report on several elements within one working day following the irradiation. This opportunity is one major focus of this publication and examples of analytical protocols are given in Section 4.

(3) Sensitivity: There are several elements where measurement of the short half-life radionuclide has very good sensitivity, e.g., Ag, Al, Ar, As, Au, Br, Co, Cs, Cu, Dy, Er, Eu, Ga, Gd, Hf, Ho, I, In, Ir, La, Lu, Mn, Mo, Na, Nd, Pd, Re, Rh, Sb, Sc, Se, Sm, Sr, U, V, W and Yb. A theoretical parameter is derived in Section 5 as a first indication of the (interference free) sensitivity that may be obtained by measuring short half-life, medium half-live (MHL) or long half-life (LHL) radionuclides from the same element.

(4) Selectivity: The short half-life radionuclide can often be measured with less spectral interferences than the longer half-life radionuclide produced from the same element, like for Se, Sm, Cu or Zn. Short-lived NAA will suffer more from fast neutron threshold interferences, but less from fission interferences. Cyclic and epithermal NAA (ENAA) are advantageous for short lived NAA. More examples thereof are provided in Section 6 of this publication.

(5) Safety: NAA based on short half-life radionuclides requires short irradiation times. This implies lower risk of radiolysis, decomposition and pressure build-up, which can be advantageous when analysing organic and biological materials. Irradiation and counting facilities may be integrated into a fully automatic system with no intervention, which

contributes to limiting the radiation dose to personnel. This and other aspects are described in Section 7.

The five specific advantages of NAA using short half-life radionuclides add up to other advantages. These additional benefits include: the ability to analyse material without chemical destruction, the absence of interference by chemical speciation of the elements, the unique feature that results are less dependent on the matrix of the samples when compared to chemical techniques, the self-validation characteristics, and the intrinsic high degree of trueness. All these benefits increase the competitiveness of NAA.

There are, however, specific requirements on the facilities for irradiation and counting to take optimal advantage of these features of NAA with short half-life radionuclides. To take optimal advantage of the 'speed' feature of short half-life radionuclides, the irradiation facility needs to allow not only for rapid and reproducible transfer of the irradiation container to the counting position, but also a swift removal of the sample vial from the irradiation container prior to its counting. The short half-life radionuclide may also decay significantly during the counting of the induced activity, and measures are therefore needed to correct for this, especially when measuring a mixture of radionuclides with different half-lives. Irradiation and counting facilities, including their design features are described in Sections 8 and 9, respectively.

3. SINGLENESS

The characteristics of the chemical elements that can only be measured by NAA on the basis of short half-life radionuclides are shown in Table 1. Most of the gamma ray peaks of these radionuclides can be measured without spectrum interference, resulting in unequivocal identification of the radionuclides. The radionuclides formed from neutron activation of the elements Al, Mg, Mn, V and often also Si can be measured simultaneously in samples from typical niches in NAA such as geosciences and environmental sciences. The radionuclide ^{8}Li, activation product from B or Li, emits very high energy beta radiation that can be measured using a plastic scintillator or Cerenkov detector operating in the multichannel scaling mode. This opportunity is further discussed in Section 9.

TABLE 1. ELEMENTS WITH ONLY SHORT HALF-LIFE NAA FORMED RADIONUCLIDES

Element	Nuclear reaction	Half-life of the radionuclide(s) formed	Relevant radiation to be measured (gamma radiation unless otherwise mentioned)
Al	^{27}Al (n,g)^{28}Al	2.25 min	1779.0 keV
Ar	^{40}Ar (n,g)^{41}Ar	1.83 h	1293.6 keV
B	^{11}B (n,a)^{8}Li	0.84 s	b radiation 12 MeV
Be	^{9}Be (n,a)^{6}He	0.81 s	b radiation 3.5 MeV
Cl	^{37}Cl (n,g)^{38m,38}Cl	0.715s resp. 37.23 min	671.36 keV resp. 1642.7 and 2167.4 keV
F	^{19}F (n,g)^{20}F	11.07 s	1633.6 keV
	^{19}F (n,a)^{16}N	7.1 s	6.1 MeV
	^{19}F(n,p)^{19}O	27 s	197.14 keV
I	^{127}I(n,g)^{128}I	25 min	442.9 keV
Li	^{7}Li(n,g)^{8}Li	0.84 s	b radiation 12 MeV
Mg	^{26}Mg(n,g)^{27}Mg	9.46 min	843.8 keV; 1014.5 keV
Mn*	^{55}Mn(n,g)^{56}Mn	2.579 h	846.8 keV; 1810.7 keV; 2113.1 keV
Nb	^{93}Nb(n,g)^{94m}Nb	6.26 min	871 keV
O	^{18}O (n,g)^{19}O	26.88 s	197.14 keV
	^{16}O(n,p)^{16}N	7.1 s	6.1 MeV
	^{17}O(n,p)^{17}N	4.2 s	870.7 keV
Pb	^{206}Pb (n,g)^{207m}Pb	0.81 s	569.7 keV
Rh	^{103}Rh (n,g)^{104m,104}Rh	4.34 min resp. 42.3 s	51.4 keV resp. 555.8 keV
S	^{36}S (n,g)^{37}S	5.05 min	3103.4 keV
Si*	^{29}Si(n,p)^{29}Al	6.56 min	1273.4 keV
	^{30}Si (n,a)^{28}Al	2.25 min	1779.0 keV
	^{30}Si (n,g)^{31}Si	2.62 h	1266.1 keV
Ti	^{50}Ti (n,g)^{51}Ti	5.76 min	320.1 keV
V	^{51}V (n,g)^{52}V	3.74 min	1434.1 keV

* Mn and Si can also be determined in MHL protocols, but not in LHL protocols.

Practical difficulties may occur in the simultaneous measurement of Mg and Mn as their main gamma ray lines at 843.8 keV and 846.8 keV may be difficult to resolve depending on the performance of the detector used. However, the less intense gamma rays at 1014.4 keV and 1810.7 keV emitted by ^{27}Mg and ^{56}Mn respectively, may resolve the situation. These peaks are interference free and the half-lives of each emitter are very different. Measurements of the same sample after different decay times will contribute to resolve an eventual multiplet of both gamma rays. Also, the gamma ray of ^{29}Al at 1273.4 keV may be interfered by the 1267 keV double escape peak of the 1779.0 keV gamma ray of ^{28}Al. As for the case of ^{27}Mg and ^{56}Mn, measurements after different decay times will resolve the situation for ^{28}Al and ^{29}Al.

The radionuclide ^{8}Li, activation product from B or Li, emits very high-energy beta radiation that can be measured using a plastic scintillator or Cerenkov detector operating in the multichannel scaling mode. This opportunity is further discussed in Section 9.

NAA is a strong candidate for the measurement of total F, Cl, I and Br in different matrices, as the volatility of these elements and their use in mineral acids makes dissolution and contamination a problem with other techniques. It has already been mentioned in the introduction that F, Cl, and I can only be measured by short half-life radionuclides. The radionuclide ^{82}Br (half-life 35 h) is the most common radionuclide for measuring Br, whereas the radionuclides ^{80}Br (half-life 17.7 m), ^{80m}Br (half-life 4.4 h) and ^{82m}Br (half-life 6.1 m) could also be considered for measuring Br, especially since the activity of ^{80}Br is significantly higher than of ^{82}Br. This is further elaborated upon in Section 4. Measurement of ^{20}F is often difficult if the sample also contains the element Na, due to the interfering reaction ^{23}Na(n,a)^{20}F. In such cases, the use of the high energy gamma rays (higher than 6 MeV), emitted by ^{16}N following the fast neutron activation of F, can also be considered for interference free measurement of F. Although in principle ^{16}N is also produced in the air in the sample vial, the quantity thereof is most likely insignificant. Similar interfering nuclear threshold reactions leading to the same radionuclide occur with the elements Si, Al, Mg and Mn. The extent thereof and approaches for correction are discussed in Section 5.

Similar interfering nuclear threshold reactions leading to the same radionuclide occur with the elements Si, Al, Mg and Mn. The extent thereof and approaches for correction are discussed in Section 5.

4. SPEED

4.1 CATEGORIES OF RADIONUCLIDES WITH SHORT HALF-LIVES

Radionuclides are further sub-categorized in this publication as follows, with associated typical experimental conditions (protocols):

— Ultra Short Half-Life radionuclides (USHL): typical irradiation of a few to 30 seconds, decay limited to the travel time of the sample (usually less than a second or a few seconds), counting several seconds, to be used for radionuclides with a half-life lower than around 100 s;
— Short Half-Life radionuclides (SHL): irradiation of several minutes to 10 minutes, several seconds or minutes decay, counting a few minutes, to be used for radionuclides with a half-life typically a few minutes to about 1 hour;
— Medium Half-Life radionuclides (MHL): irradiation from several minutes to around 15 minutes, from around half an hour to maximum a few hours of decay, counting from around half an hour to a few hours, to be used for radionuclides with a half-life typically from about one hour to a maximum of around three days. It is noted that even medium half-life NAA protocol results can be supplied within one day and as such the MHL protocol was integrated in this section;
— Long Half-Life radionuclides (LHL): irradiation one to several hours, several days of decay, counting a few hours to days for radionuclides with a half-life longer than a few days. It is noted that these conditions do not allow reporting within one day. As such, this protocol is not further elaborated in this publication.

4.2 FAST ANALYSIS PROTOCOLS

Many combinations of irradiation time t_{irr}, decay time t_d and measurement time t_c can be used for measuring the short half-life radionuclides of interest. Decades of practice of NAA with short half-radionuclides for a variety of applications resulted in some 'basic' sets of typical conditions with an outlook for maximizing the detectability of short half-life, medium and long half-life radionuclides. Examples of such protocols are given in Table 2. An overview of the elements and the associated isotope formed, that can be used for protocols measuring ultra-short, short and medium half-life radionuclides, is given in Table 3 (data on half-lives from [21]). It can be derived from Tables 2 and 3 that many elements are measurable with an analysis protocol which can be completed within one working day, including on-line spectrum analysis, interpretation and reporting.

TABLE 2. ANALYTICAL SEQUENCE FOR DIFFERENT PROTOCOLS

Protocol	$t_{1/2}$	t_{irr}	t_d	t_c
Ultra Short half-life radionuclide NAA	< 100 s	10–30 s	1–10 s	10–30 s
Short half-life radionuclide NAA	1–60 min	1–10 min	1 s – 30 min	1–30 min
Medium half-life radionuclide NAA	60 min – 2 d	2–15 min	0.5–4 h	0.5–4 h
Long half-life radionuclide NAA	> 2 d	1–24 h	1–30 d	1 h – several d

TABLE 3. ELEMENTS THAT CAN BE DETERMINED USING THE NAA PROTOCOLS OF TABLE 2

Protocol USHL using short half-life radionuclides:
$t_{1/2}$ < 100 s; t_{irr}: 10 s – 30 s; t_d: 1 s -10 s; t_c: 10 s – 30 s

Element analysed	Target Isotope	Formed Isotope	$T_{1/2}$
Cl	Cl-37	Cl-38m	0.715 s
Pb	Pb-206	Pb-207m	0.81 s
Be	Be-9	He-6	0.81 s
Li	Li-7	Li-8	0.84 s
B	B-11	Li-8	0.84 s
In	In-115	In-116m2	2.18 s
Er	Er-166	Er-167m	2.27 s
W	W-182	W-183m	5.3 s
Yb	Yb-176	Yb-177m	6.41 s
O	O-16	N-16	7.13 s
F	F-19	F-20	11.07 s
Pt	Pt-198	Pt-199m	13.6 s
In	In-115	In-116	14.1 s
Se	Se-76	Se-77m	17.36 s
Hf	Hf-178	Hf-179m1	18.67 s
Sc	Sc-45	Sc-46m	18.75 s
Pd	Pd-106	Pd-107m	21.3 s
Ag	Ag-109	Ag-110	24.6 s
O	O-18	O-19	26.88 s
Rh	Rh-103	Rh-104	42.3 s
Ge	Ge-74	Ge-75m	47.7 s
Ge	Ge-76	Ge-77m	53.7 s
Ce	Ce-138	Ce-139m	57.6 s
Rb	Rb-85	Rb-86m	61.02 s
Se	Se-82	Se-83m	70.1 s
Dy	Dy-164	Dy-165m	75.4 s
Ir	Ir-191	Ir-192m	87 s
Sb	Sb-123	Sb-124m1	93 s
U	U-235	Br-87	55.7 s
		Br-88	16.3 s
		Br-89	4.4 s
		Br-90	1.9 s
		I-137	24.5 s
		I-138	6.2 s
		I-139	2.3 s
		I-140	0.86 s
		Cs-143	1.8 s
		Cs-144	1.0 s

TABLE 3. ELEMENTS THAT CAN BE DETERMINED USING THE NAA PROTOCOLS OF TABLE 2 (Cont.)

Protocol SHL using short half-life radionuclides:
$t_{1/2}$: 1–60 min; t_{irr}: 1–10 min; t_d: 1 s – 30 min; t_c: 1–30 min

Element	Target Isotope	Radionuclide produced	$t_{1/2}$
Al	Al-27	Al-28	2.25 min
Ag	Ag-107	Ag-108	2.38 min
Zn	Zn-70	Zn-71	2.42 min
Cr	Cr-54	Cr-55	3.50 min
Gd	Gd-160	Gd-161	3.66 min
V	V-51	V-52	3.74 min
Se	Se-78	Se-79m	3.92 min
Sb	Sb-121	Sb-122m2	4.191 min
Rh	Rh-103	Rh-104m	4.34 min
Pd	Pd-108	Pd-109m	4.70 min
S	S-36	S-37	5.05 min
Cu	Cu-65	Cu-66	5.12 min
Hg	Hg-204	Hg-205	5.2 min
Ti	Ti-50	Ti-51	5.76 min
Nb	Nb-93	Nb-94m	6.26 min
Si	Si-29	Al-29	6.56 min
Ca	Ca-48	Ca-49	8.718 min
Mg	Mg-26	Mg-27	9.458 min
Sn	Sn-124	Sn-125m	9.52 min
Co	Co-59	Co-60m	10.47 min
Nd	Nd-150	Nd-151	12.44 min
Mo	Mo-100	Tc-101	14.2 min
Ba	Ba-130	Ba-131m	14.6 min
Mo	Mo-100	Mo-101	14.61 min
Ta	Ta-181	Ta-182m2	15.8 min
Br	Br-79	Br-80	17.68 min
Rb	Rb-87	Rb-88	17.77 min
Se	Se-80	Se-81	18.45 min
Re	Re-187	Re-188m	18.6 min
Ga	Ga-69	Ga-70	21.14 min
Th	Th-232	Th-233	21.83 min
Sm	Sm-154	Sm-155	22.2 min
Se	Se-82	Se-83	22.3 min
Pd	Pd-110	Pd-111	23.4 min
U	U-238	U-239	23.5 min
I	I-127	I-128	24.99 min
Pt	Pt-198	Pt-199	30.8 min
Cl	Cl-37	Cl-38	37.23 min
Sn	Sn-122	Sn-123m	40.06 min
Hg	Hg-198	Hg-199m	42.7 min
Cd	Cd-110	Cd-111m	48.54 min
In	In-115	In-116m1	54.29 min
Se	Se-80	Se-81m	57.28 min

TABLE 3. ELEMENTS THAT CAN BE DETERMINED USING THE NAA PROTOCOLS OF TABLE 2 (Cont.)

Protocol MHL using medium half-life radionuclides:
$t_{1/2}$: 60 min to 2 d; t_{irr}: 2–15 min; t_d: 0.5 h – 4 h; t_c: 0.5 h – 4 h

Element	Target Isotope	Radionuclide produced	$t_{1/2}$
Sr	Sr-84	Sr-85m	67.63 min
Te	Te-128	Te-129	69.6 min
Ge	Ge-74	Ge-75	82.78 min
Ba	Ba-138	Ba-139	82.9 min
Pt	Pt-196	Pt-197m	95.4 min
Eu	Eu-151	Eu-152m2	96 min
Nd	Nd-148	Nd-149	1.73 h
Ar	Ar-40	Ar-41	1.827 h
Yb	Yb-176	Yb-177	1.911 h
Dy	Dy-164	Dy-165	2.334 h
Cd	Cd-116	Cd-117 / In-117	2.49 h / 43.2 min
Ni	Ni-64	Ni-65	2.517 h
Mn	Mn-55	Mn-56	2.579 h
Si	Si-30	Si-31	2.621 h
Sr	Sr-86	Sr-87m	2.815 h
Cs	Cs-133	Cs-134m	2.91 h
Y	Y-89	Y-90m	3.19 h
Cd	Cd-116	Cd-117m	3.36 h
Lu	Lu-175	Lu-176m	3.635 h
Zn	Zn-70	Zn-71m	4.14 h
Ru	Ru-104	Ru-105 / Rh-105m	4.44 h / 42.8 s
Cd	Cd-114	Cd-115 / In-115m	53.46 h / 4.486 h
Pd	Pd-110	Pd-111m	5.5 h
Hf	Hf-179	Hf-180m	5.5 h
Cd	Cd-106	Cd-107	6.5 h
Er	Er-170	Er-171	7.516 h
Ce	Ce-136	Ce-137	9.0 h
Eu	Eu-151	Eu-152m1	9.312 h
Te	Te-126	Te-127	9.35 h
Ge	Ge-76	Ge-77	11.21 h
K	K-41	K-42	12.36 h
Cu	Cu-63	Cu-64	12.7 h
Os	Os-190	Os-191m	13.1 h
Pd	Pd-108	Pd-109 / Ag-109m	13.59 h / 39.8 s
Zn	Zn-68	Zn-69m	13.76 h
Ga	Ga-71	Ga-72	14.1 h
Na	Na-23	Na-24	14.96 h
Zr	Zr-96	Zr-97 / Nb-97m / Nb-97	16.75 h / 58.7 s / 72.1 min
Re	Re-187	Re-188	17.0 h
Gd	Gd-158	Gd-159	18.48 h

TABLE 3. ELEMENTS THAT CAN BE DETERMINED USING THE NAA PROTOCOLS OF TABLE 2 (Cont.)

Protocol MHL using medium half-life radionuclides:
$t_{1/2}$: 60 min to 2 d; t_{irr}: 5–15 min; t_d: 0.5 h – 4 h; t_c: 0.5 h – 4 h

Element	Target Isotope	Radionuclide produced	$t_{1/2}$
Pr	Pr-141	Pr-142	19.12 h
Ir	Ir-193	Ir-194	19.2 h
Pt	Pt-196	Pt-197	19.89 h
W	W-186	W-187	24.00 h
Hg	Hg-196	Hg-197m	23.8 h
As	As-75	As-76	26.24 h
Ho	Ho-165	Ho-166	26.83 h
Nd	Nd-150	Pm-151	28.4 h
Ba	Ba-134	Ba-135m	28.7 h
Os	Os-192	Os-193	29.83 h
Ce	Ce-142	Ce-143	33.0 h
Te	Te-130	Te-131m	33.25 h
Ce	Ce-136	Ce-137m	34.4 h
Br	Br-81	Br-82	35.3 h
Ru	Ru-104	Rh-105	35.34 h
Ba	Ba-132	Ba-133m	38.9 h
La	La-139	La-140	40.286 h
Sm	Sm-152	Sm-153	46.3 h
Nd	Nd-148	Pm-149	53.08 h
Cd	Cd-114	Cd-115	53.46 h
U	U-238	Np-239	56.54 h
Hg	Hg-196	Hg-197	64.14 h
Au	Au-197	Au-198	64.68 h
Sb	Sb-121	Sb-122	65.371 h
Mo	Mo-98	Mo-99 / Tc-99m	65.92 h / 6.01 h
Ru	Ru-96	Ru-97	2.83 d

4.3 OVERLAPPING IRRADIATION, DECAY AND COUNTING PERIODS

Soils, sediments, rocks and other material of geological origin, often contain Al with mass fractions that can go up to several percent and silicon mass fractions that can go up to several tens of percent. The neutron activation induced ^{28}Al activity is often dominant at the end of irradiation, and the high Compton background hinders the measurement of other elements (such as Mg, Ti or V) by their short half-life radionuclides. The decay time for the optimal signal (the activities of the other radionuclides) to noise (due to the ^{28}Al activity) has to be established experimentally. If advanced knowledge is available on the composition of the materials, the induced activities of the various radionuclides can be estimated, and a plot can help to establish a suitable optimal decay time (see Figure 1).

Optimal decay times for NAA using short half-life radionuclides on geological material may vary from a few minutes up to even 30 minutes. Since the samples to be measured are irradiated one-by-one, the decay time of each sample can be used to irradiate the next sample or even multiple next samples in such a way that the samples can be counted immediately after each

other. This has been a routine practice at the Reactor Institute Delft, Netherlands. Their experimental conditions were:

— Thermal neutron flux: 1.6×10^{13} $cm^{-2}s^{-1}$, thermal/fast ratio ca. 20;
— Sample mass: ca. 200 mg;
— Irradiation time: 7 s;
— Transfer time: 1.1 s;
— Decay time sample: 1200 s;
— Counting time sample: 300 s;
— Decay time flux monitor (^{69m}Zn) 1530 s;
— Counting time flux monitor: 30 s;
— Time for changing samples and data storage: 30 s;
— Detector: Ge; 10% relative efficiency; sample to endcap distance: 5 cm.

The total time needed for irradiation and counting of 1 sample plus flux monitor is about 26 minutes, but by using overlapping irradiations and countings, about 9 samples can still be processed within 1 hour (see Figure 2). It is labour intensive and requires a well-thought approach for timekeeping using at least two timers; a timer for the gap between the successive irradiation and a timer for the first decay time. The latter one can be used for the counting and sample changing periods as well.

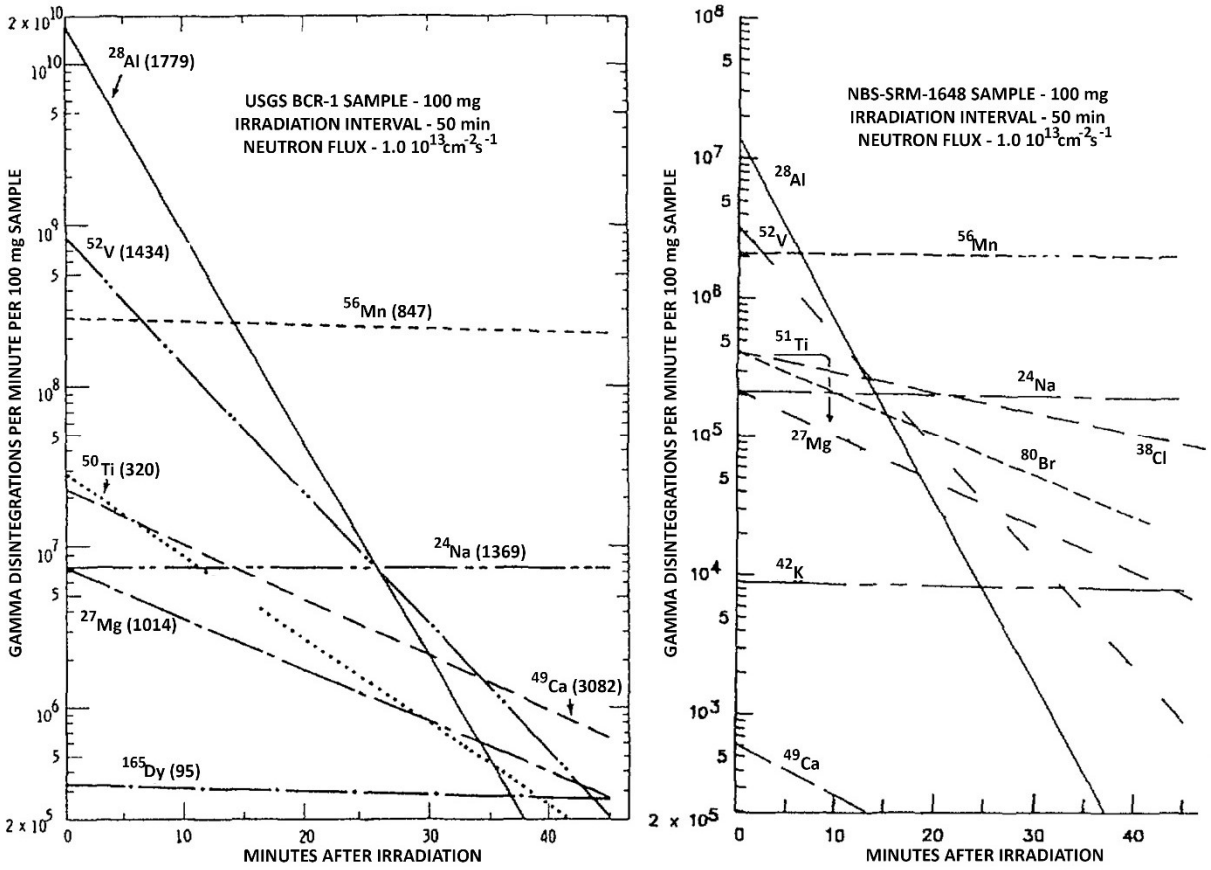

FIG. 1. Induced gamma activities of short half-life radionuclides and their decays with time in a USGS BCR-1 sample (left) and an NIST SRM 1648 urban dust sample (right) (adapted from [22]).

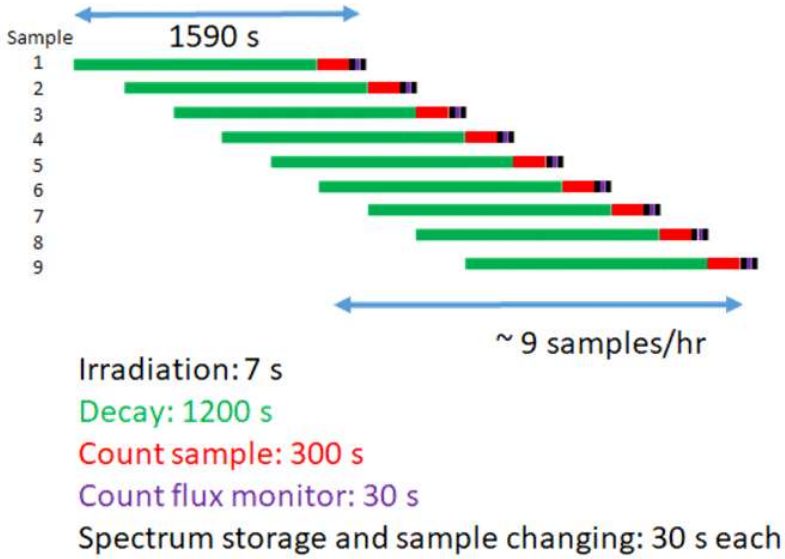

FIG. 2. Scheme with overlapping irradiations, decays and countings as used for measuring short half-life radionuclides for NAA of soils, sediments and geological samples at Reactor Institute Delft (courtesy of P. Bode, TU Delft).

5. SENSITIVITY

5.1 CONCEPTS

Sensitivity is defined in the International Vocabulary of Metrology – Terms and Concepts [23] as the quotient of the change in an indication of a measuring system and the corresponding change in a value of a quantity being measured. The detection limit is defined as the measured quantity value, obtained by a given measurement procedure, for which the probability of falsely claiming the absence of a component in a material is β, given a probability α of falsely claiming its presence.

The concepts of both sensitivity and detection limit are taken together to determine the extent by which NAA using short half-life radionuclides would yield a sufficient number of interference free counts in the gamma ray peak in order to enable well quantifiable results. Based upon the reaction rate equation this number of counts can be calculated theoretically, and thus the suitability of NAA for a particular application can be determined. The number of counts obtained is indeed purely theoretical since, background and specific interferences are not taken into account.

According to the Eurachem validation guide [24] the 'working range' is the interval over which the method provides results with an acceptable uncertainty. The lower end of the working range is bounded by the limit of quantification which is related to the analytical sensitivity. Detection and quantification limits in NAA are largely determined by the composition of the sample and are thus sample specific. The upper end of the working range is defined by mass fractions at which significant anomalies in the analytical sensitivity are observed. In principle, a working range in NAA may stretch from the limit of detection to a 100% mass fraction. However, the working range in NAA with short half-life radionuclides will be limited by count rate and dead time issues at higher mass fractions. Sample masses as small as 0.01 mL to 0.1 mL in volume or a few tens to a few hundreds of milligrams may be used to avoid high count rates depending on the sample matrix and the neutron flux.

Besides RNAA or Compton suppression systems, there are different methodologies for improving the sensitivity of NAA using short half-life radionuclides that are discussed in this document:

— Cyclic activation analysis in which a sample undergoes different cycles of irradiation-transfer-count-return, in sequence;
— Epithermal NAA, where a thermal neutron filter such as Cd or B is used.

The physical characteristics of NAA and the availability of a complete measurement equation [25] allows for estimating theoretical, i.e. interference free, sensitivities on the basis of minimum detectable amounts of the elements under stipulated experimental conditions. This is further elaborated in the paragraphs below for reactor based NAA, as the neutron flux and energy distributions in the irradiation position are usually well known, and consequently the estimate of the activation cross-section is also usually well known. Such theoretical estimations are less easy to make for NAA in which D–D (2.45 MeV), D–T (14 MeV) neutron generators or isotopic neutron sources (^{252}Cf, Am–Be or Pu–Be) are used. The neutron flux and neutron energy distributions depend also on the materials used for constructing the irradiation assembly, which makes it difficult to use appropriate values for activation cross-sections (provided these are available for fast neutron activation). Information on sensitivities obtained experimentally

by using 2.45 MeV and 14 MeV neutron generators [26–28] and for the use of ^{252}Cf sources [29] have been published.

5.2 THE SHL SENSITIVITY FACTOR

Using the Høgdahl convention, the net peak area produced by (n,γ) reaction is given in Eq. 1 [30]:

$$N_{p,x} = m_x . \frac{\mathrm{N_{Av}} \theta_x I_{\gamma,x}}{M_x} . \left(\varphi_{th}\sigma_{th,x} + \varphi_{epi} I_{0,x}\right) . (SDC)_x . \varepsilon . t_c \quad (1)$$

Where $N_{p,x}$ is the number of counts in the peak for a specific isotope for element x, N_{av} is the Avogadro constant, M_x the atomic mass, ε the full energy peak efficiency, $I_{\gamma,x}$ the gamma ray emission probability, m_x the mass of the target element x in the sample ($m_x = w \, . \, c_x$ with w the sample weight and c_x the mass fraction), θ_x the abundance of the target isotope, $\sigma_{th,x}$ the neutron capture cross-section, φ_{epi} the epithermal neutron flux, φ_{th} the thermal neutron flux, $I_{0,x}$ resonance integral, S [$= (1 - e^{-\lambda t_{irr}})$] the irradiation factor, D [$= e^{-\lambda t_d}$] the decay factor, C [$= \left(1 - e^{-\lambda t_c}\right)/\lambda t_c$] the counting factor with λ the decay constant, and t_{irr}, t_d and t_c are the irradiation, decay and measuring time, respectively. Note that in Eq. 1, in the interest of simplicity, the corrections for neutron and gamma ray self-attenuation, geometrical effects during irradiation and counting, and coincidence effects are not mentioned. The equation clearly shows that analytical sensitivity is not only determined by the cross-section, but also by the mass of the target element, the isotopic and gamma abundance, the neutron flux and the analytical sequence scheme irradiation/decay/counting.

Calculations of the sensitivity reported in this section were made with specific protocols (see Table 4):

— Two short irradiations: a very short one for measuring radionuclides with half-lives in the order of seconds and a 10 min irradiation for measuring all other short half-life radionuclides;
— One long irradiation of 4 hours for measuring long half-life radionuclides.

In both cases, an irradiation with the following experimental conditions was used: thermal neutron flux of 10^{12} cm^{-2} s^{-1}, j_{th}/j_{epi} thermal to epithermal neutron flux ratio = 20, measurements at endcap distance 2 cm on a 40% Ge detector.

TABLE 4. IRRADIATION, DECAY AND COUNTING PROTOCOLS USED FOR THE SENSITIVITY CALCULATION

NAA using short half-life radionuclides				**NAA using long half-life radionuclides**			
$t_{1/2}$	t_{irr}	t_d	t_c	$t_{1/2}$	t_{irr}	t_d	t_c
Seconds	30 s	1 s	30 s				
Minutes	10 min	2 min	5 min				
< 2h	10 min	1 h	1 h	> 2 h	4 h	1 h	1 h
				Days	4 h	14 d	24 h
				Years	4 h	14 d	24 h

A sensitivity factor S_{SHL} was defined as $S_{SHL} = m_x$, the mass of the target element (expressed in µg) needed to obtain $N_{p,x} = 100$ counts in the corresponding main gamma ray peak of the formed radionuclide.

In Table 5 in the last column -log(S_{SHL}) was calculated based upon available nuclear data:

— Gamma ray emission probability, isotopic abundance of the target isotope, half-lives and Eγ from [21] ;
— Neutron capture cross-section and resonance integrals from [31–36].

As an example, if $S_{SHL} = 1$ µg or -log(S_{SHL}) = 0, a mass of the target element of $m_x = 1$ µg would yield $N_{p,x} = 100$ counts. On the other hand, if $S_{SHL} = 1000$ µg or -log(S_{SHL}) = -3, a mass of 1 mg would yield 100 counts. Whereas if $S_{SHL} = 0.001$ µg or -log(S_{SHL}) = 3, a mass of 1 ng would yield to 100 counts. Again, this is purely theoretical based upon Eq. 1 since no background and no interferences were taken into account. Theoretically, without background, a net peak area $N_{p,x} = 100$ counts would correspond to 10% uncertainty due to the counting statistics ($\frac{\sqrt{N_{p,x}}}{N_{p,x}} = 10\%$). There will be a loss of sensitivity if ^{28}Al or ^{56}Mn would contribute to the Compton continuum and to the background counts for the peak of interest. For instance, if the background counts at the peak of interest would be $B_{p,x} = 150$ counts, a sensitivity corresponding to 100 net counts in the peak would theoretically correspond to 20% counting statistics ($\frac{\sqrt{N_{px}+2B_{p,x}}}{N_{p,x}} * 100\% = 20\%$) and as such, a loss in sensitivity and a higher detection limit will be obtained. The last column is expressed in –log values whereby a green colour reflects a very good analytical sensitivity, and a bright red colour refers to less good analytical sensitivity.

It is, however, more valid to express S_{SHL} expressed as a range (in mass units), as given in table 5. This is due to the fact that 1) the calculation is only valid for the particular protocol mentioned in table 4, and 2) as mentioned in Eq. 1, many sources of uncertainties on the nuclear data have to be taken into account (e.g. thermal neutron flux, resonance integral, isotopic abundance, detector efficiency, etc) likely leading to expanded uncertainties in the order of 6 to 20 %. The log value in the table for SHL then allows for better comparison with the data for LHL.

In the calculation used to obtain the values in Table 5, another simplification was made in terms of complex activation/decay schemes. Most of the nuclides are produced by direct (n,γ) reactions and a quite straightforward "parent/daughter" relation can be assumed. Some radionuclides however are produced by branched decay. In those cases where the half-life of the respective daughter radionuclide was shorter than the half-life of the mother it was assumed that equilibrium was reached (e.g., for ^{109}Pd/^{109m}Ag). In those cases where the half-life of the respective daughter was longer than the half-life of the parent radionuclide it was assumed that the daughter was counted sufficiently long after the metastable state had decayed (e.g. ^{134m}Cs/^{134}Cs). Due to this simplification, actual experimental values may differ slightly from the calculated data depending on the time when measurements have started.

It can be derived from Table 5 that quite a number of elements exists for which the sensitivity by measuring short half-life radionuclides is theoretically sufficient to determine masses at the µg level: Eu, Dy, In, Mn, Au, Rh, V, U, Lu, Hf, Sc, Ir, Re, Ar, Co, Ho, I, Cs, As, Br, W, Er, Sm, La, Na, Al, Se, Ga, Yb, Ag, Nd (under the stipulated experimental protocol mentioned in Table 4).

TABLE 5: THEORETICAL SENSITIVITY FACTORS OBTAINED USING A SPECIFIC ANALYTICAL SEQUENCE IN NAA

SHL-NAA - Short Irradiation – Theoretical sensitivity factor SHL						
Element analysed	**Target Isotope**	**Formed Isotope**	**$T_{1/2}$**	**E_γ (keV)**	**Estimated range of S_{SHL}**	**- log (S_{SHL})**
O	O-18	O-19	26.88 s	197.14	5–10 mg	-4.0
F	F-19	F-20	11.07 s	1633.6	1–2 µg	-0.2
Na	Na-23	Na-24	14.96 h	1368.6	5–10 ng	1.8
	Na-23	Na-24	14.96 h	2754.0	20–50 ng	1.6
Mg	Mg-26	Mg-27	9.46 min	843.8	200–500 ng	0.3
	Mg-26	Mg-27	9.46 min	1014.5	1–2 µg	-0.1
Al	Al-27	Al-28	2.25 min	1779.0	5–10 ng	1.8
Si	Si-30	Si-31	2.621 h	1266.1	1–2 mg	-3.0
S	S-36	S-37	5.05 min	3103.4	100–200 µg	-2.1
Cl	Cl-37	Cl-38m	0.715s	671.3	20 - 50 µg	-1.6
	Cl-37	Cl-38	37.23 min	1642.7	200–500 ng	0.7
	Cl-37	Cl-38	37.23 min	2167.4	100–200 ng	0.7
Ar	Ar-40	Ar-41	1.827 h	1293.6	1–2 ng	2.4
K	K-41	K-42	12.36 h	1524.6	0.5–1 µg	0.2
Ca	Ca-48	Ca-49	8.718 min	3084.4	2–5 µg	-0.4
Sc	Sc-45	Sc-46m	18.75 s	142.5	0.5–1 ng	2.7
Ti	Ti-50	Ti-51	5.76 min	320.1	100–200 ng	0.8
V	V-51	V-52	3.74 min	1434.1	0.2–0.5 ng	3.1
Cr	Cr-54	Cr-55	3.50 min	1528.0	10–20 µg	-1.1
Mn	Mn-55	Mn-56	2.579 h	846.8	0.1–0.2 ng	3.6
	Mn-55	Mn-56	2.579 h	1810.7	0.5–1 ng	2.8
	Mn-55	Mn-56	2.579 h	2113.1	1–2 ng	2.5
Fe	No short lived equivalent					
Co	Co-59	Co-60m	10.47 min	58.6	1–2 ng	2.4
	Co-59	Co-60m	10.47 min	1332.5	50–100 ng	1.1
Ni	Ni-64	Ni-65	2.517 h	1481.8	1–2 µg	-0.1
Cu	Cu-63	Cu-64	12.7 h	1345.8	1–2 µg	-0.1
	Cu-65	Cu-66	5.12 min	1039.2	50–100 ng	1.2
Zn	Zn-68	Zn-69m	13.76 h	438.6	0.5–1 µg	0.2
	Zn-70	Zn-71	2.42 min	121.5	200–500 µg	-2.6
	Zn-70	Zn-71m	4.14 h	386.4	50–100 µg	-1.7
Ga	Ga-71	Ga-72	14.1 h	630.0	5–10 ng	1.7
	Ga-71	Ga-72	14.1 h	834.1	2–5 ng	2.2
	Ga-69	Ga-70	21.14 min	176.1	0.5–1 µg	0.3
	Ga-69	Ga-70	21.14 min	1039.5	0.5–1 µg	0.3
Ge	Ge-74	Ge-75	82.78 min	198.6	2–5 µg	-0.6
	Ge-74	Ge-75m	47.7 s	139.7	0.5–1 µg	0.0
	Ge-76	Ge-77	11.21 h	211.0	2–5 µg	-0.4
	Ge-76	Ge-77	11.21 h	416.3	5–10 µg	-0.7
	Ge-76	Ge-77m	53.7 s	159.7	20–50 µg	-1.4
As	As-75	As-76	26.24 h	559.1	2–5 ng	2.1

TABLE 5: THEORETICAL SENSITIVITY FACTORS OBTAINED USING A SPECIFIC ANALYTICAL SEQUENCE IN NAA (Cont.)

SHL-NAA - Short Irradiation – Theoretical sensitivity factor SHL						
Element analysed	**Target Isotope**	**Formed Isotope**	**$T_{1/2}$**	**E_γ (keV)**	**Sensitivity Factor S_{SHL}**	**- log (S_{SHL})**
Se	Se-76	Se-77m	17.36 s	162.0	5–10 ng	1.8
	Se-82	Se-83m	70.1 s	356.7	200–500 µg	-2.6
	Se-78	Se-79m	3.92 min	95.7	100–200 ng	0.9
	Se-80	Se-81	18.45 min	276.0	1–2 µg	-0.2
	Se-80	Se-81m	57.28 min	103.0	0.5–1 µg	0.0
	Se-82	Se-83	22.3 min	356.7	1–2 µg	-0.2
Br	Br-79	Br-80	17.68 min	616.3	5–10 ng	1.9
	Br-81	Br-82	35.3 h	554.3	5–10 ng	1.7
Rb	Rb-87	Rb-88	17.77 min	898.0	0.5–1 µg	0.1
	Rb-87	Rb-88	17.77 min	1836.0	0.5–1 µg	0.1
	Rb-85	Rb-86m	61.02 s	556.1	0.5–1 µg	0.1
Sr	Sr-84	Sr-85m	67.63 min	231.9	1–2 µg	-0.2
	Sr-86	Sr-87m	2.815 h	388.5	20–50 ng	1.4
Y	Y-89	Y-90m	3.19 h	202.5	1–2 µg	-0.3
	Y-89	Y-90m	3.19 h	479.5	2–5 µg	-0.5
Zr	Zr-96	Zr-97 / Nb-97m / Nb-97	16.75 h / 58.7 s / 72.1 min	657.9	2–5 µg	-0.4
	Zr-96	Zr-97 / Nb-97m / Nb-97	16.8 h / 58.7 s	743.4	2–5 µg	-0.5
Nb	Nb-93	Nb-94m	6.26 min	871	0.5–1 µg	0.1
Mo	Mo-98	Mo-99 / Tc-99m	65.92 h / 6.01 h	140.5	2–5 µg	-0.4
	Mo-100	Mo-101	14.61 min	590.1	0.5–1 µg	0.2
	Mo-100	Tc-101	14.2 min	306.8	50–100 ng	1.0
Ru	Ru-104	Ru-105 / Rh-105m	4.44 h / 42.8 s	724.2	100–200 ng	1.0
	Ru-104	Rh-105	35.34 h	319.2	200–500 ng	0.4
	Ru-96	Ru-97	2.83 d	215.7	1–2 µg	-0.2
Rh	Rh-103	Rh-104	42.3 s	555.8	5–10 ng	1.9
	Rh-103	Rh-104m	4.34 min	51.4	0.2–0.5 ng	3.2
Pd	Pd-106	Pd-107m	21.3 s	214.9	5–10 µg	-0.8
	Pd-108	Pd-109	13.59 h	311.4	5–10 µg	-0.8
	Pd-108	Pd-109 / Ag-109m	13.59 h / 39.8 s	88.0	20–50 ng	1.3
	Pd-110	Pd-111	23.4 min	580.0	20–50 µg	-1.4
	Pd-110	Pd-111m	5.5 h	172.2	5–10 µg	-0.7
	Pd-108	Pd-109m	4.70 min	188.9	20–50 ng	1.4
Ag	Ag-107	Ag-108	2.38 min	434.0	50–100 ng	1.2
	Ag-107	Ag-108	2.38 min	633.0	5–10 ng	1.7
	Ag-109	Ag-110	24.6 s	657.5	5–10 ng	1.8

TABLE 5: THEORETICAL SENSITIVITY FACTORS OBTAINED USING A SPECIFIC ANALYTICAL SEQUENCE IN NAA (Cont.)

SHL-NAA - Short Irradiation – Theoretical sensitivity factor SHL						
Element analysed	**Target Isotope**	**Formed Isotope**	**$T_{1/2}$**	**E_γ (keV)**	**Sensitivity Factor S_{SHL}**	**- log (S_{SHL})**
Cd	Cd-114	Cd-115	53.46 h	527.9	0.5–1 µg	0.0
	Cd-114	Cd-115 / In-115m	4.486 h	336.2	200–500 ng	0.4
	Cd-110	Cd-111m	48.54 min	245.4	200–500 ng	0.5
	Cd-106	Cd-107	6.5 h	93.1	5–10 µg	-0.8
	Cd-116	Cd-117	2.49 h	273.3	2–5 µg	-0.3
	Cd-116	Cd-117m	3.36 h	1066.0	10–20 µg	-1.1
	Cd-116	Cd-117 / In-117	2.49 h /43.2 min	553.0	1–2 µg	0.1
In	In-115	In-116m1	54.29 min	1097.3	0.05–0.1 ng	3.8
	In-115	In-116m2	2.18 s	162.4	1–2 ng	2.6
	In-115	In-116	14.1 s	1293.6	50–100 ng	1.1
Sn	Sn-122	Sn-123m	40.06 min	160.3	0.5–1 µg	0.1
	Sn-124	Sn-125m	9.52 min	332.1	100–200 ng	0.9
Sb	Sb-123	Sb-124m1	93 s	498.4	5–10 µg	-0.8
	Sb-123	Sb-124m1	93 s	602.7	5–10 µg	-0.8
	Sb-121	Sb-122m2	4.191 min	61.4	20–50 ng	1.4
	Sb-121	Sb-122	65.371 h	564.2	5–10 ng	1.9
I	I-127	I-128	24.99 min	442.9	2–5 ng	2.3
Te	Te-128	Te-129	69.6 min	459.6	0.5–1 µg	0.3
	Te-126	Te-127	9.35 h	417.9	5–10 µg	-0.8
	Te-130	Te-131m	33.25 h	773.7	10–20 µg	-1.2
Cs	Cs-133	Cs-134m	2.91 h	127.42	2–5 ng	2.3
Ba	Ba-132	Ba-133m	38.9 h	275.9	100–200 µg	-2.3
	Ba-134	Ba-135m	28.7 h	268.2	5–10 µg	-0.7
	Ba-138	Ba-139	82.9min	165.9	100–200 ng	0.7
	Ba-130	Ba-131m	14.6 min	108.4	2–5 µg	-0.4
La	La-139	La-140	40.286 h	487.0	5–10 ng	1.9
	La-139	La-140	40.286 h	1596.2	5–10 ng	1.8
Ce	Ce-136	Ce-137m	34.4 h	254.3	20–50 µg	-1.5
	Ce-136	Ce-137	9.0 h	447.2	50–100 µg	-1.9
	Ce-138	Ce-139m	57.6 s	754.2	100–200 µg	-2.3
	Ce-142	Ce-143	33.0 h	293.3	0.5–1 µg	0.1
Pr	Pr-141	Pr-142	19.12 h	1575.6	100–200 ng	0.8
Nd	Nd-148	Nd-149	1.73 h	211.3	50–100 ng	1.2
	Nd-148	Pm-149	53.08 h	286.0	10–20 µg	-1.0
	Nd-150	Nd-151	12.44 min	255.7	200–500 ng	0.5
	Nd-150	Pm-151	28.4 h	340.1	1–2 µg	-0.3

TABLE 5: THEORETICAL SENSITIVITY FACTORS OBTAINED USING A SPECIFIC ANALYTICAL SEQUENCE IN NAA (Cont.)

SHL-NAA - Short Irradiation – Theoretical sensitivity factor SHL						
Element analysed	**Target Isotope**	**Formed Isotope**	**$T_{1/2}$**	**E_γ (keV)**	**Sensitivity Factor S_{SHL}**	**- log (S_{SHL})**
Sm	Sm-152	Sm-153	46.3 h	69.7	5–10 ng	1.9
	Sm-152	Sm-153	46.3 h	103.2	0.5–1 ng	2.8
	Sm-154	Sm-155	22.2 min	141.4	100–200 ng	0.9
	Sm-154	Sm-155	22.2 min	245.7	50–100 ng	1.1
Eu	Eu-151	Eu-152m1	9.312 h	121.8	0.02–0.05 ng	4.1
	Eu-151	Eu-152m1	9.312 h	841.6	0.05–0.1 ng	4.0
	Eu-151	Eu-152m2	96 min	89.8	5–10 ng	1.9
Gd	Gd-158	Gd-159	18.48 h	363.5	100–200 ng	0.8
	Gd-160	Gd-161	3.66 min	360.9	5–10 ng	1.7
Tb	No short lived equivalent					
Dy	Dy-164	Dy-165	2.334 h	94.7	0.05–0.1 ng	3.9
	Dy-164	Dy-165	2.334 h	361.7	0.2–0.5 ng	3.1
	Dy-164	Dy-165m	75.4 s	515.5	5–10 ng	1.8
Ho	Ho-165	Ho-166	26.83 h	80.6	2–5 ng	2.3
	Ho-165	Ho-166	26.83 h	1379.4	100–200 ng	0.9
Er	Er-170	Er-171	7.516 h	308.3	5–10 ng	1.9
	Er-166	Er-167m	2.27 s	207.8	50–100 ng	1.2
Tm	No short lived equivalent					
Yb	Yb-176	Yb-177	1.911 h	150.4	20–50 ng	1.4
	Yb-176	Yb-177m	6.41 s	104.5	200–500 ng	0.6
Lu	Lu-175	Lu-176m	3.635 h	88.4	0.5–1 ng	2.9
Hf	Hf-178	Hf-179m1	18.67 s	214.3	0.5–1 ng	2.8
	Hf-179	Hf-180m	5.5 h	215.4	50–100 ng	1.1
	Hf-179	Hf-180m	5.5 h	332.3	50–100 ng	1.0
	Hf-179	Hf-180m	5.5 h	443.2	100–200 ng	0.9
Ta	Ta-181	Ta-182m2	15.8 min	171.6	200–500 ng	0.4
W	W-186	W-187	24.00 h	479.5	5–10 ng	2.0
	W-186	W-187	24.00 h	685.8	5–10 ng	2.0
	W-182	W-183m	5.3 s	107.9	1–2 µg	-0.2
Re	Re-187	Re-188	17.0 h	155.0	1–2 ng	2.6
	Re-187	Re-188m	18.6 min	105.8	20–50 ng	1.5
Os	Os-192	Os-193	29.83 h	460.5	1–2 µg	0.0
	Os-190	Os-191m	13.1 h	74.4	0.5–1 mg	-3.0
Ir	Ir-193	Ir-194	19.2 h	328.4	0.5–1 ng	2.7
	Ir-191	Ir-192m	87 s	56.7	2–5 µg	-0.4
Pt	Pt-198	Pt-199m	29.83 h	460.5	1–2 µg	-0.2
	Pt-198	Pt-199	30.8 min	543.0	200–500 ng	0.6
	Pt-196	Pt-197m	95.4 min	346.5	10–20 µg	-1.4
	Pt-196	Pt-197	19.89 h	191.4	2–5 µg	-0.4
Au	Au-197	Au-198	64.68 h	411.8	0.2–0.5 ng	3.1

TABLE 5: THEORETICAL SENSITIVITY FACTORS OBTAINED USING A SPECIFIC ANALYTICAL SEQUENCE IN NAA (Cont.)

SHL-NAA - Short Irradiation – Theoretical sensitivity factor SHL						
Element analysed	**Target Isotope**	**Formed Isotope**	**$T_{1/2}$**	**E_γ (keV)**	**Sensitivity Factor S_{SHL}**	**- log(S_{SHL})**
Hg	Hg-196	Hg-197	64.14 h	77.4	100–200 ng	1.0
	Hg-196	Hg-197m	23.8 h	134.0	0.5–1 µg	0.2
	Hg-204	Hg-205	5.2 min	203.7	5–10 µg	-0.8
	Hg-198	Hg-199m	42.7 min	158.3	2–5 µg	-0.4
Pb	Pb-206	Pb-207m	0.8 s	569.7	200–500 µg	-2.5
Th	Th-232	Th-233	21.83 min	459.2	100–200 ng	0.9
U	U-238	U-239	23.5 min	74.7	0.5–1 ng	3.0
	U-238	Np-239	56.54 h	277.6	20–50 ng	1.4

5.3 SENSITIVITY OF NAA WITH SHORT HALF-LIFE RADIONUCLIDES VERSUS NAA WITH LONG HALF-LIFE RADIONUCLIDES

Table 6 shows a comparison of the sensitivity for NAA using long half-life vs using short half-life radionuclides. The data shows that, in many cases, NAA using long half-life radionuclides is more sensitive than NAA using short half-life radionuclides. This effect might be reinforced for very long half-life radionuclides as they will be less influenced by the Compton background of ^{28}Al, ^{56}Mn and ^{24}Na. There are a number of elements for which NAA using short half-life radionuclides is as, or even more, favourable than long half-life NAA e.g., Ca, In, Ba and Sn as shown in Table 6. Some elements can only be measured using the short half-life radionuclides.

Note that the same analytical sequence of irradiation, decay and counting sequence as used for Table 4 was used for the sensitivity calculation in Table 6.

TABLE 6. SENSITIVITY OF NAA USING SHORT HALF LIFE RADIONUCLIDES (SHL) VERSUS NAA USING LONG HALF-LIFE RADIONUCLIDES (LHL)

NAA using short half-life radionuclides, short irradiation						NAA using medium/long half-life radionuclides, long irradiation					
Element	**Target isotope**	**Formed isotope**	**$T_{1/2}$**	**E_γ (keV)**	**-log (S_{SHL})**	**Element**	**Target isotope**	**Formed isotope**	**$T_{1/2}$**	**E_γ (keV)**	**-log (S_{LHL})**
O	O-18	O-19	26.88 s	197.14	-4.0	**O**	No long lived equivalent				
F	F-19	F-20	11.07 s	1633.6	-0.2	**F**	No long lived equivalent				
Na	Na-23	Na-24	14.96 h	1368.6	1.8	**Na**	Na-23	Na-24	14.96 h	1368.6	3.2
	Na-23	Na-24	14.96 h	2754.0	1.6		Na-23	Na-24	14.96 h	2754.0	2.9
Mg	Mg-26	Mg-27	9.458 min	843.8	0.3	**Mg**	No long lived equivalent				
	Mg-26	Mg-27	9.458 min	1014.5	-0.1						
Al	Al-27	Al-28	2.25 min	1779.0	1.8	**Al**	No long lived equivalent				
Si	Si-30	Si-31	2.621 h	1266.1	-3.0	**Si**	Si-30	Si-31	2.621 h	1266.1	-1.9
S	S-36	S-37	5.05 min	3103.4	-2.1	**S**	No long lived equivalent				
Cl	Cl-37	Cl-38m	0.715s	671.3	-1.6	**Cl**	No long lived equivalent				
	Cl-37	Cl-38	37.23 min	1642.7	0.7						
	Cl-37	Cl-38	37.23 min	2167.4	0.7						
Ar	Ar-40	Ar-41	1.827 h	1293.6	2.4	**Ar**	Ar-40	Ar-41	1.827 h	1293.6	3.5
K	K-41	K-42	12.36 h	1524.6	0.2	**K**	K-41	K-42	12.36 h	1524.6	1.5
Ca	Ca-48	Ca-49	8.718 min	3084.4	-0.4	**Ca**	Ca-46	Ca-47	4.536 d	1297.1	-1.9
							Ca-46	Sc-47	3.349 d	159.4	-1.1
Sc	Sc-45	Sc-46m	18.75 s	142.5	2.7	**Sc**	Sc-45	Sc-46	83.83 d	889.3	4.0
							Sc-45	Sc-46	83.83 d	1120.5	3.9
Ti	Ti-50	Ti-51	5.76 min	320.1	0.8	**Ti**	No long lived (n,γ) equivalent, consider using the $^{47}Ti(n,p)^{47}$ Sc threshold reaction				
V	V-51	V-52	3.74 min	1434.1	3.1	**V**	No long lived equivalent				
Cr	Cr-54	Cr-55	3.5 min	1528.0	-1.1	**Cr**	Cr-50	Cr-51	27.7 d	320.1	2.0
Mn	Mn-55	Mn-56	2.579 h	846.8	3.6	**Mn**	Mn-55	Mn-56	2.579 h	846.8	4.8
	Mn-55	Mn-56	2.579 h	1810.7	2.8		Mn-55	Mn-56	2.579 h	1810.7	4.0
	Mn-55	Mn-56	2.579 h	2113.1	2.5		Mn-55	Mn-56	2.579 h	2113.1	3.7

TABLE 6. SENSITIVITY OF NAA USING SHORT HALF LIFE RADIONUCLIDES (SHL) VERSUS NAA USING LONG HALF-LIFE RADIONUCLIDES (LHL) (Cont.)

NAA using short half-life radionuclides, short irradiation						NAA using medium/long half-life radionuclides, long irradiation					
Element	**Target isotope**	**Formed isotope**	**$T_{1/2}$**	**E_γ (keV)**	**-log (S_{SHL})**	**Element**	**Target isotope**	**Formed isotope**	**$T_{1/2}$**	**E_γ (keV)**	**-log (S_{LHL})**
Fe	No short lived equivalent					**Fe**	Fe-58	Fe-59	44.5 d	1099.3	0.0
							Fe-58	Fe-59	44.5 d	1291.6	-0.2
Co	Co-59	Co-60m	10.47 min	58.6	2.4	**Co**	Co-59	Co-60	1925.3 d	1173.2	2.7
	Co-59	Co-60m	10.47 min	1332.5	1.1		Co-59	Co-60	1925.3 d	1332.5	2.6
Ni	Ni-64	Ni-65	2.518 h	1481.8	-0.1	**Ni**	Ni-64	Ni-65	2.518 h	1481.8	1.0
							Consider using the $^{58}Ni(n,p)^{58}Co$ threshold reaction				
Cu	Cu-63	Cu-64	12.7 h	1345.8	-0.1	**Cu**	Cu-63	Cu-64	12.7 h	1345.8	1.3
	Cu-65	Cu-66	5.12 min	1039.2	1.2						
Zn	Zn-68	Zn-69m	13.76 h	438.6	0.2	**Zn**	Zn-68	Zn-69m	13.76 h	438.6	1.5
	Zn-70	Zn-71	2.42 min	121.5	-2.6		Zn-64	Zn-65	244.3 d	1115.5	1.2
	Zn-70	Zn-71m	4.14 h	386.4	-1.7		Zn-70	Zn-71m	4.14 h	386.3	-0.5
Ga	Ga-71	Ga-72	14.1 h	630.0	1.7	**Ga**	Ga-71	Ga-72	14.1 h	630.0	3.0
	Ga-71	Ga-72	14.1 h	834.1	2.2		Ga-71	Ga-72	14.1 h	834.1	3.5
	Ga-69	Ga-70	21.14 min	176.1	0.3		Ga-71	Ga-72	14.1 h	2201.7	2.7
	Ga-69	Ga-70	21.14 min	1039.5	0.3						
Ge	Ge-74	Ge-75	82.78 min	198.6	-0.6	**Ge**	Ge-76	Ge-77	11.21 h	211.0	0.9
	Ge-74	Ge-75m	47.7 s	139.7	0.0		Ge-76	Ge-77	11.21 h	416.3	0.7
	Ge-76	Ge-77	11.21 h	211.0	-0.4						
	Ge-76	Ge-77	11.21 h	416.3	-0.7						
	Ge-76	Ge-77m	53.7 s	159.7	-1.4						
As	As-75	As-76	26.24 h	559.1	2.1	**As**	As-75	As-76	26.24 h	559.1	3.5

TABLE 6. SENSITIVITY OF NAA USING SHORT HALF LIFE RADIONUCLIDES (SHL) VERSUS NAA USING LONG HALF-LIFE RADIONUCLIDES (LHL) (Cont.)

NAA using short half-life radionuclides, short irradiation						NAA using medium/long half-life radionuclides, long irradiation					
Element	**Target isotope**	**Formed isotope**	**$T_{1/2}$**	**E_γ (keV)**	**-log (S_{SHL})**	**Element**	**Target isotope**	**Formed isotope**	**$T_{1/2}$**	**E_γ (keV)**	**-log (S_{LHL})**
Se	Se-76	Se-77m	17.36 s	162.0	1.8	**Se**	Se-74	Se-75	119.781 d	136.0	2.3
	Se-82	Se-83m	70.1 s	356.7	-2.4		Se-74	Se-75	119.781 d	264.7	2.2
	Se-78	Se-79m	3.92 min	95.7	0.9		Se-74	Se-75	119.781 d	279.5	1.8
	Se-80	Se-81	18.45 min	276.0	-0.2		Se-80	Se-81m	57.28 min	103.0	1.7
	Se-80	Se-81m	57.28 min	103.0	0.0						
	Se-82	Se-83	22.3 min	356.7	-0.2						
Br	Br-79	Br-80	17.68 min	616.3	1.9	**Br**	Br-81	Br-82	35.3 h	554.3	3.1
	Br-81	Br-82	35.3 h	554.3	1.7						
Rb	Rb-87	Rb-88	17.77 min	898.0	0.1	**Rb**	Rb-85	Rb-86	18.63 d	1077.0	1.4
	Rb-87	Rb-88	17.77 min	1836.0	0.1						
	Rb-85	Rb-86m	61.02 s	556.1	0.1						
Sr	Sr-84	Sr-85m	67.63 min	231.9	-0.2	**Sr**	Sr-84	Sr-85	64.84 d	514.0	0.3
	Sr-86	Sr-87m	2.815 h	388.5	1.4		Sr-86	Sr-87m	2.815 h	388.5	2.6
Y	Y-89	Y-90m	3.19 h	202.5	-0.3	**Y**	Y-89	Y-90m	3.19 h	202.5	0.9
	Y-89	Y-90m	3.19 h	479.5	-0.5		Y-89	Y-90m	3.19 h	479.5	0.7
Zr	Zr-96	Zr-97 / Nb-97m / Nb-97	16.75 h / 58.7 s / 72.1 min	657.9	-0.4	**Zr**	Zr-94	Zr-95 / Nb-95	64.02 d / 34.97 d	765.8	-1.5
	Zr-96	Zr-97 / Nb-97m / Nb-97	16.75 h / 58.7 s / 72.1 min	743.4	-0.5		Zr-94	Zr-95	64.02 d	756.7	0.2
							Zr-96	Zr-97/Nb-97m/Nb-97	16.75h/58.7s/72.1min	657.9	0.9
Nb	Nb-93	Nb-94m	6.26 min	871	0.1	**Nb**	No long lived equivalent				
Mo	Mo-98	Mo-99 / Tc-99m	65.92 h / 6.01 h	140.5	-0.4	**Mo**	Mo-98	Mo-99 / Tc-99m	65.92 h / 6.01 h	140.5	1.3
	Mo-100	Mo-101	14.61 min	590.1	0.2						
	Mo-100	Tc-101	14.2 min	306.8	1.0						

TABLE 6. SENSITIVITY OF NAA USING SHORT HALF LIFE RADIONUCLIDES (SHL) VERSUS NAA USING LONG HALF-LIFE RADIONUCLIDES (LHL) (Cont.)

NAA using short half-life radionuclides, short irradiation						NAA using medium/long half-life radionuclides, long irradiation					
Element	**Target isotope**	**Formed isotope**	**$T_{1/2}$**	**E_γ (keV)**	**-log (S_{SHL})**	**Element**	**Target isotope**	**Formed isotope**	**$T_{1/2}$**	**E_γ (keV)**	**-log (S_{LHL})**
Ru	Ru-104	Ru-105 / Rh-105m	4.44 h / 42.8 s	724.2	1.0	**Ru**	Ru-96	Ru-97	2.83 d	215.7	1.0
	Ru-104	Rh-105	35.34 h	319.2	0.4		Ru-102	Ru-103	39.35 d	497.1	2.2
	Ru-96	Ru-97	2.83 d	215.7	-0.2		Ru-104	Rh-105	35.34 h	318.9	1.4
							Ru-104	Ru-105 / Rh-105m	4.44 h / 42.8 s	724.2	2.2
Rh	Rh-103	Rh-104	42.3 s	555.8	1.9	**Rh**	No long lived equivalent				
	Rh-103	Rh-104m	4.34 min	51.4	3.2						
Pd	Pd-106	Pd-107m	21.3 s	214.9	-0.8	**Pd**	Pd-108	Pd-109	13.59 h	311.4	0.5
	Pd-108	Pd-109	13.59 h	311.4	-0.8		Pd-108	Pd-109 / Ag-109m	13.59 h / 39.8 s	88.0	2.7
	Pd-108	Pd-109 / Ag-109m	13.59 h / 39.8 s	88.0	1.3						
	Pd-110	Pd-111	23.4 min	580.0	-1.4						
	Pd-110	Pd-111m	5.5 h	172.2	-0.7						
	Pd-108	Pd-109m	4.70 min	188.9	1.4						
Ag	Ag-107	Ag-108	2.38 min	434.0	1.2	**Ag**	Ag-109	Ag-110m	249.8 d	657.8	2.3
	Ag-107	Ag-108	2.38 min	633.0	1.7		Ag-109	Ag-110m	249.8 d	937.5	1.8
	Ag-109	Ag-110	24.6 s	657.5	1.8						
Cd	Cd-114	Cd-115	53.46 h	527.9	0.0	**Cd**	Cd-114	Cd-115	53.46 h	527.9	1.4
	Cd-114	Cd-115 / In-115m	53.46 h / 4.486 h	336.2	0.4		Cd-114	Cd-115 / In-115m	53.46 h / 4.486 h	336.2	1.7
	Cd-110	Cd-111m	48.54 min	245.4	0.5		Cd-106	Cd-107	6.5 h	93.1	0.4
	Cd-106	Cd-107	6.5 h	93.1	-0.8		Cd-116	Cd-117	2.49 h	273.3	0.9
	Cd-116	Cd-117	2.49 h	273.3	-0.3		Cd-116	Cd-117m	3.36 h	1066.0	+0.1
	Cd-116	Cd-117m	3.36 h	1066.0	-1.1		Cd-116	Cd-117 / In-117	2.49 h / 43.2 min	553.0	1.3
	Cd-116	Cd-117 / In-117	2.49 h / 43.2 min	553.0	+0.1						

TABLE 6. SENSITIVITY OF NAA USING SHORT HALF LIFE RADIONUCLIDES (SHL) VERSUS NAA USING LONG HALF-LIFE RADIONUCLIDES (LHL) (Cont.)

NAA using short half-life radionuclides, short irradiation						NAA using medium/long half-life radionuclides, long irradiation					
Element	**Target isotope**	**Formed isotope**	**$T_{1/2}$**	**E_γ (keV)**	**-log (S_{SHL})**	**Element**	**Target isotope**	**Formed isotope**	**$T_{1/2}$**	**E_γ (keV)**	**-log (S_{LHL})**
In	In-115	In-116m1	54.29 min	1097.3	3.8	**In**	In-113	In-114m	49.51 d	190.3	1.9
	In-115	In-116m2	2.18 s	162.4	2.6		In-113	In-114m	49.51 d	558.4	1.0
	In-115	In-116	14.1 s	1293.6	1.1						
Sn	Sn-122	Sn-123m	40.06 min	160.3	0.1	**Sn**	Sn-112	Sn-113	115.1 d	255.1	-1.0
	Sn-124	Sn-125m	9.52 min	332.1	0.9		Sn-112	In-113m / Sn-113	1.658 h / 115.1 d	391.7	0.3
							Sn-116	Sn-117m	13.6 d	158.5	0.6
							Sn-124	Sn-125	9.64 d	1067.1	-1.7
Sb	Sb-123	Sb-124m1	93 s	498.4	-0.8	**Sb**	Sb-121	Sb-122	65.371 h	564.2	3.0
	Sb-123	Sb-124m1	93 s	602.7	-0.8		Sb-121	Sb-122	65.371 h	692.7	1.7
	Sb-121	Sb-122m2	4.191 min	61.4	1.4		Sb-123	Sb-124	60.2 d	602.7	2.9
	Sb-121	Sb-122	65.371 h	564.2	1.9		Sb-123	Sb-124	60.2 d	1691.0	2.3
I	I-127	I-128	24.99 min	442.9	2.3	**I**	No long lived equivalent				
Te	Te-128	Te-129	69.6 min	459.6	0.3	**Te**	Te-130	Te-131m / I-131	33.25 h / 8.025 d	364.5	1.6
	Te-126	Te-127	9.35 h	417.9	-0.8		Te-130	Te-131m	33.25 h	773.7	0.1
	Te-130	Te-131m	33.25 h	773.7	-1.2		Te-128	Te-129	69.6 min	459.6	1.2
							Te-126	Te-127	9.35 h	417.9	0.5
Cs	Cs-133	Cs-134m	2.91 h	127.42	2.3	**Cs**	Cs-133	Cs-134	2.0644 y	604.7	3.0
							C -133	Cs-134	2.0644 y	795.9	2.9
Ba	Ba-132	Ba-133m	38.9 h	275.9	-2.3	**Ba**	Ba-130	Ba-131	11.5 d	496.3	0.7
	Ba-134	Ba-135m	28.7 h	268.2	-0.7		Ba-134	Ba-135m	28.7 h	268.2	0.6
	Ba-138	Ba-139	82.9 min	165.9	0.7		Ba-132	Ba-133m	38.9 h	275.9	-1.0
	Ba-130	Ba-131m	14.6 min	108.4	-0.4						
La	La-139	La-140	40.286 h	487.0	1.9	**La**	La-139	La-140	40.286 h	487.0	3.2
	La-139	La-140	40.286 h	1596.2	1.8		La-139	La-140	40.286 h	1596.2	3.2

TABLE 6. SENSITIVITY OF NAA USING SHORT HALF LIFE RADIONUCLIDES (SHL) VERSUS NAA USING LONG HALF-LIFE RADIONUCLIDES (LHL) (Cont.)

NAA using short half-life radionuclides, short irradiation						NAA using medium/long half-life radionuclides, long irradiation					
Element	**Target isotope**	**Formed isotope**	**$T_{1/2}$**	**E_γ (keV)**	**-log (S_{SHL})**	**Element**	**Target isotope**	**Formed isotope**	**$T_{1/2}$**	**E_γ (keV)**	**-log (S_{LHL})**
Ce	Ce-136	Ce-137m	34.4 h	254.3	-1.5	**Ce**	Ce-136	Ce-137m	34.4 h	254.3	-0.2
	Ce-136	Ce-137	9.0 h	447.2	-1.9		Ce-136	Ce-137	9.0 h	447.2	-0.6
	Ce-138	Ce-139m	57.6 s	754.24	-2.3		Ce-140	Ce-141	32.50 d	145.4	2.2
	Ce-142	Ce-143	33.0 h	293.3	0.1		Ce-142	Ce-143	33.1 h	293.3	1.5
Pr	Pr-141	Pr-142	19.12 h	1575.6	0.8	**Pr**	Pr-141	Pr-142	19.12 h	1575.6	2.2
Nd	Nd-148	Nd-149	1.73 h	211.3	1.2	**Nd**	Nd-146	Nd-147	11.0 d	91.1	1.9
	Nd-148	Pm-149	53.08 h	286.0	-1.0		Nd-148	Nd-149	1.73 h	211.3	2.3
	Nd-150	Nd-151	12.44 min	255.7	0.5		Nd-148	Pm-149	53.08 h	286.0	0.3
	Nd-150	Pm-151	28.4 h	340.1	-0.3		Nd-150	Pm-151	28.4 h	340.1	1.1
Sm	Sm-152	Sm-153	46.3 h	69.7	1.9	**Sm**	Sm-152	Sm-153	46.3 h	69.7	3.3
	Sm-152	Sm-153	46.3 h	103.2	2.8		Sm-152	Sm-153	46.3 h	103.2	4.2
	Sm-154	Sm-155	22.2 min	141.4	0.9						
	Sm-154	Sm-155	22.2 min	245.7	1.1						
Eu	Eu-151	Eu-152m1	9.312 h	121.8	4.1	**Eu**	Eu-151	Eu-152	13.52y	121.8	3.7
	Eu-151	Eu-152m1	9.312 h	841.6	4.0		Eu-151	Eu-152	13.52 y	1408.0	3.0
	Eu-151	Eu-152m2	96 min	89.8	1.9						
Gd	Gd-158	Gd-159	18.48 h	363.5	0.8	**Gd**	Gd-152	Gd-153	240.4 d	97.4	1.7
	Gd-160	Gd-161	3.66 min	360.9	1.7		Gd-152	Gd-153	240.4 d	103.2	1.5
							Gd-158	Gd-159	18.48 h	363.5	2.1
Tb	No short lived equivalent					**Tb**	Tb-159	Tb-160	72.3 d	86.8	3.3
							Tb-159	Tb-160	72.3 d	879.4	3.2
Dy	Dy-164	Dy-165	2.334 h	94.7	3.9	**Dy**	Dy-164	Dy-165	2.334 h	94.7	5.0
	Dy-164	Dy-165	2.334 h	361.7	3.1		Dy-164	Dy-165	2.334 h	361.7	4.2
	Dy-164	Dy-165m	75.4 s	515.5	1.8						

TABLE 6. SENSITIVITY OF NAA USING SHORT HALF LIFE RADIONUCLIDES (SHL) VERSUS NAA USING LONG HALF-LIFE RADIONUCLIDES (LHL) (Cont.)

NAA using short half-life radionuclides, short irradiation						NAA using medium/long half-life radionuclides, long irradiation					
Element	**Target isotope**	**Formed isotope**	**$T_{1/2}$**	**E_γ (keV)**	**-log (S_{SHL})**	**Element**	**Target isotope**	**Formed isotope**	**$T_{1/2}$**	**E_γ (keV)**	**-log (S_{LHL})**
Ho	Ho-165	Ho-166	26.83 h	80.6	2.3	**Ho**	Ho-165	Ho-166	26.83 h	80.6	3.7
	Ho-165	Ho-166	26.83 h	1379.4	0.9		Ho-165	Ho-166	26.83 h	1379.4	2.3
Er	Er-170	Er-171	7.516 h	308.3	1.9	**Er**	Er-170	Er-171	7.516 h	308.3	3.3
	Er-166	Er-167m	2.27 s	207.8	1.2						
Tm	No short lived equivalent					**Tm**	Tm-169	Tm-170	128.6 d	84.3	2.9
Yb	Yb-176	Yb-177	1.911 h	150.4	1.4	**Yb**	Yb-168	Yb-169	32.02 d	198.0	2.9
	Yb-176	Yb-177m	6.41 s	104.5	0.6		Yb-174	Yb-175	4.185 d	396.3	2.9
							Yb-176	Yb-177	1.911 h	150.4	2.5
Lu	Lu-175	Lu-176m	3.635 h	88.4	2.9	**Lu**	Lu-175	Lu-176m	3.635 h	88.4	4.1
							Lu-176	Lu-177	6.64 d	208.4	3.7
Hf	Hf-178	Hf-179m1	18.67 s	214.3	2.8	**Hf**	Hf-174	Hf-175	70 d	343.4	2.2
	Hf-179	Hf-180m	5.5 h	215.4	1.1		Hf-180	Hf-181	42.39 d	345.9	2.3
	Hf-179	Hf-180m	5.5 h	332.3	1.0		Hf-180	Hf-181	42.39 d	482.2	3.0
	Hf-179	Hf-180m	5.5 h	443.2	0.9						
Ta	Ta-181	Ta-182m2	15.8 min	171.6	0.4	**Ta**	Ta-181	Ta-182	114.7 d	1121.3	3.0
							Ta-181	Ta-182	114.7 d	1221.4	2.9
W	W-186	W-187	24.00 h	479.5	2.0	**W**	W-186	W-187	24.00 h	479.5	3.3
	W-186	W-187	24.00 h	685.8	2.0		W-186	W-187	24.00 h	685.8	3.3
	W-182	W-183m	5.3 s	107.9	-0.2						
Re	Re-187	Re-188	17.0 h	155.0	2.6	**Re**	Re-185	Re-186	3.718 d	137.2	3.4
	Re-187	Re-188m	18.6 min	105.8	1.5		Re-187	Re-188	17.0 h	155.0	4.0
Os	Os-192	Os-193	29.83 h	460.5	0.0	**Os**	Os-184	Os-185	93.6 d	646.1	1.7
	Os-190	Os-191m	13.1 h	74.4	-3.0		Os-190	Os-191	15.4 d	129.4	2.3
							Os-192	Os-193	29.83 h	460.5	1.3

TABLE 6. SENSITIVITY OF NAA USING SHORT HALF LIFE RADIONUCLIDES (SHL) VERSUS NAA USING LONG HALF-LIFE RADIONUCLIDES (LHL) (Cont.)

NAA using short half-life radionuclides, short irradiation						NAA using medium/long half-life radionuclides, long irradiation					
Element	**Target isotope**	**Formed isotope**	**$T_{1/2}$**	**E_γ (keV)**	**-log (S_{SHL})**	**Element**	**Target isotope**	**Formed isotope**	**$T_{1/2}$**	**E_γ (keV)**	**-log (S_{LHL})**
Ir	Ir-193	Ir-194	19.2 h	328.4	2.7	**Ir**	Ir-191	Ir-192	73.83 d	316.5	4.8
	Ir-191	Ir-192m	87 s	56.7	-0.4		Ir-191	Ir-192	73.83 d	468.1	4.5
Pt	Pt-198	Pt-199m	13.6s	391.9	-0.2	**Pt**	Pt-198	Au-199	3.139 d	158.4	1.7
	Pt-198	Pt-199	30.8m	543	0.6		Pt-198	Au-199	3.139 d	208.2	1.0
	Pt-196	Pt-197m	95.4m	346.5	-1.4		Pt-196	Pt-197	19.89 h	191.4	1.0
	Pt-196	Pt-197	19.89h	191.4	-0.4						
Au	Au-197	Au-198	64.68 h	411.8	3.1	**Au**	Au-197	Au-198	64.68 h	411.8	4.5
Hg	Hg-196	Hg-197	64.14 h	77.4	1.0	**Hg**	Hg-196	Hg-197	64.14 h	77.4	2.4
	Hg-196	Hg-197m	23.8 h	134.0	0.2		Hg-196	Hg-197m	23.8 h	134.0	1.6
	Hg-204	Hg-205	5.2 min	203.7	-0.8		Hg-202	Hg-203	46.61 d	279.2	2.5
	Hg-198	Hg-199m	42.7 min	158.3	-0.4						
Pb	Pb-206	Pb-207m	0.8 s	569.7	-2.5	**Pb**	No long lived equivalent				
Th	Th-232	Th-233	21.83 min	459.2	0.9	**Th**	Th-232	Pa-233	26.97 d	300.1	2.4
							Th-232	Pa-233	26.97 d	311.9	3.2
U	U-238	U-239	23.5 min	74.7	3.0	**U**	U-238	Np-239	2.356 d	106.1	2.7
	U-238	Np-239	56.54 h	277.6	1.4		U-238	Np-239	2.356 d	228.2	2.2
							U-238	Np-239	2.356 d	277.6	2.3

5.4 CYCLIC SHORT-LIVED NAA

A problem inherent in the use of very short half-life radionuclides concerns the fact that the effective detection time has to be shortened as much as possible since the resulting spectrum would otherwise favour radionuclides with longer half-lives. Short measuring times will however limit the counting statistics of the short half-life radionuclides under interest. The problem may be solved by cyclic activation, i.e. so-called cyclic NAA.

In cyclic activation analysis a sample goes through a specific time sequence of operations whereby the sample is activated, decayed, counted and then irradiated again several times (n cycles of irradiate transfer-count-return, in sequence). NAA expert practitioners usually fine tune the irradiation time, decay time, and counting time and a sufficient waiting time between all cycles in order to optimize the signal-to-noise of the short half-life radionuclides of interest versus the longer-lived radionuclides present in the sample. By summing all collected spectra into a single spectrum, the counting statistics and the associated signal-to-noise ratio of the short half-life nuclides in the matrix will be enhanced when compared to the more conventional one shot analysis. Cyclic activation is mainly applied for measuring ultra short half-life radionuclides ($t_{1/2}$ < 100 s). Very detailed summaries and reviews of the advantages and disadvantages, the different types of and different applications in different matrices of cyclic NAA are available in the literature [37–42].

Care needs to be taken if some of the major elements in the sample yield short half-life radionuclides such as ^{28}Al or ^{56}Mn since the Compton background generate by these nuclides will also increase gradually over the different cycles and one cannot allow for a long decay between cycles. To avoid the accumulation of the longer-lived nuclide activity, cyclic activation can be performed using a series of fresh subsamples (referred to as pseudo-cyclic NAA [43])

The key concepts to be implemented in the design of cyclic NAA are:

— High level of automation, meaning minimum need for user intervention during measurement and an efficient user interface keeping control of all the data concerning the irradiation-measurement-data processing cycle;
— High level of flexibility, so that the system is able to measure both short lived and long lived activation products (e.g. knowledge of Na for determination of the ^{23}Na(n,α)^{20}F threshold interference correction);
— High level of simplicity, in that the system needs to be cost effective, simple to run by an operator, can automatically, and in a reproducible way cycle the position of the sample and the associated irradiation, decay, cycle and measurement times;
— Reproducible, well known and sufficiently short transport time to the detector system - preferably reproducibility is on the order of 1% or lower;
— A proper counting system dealing with dead time and pile up corrections (see Section 9.3);
— A well characterized irradiation vial, since impurities in the vial will lead to interferences in the spectrum and a blank subtraction will need to be made. The same is true for the peak of ^{41}Ar in the spectrum, which is formed by activation of argon in the air in the vial.

Cyclic NAA offers several advantages:

— Improvement of analytical sensitivity and detection limit;
— Very short total turn-around time as it is mainly suited for NAA on the basis of radionuclides with half-lives less than 100 s (USHL);

— Many elements can be easily determined using cyclic NAA (see first part of Table 3);
— Suitable for within-item and between-item homogeneity studies using different aliquots of the same item due to the very short turn-around time cyclic NAA.

5.5 EPITHERMAL SHORT-LIVED NAA

There are many radionuclides with a 1/v behaviour of the activation cross-section vs the neutron energy both in the thermal and epithermal neutron energy region, but there is also a number of radionuclides that have many resonances for neutron capture in the epithermal region. For those radionuclides with high cross-sections in the epithermal region versus the thermal region (or high $Q_0 = I_0/\sigma_{th}$), the epithermal contribution to the overall reaction rate will be proportionally higher. For those radionuclides with low Q_0 the thermal contribution to the total reaction rate will be higher than the epithermal contribution.

Epithermal NAA (ENAA) can be achieved by surrounding the sample with a thermal neutron absorber such as cadmium, boron or gadolinium inside of the irradiation container or alternatively using a dedicated facility where a neutron absorber is integrated into the irradiation facility itself (as described in Section 8). By using such an arrangement, thermal activation is minimized since e.g. Cd has a very high absorption cross-section in the thermal neutron region and will be virtually transparent for neutrons above the effective Cd cut-off energy, which is about 0.55 eV. Epithermal NAA will reduce the impact of low Q_0 radionuclides, which are often present in the sample and have the tendency of being interfering elements in the matrix. The benefits of ENAA are considerable for some elements, due to improved detection limits from the increased photopeak to background ratio and/or elimination of some interferences. Also, as the induced activity will be lower, the sample may be counted much closer to the detector, again leading to better detection limits.

Epithermal NAA is advantageous in cases when the Cd ratio R_{Cd} (see Eq. 2) for a given nuclide is low, with $f = j_{th}/j_{epi}$ the thermal to epithermal neutron fluence rate ratio and α the deviation of the epithermal neutron fluence rate distribution from the 1/E shape, approximated by a $1/E^{1+\alpha}$ dependence and $Q_{0(\alpha)} = I_{0(\alpha)}/\sigma_{th}$

$$R_{\mathrm{Cd}} = \frac{f + Q_0(\alpha)}{Q_0\,(\alpha)} \tag{2}$$

It can be noticed that some elements measured by short half-life radionuclides will benefit from ENAA, as in this case R_{Cd} of the nuclides of interest is lower than the corresponding R_{Cd}-ratio for nuclides formed by Al, Mn, Na and K which are often present in soils, rocks, sediments and air particulate matter. However, the advantage of using ENAA depends a lot on the sample matrix and its interfering elements. An improved factor to evaluate the impact of ENAA is the advantage factor, as defined in Eq. 3 [44, 45], where d and D denote the interfering nuclide and the nuclide under interest, respectively:

$$F_a = \frac{(R_{\mathrm{Cd}})_{\mathrm{d}}}{(R_{\mathrm{Cd}})_{\mathrm{D}}} \tag{3}$$

The calculated advantage factor for several short half-life radionuclides is given in Table 7, with $f = 20$ and $\alpha = -0.02$ and $(R_{Cd})_d$ was assumed to be 25, which is an average R_{Cd} for e.g. ^{28}Al and ^{24}Na. Examples of elements where considerable improvements can be made are given

in the left column of table 7: Zr, U, Sn, Mo, Ta, Lu, Gd, W, Pd, I, Rb, Br, Sb, Ag, Pt, Hf, In, Sr, Au, As.

The benefits of using epithermal neutrons for irradiation have been discussed by several authors, whereby both tabulated theoretical and experimental advantage factors for different matrices were determined, including the use of Compton suppression systems [38, 46–49].

ENAA has some other advantages relevant for NAA using short half-life radionuclides:

— It reduces the radioactivity dose level as many of the main contributors to the activity such as ^{24}Na, ^{28}Al, ^{56}Mn and ^{140}La are strongly minimised;
— It reduces the effect of thermal neutron fission of ^{235}U and thus the impact of fission interference. This is especially significant for e.g. Zr and Mo;
— Build-up of ^{115}Cd and ^{115}In from Cd (e.g. a Cd-cover) will be reduced with respect to ENAA with long half-life radionuclides due to the short irradiation time.

However, incorporating a neutron filter into an irradiation container introduces additional challenges, chiefly the handling of toxic metals (cadmium), high activities in irradiated neutron filters (cadmium) and potentially higher temperatures during irradiation (cadmium and especially boron).

TABLE 7. CALCULATED IMPROVEMENT FACTORS FOR ENAA USING SHORT HALF-LIFE RADIONUCLIDES with $f = 20$ and $\alpha = -0.02$

Element analysed	Target isotope	Formed isotope	F_a
O	O-18	O-19	5.6
F	F-19	F-20	2.9
Na	Na-23	Na-24	0.8
Mg	Mg-26	Mg-27	0.9
Al	Al-27	Al-28	0.9
Si	Si-30	Si-31	1.5
S	S-36	S-37	1.4
Cl	Cl-37	Cl-38m	1.0
	Cl-37	Cl-38	0.9
Ar	Ar-40	Ar-41	0.8
K	K-41	K-42	1.1
Ca	Ca-48	Ca-49	0.6
Sc	Sc-45	Sc-46m	0.7
Ti	Ti-50	Ti-51	0.9
V	V-51	V-52	0.7
Cr	Cr-54	Cr-55	0.6
Mn	Mn-55	Mn-56	1.4
Co	Co-59	Co-60m	2.4
Ni	Ni-64	Ni-65	0.9
Cu	Cu-63	Cu-64	1.5
	Cu-65	Cu-66	1.4
Zn	Zn-68	Zn-69m	3.8
	Zn-70	Zn-71	7.4
	Zn-70	Zn-71m	4.9
Ga	Ga-71	Ga-72	6.7
	Ga-69	Ga-70	8.4
Ge	Ge-74	Ge-75	2.0
	Ge-74	Ge-75m	3.0
	Ge-76	Ge-77	10.6
	Ge-76	Ge-77m	8.3
As	As-75	As-76	10.7
Se	Se-76	Se-77m	1.0
	Se-82	Se-83m	11.8
	Se-78	Se-79m	9.8
	Se-80	Se-81	3.2
	Se-80	Se-81m	4.9
	Se-82	Se-83	1.3
Br	Br-79	Br-80	9.9
	Br-81	Br-82	12.9
Rb	Rb-87	Rb-88	14.2
	Rb-85	Rb-86m	11.4
Sr	Sr-84	Sr-85m	11.2
	Sr-86	Sr-87m	4.7

TABLE 7. IMPROVEMENT FACTORS FOR ENAA USING SHORT HALF-LIFE RADIONUCLIDES with f = 20 and α = − 0.02 (Cont.)

Element analysed	Target isotope	Formed isotope	F_a
Y	Y-89	Y-90m	6.4
Zr	Zr-96	Zr-97 / Nb-97m / Nb-97	23.3
Nb	Nb-93	Nb-94m	7.3
Mo	Mo-98	Mo-99 / Tc-99m	18.7
	Mo-100	Mo-101	12.9
	Mo-100	Tc-101	12.9
Ru	Ru-104	Ru-105 / Rh-105m	10.5
	Ru-96	Ru-97	15.0
Rh	Rh-103	Rh-104	6.4
	Rh-103	Rh-104m	6.4
Pd	Pd-106	Pd-107m	10.2
	Pd-108	Pd-109	14.7
	Pd-108	Pd-109 / Ag-109m	14.7
	Pd-110	Pd-111	10.1
	Pd-110	Pd-111m	10.1
	Pd-108	Pd-109m	14.3
Ag	Ag-107	Ag-108	3.4
	Ag-109	Ag-110	12.2
Cd	Cd-114	Cd-115	16.1
	Cd-114	Cd-115 / In-115m	16.1
	Cd-110	Cd-111m	13.1
	Cd-106	Cd-107	5.4
	Cd-116	Cd-117	9.8
	Cd-116	Cd-117m	10.1
	Cd-116	Cd-117 / In-117	9.8
In	In-115	In-116m	11.5
	In-115	In-116m2	11.5
	In-115	In-116	12.3
Sn	Sn-122	Sn-123m	5.8
	Sn-124	Sn-125m	19.2
Sb	Sb-123	Sb-124m1	12.9
	Sb-121	Sb-122m	15.9
	Sb-121	Sb-122	15.9
I	I-127	I-128	14.2
Te	Te-128	Te-129	7.8
	Te-126	Te-127	8.3
	Te-130	Te-131m	2.3
Cs	Cs-133	Cs-134m	9.7
Ba	Ba-132	Ba-133m	5.9
	Ba-134	Ba-135m	22.3
	Ba-138	Ba-139	1.2
	Ba-130	Ba-131m	13.5
La	La-139	La-140	1.6

TABLE 7. IMPROVEMENT FACTORS FOR ENAA USING SHORT HALF-LIFE RADIONUCLIDES with f = 20 and α = − 0.02 (Cont.)

Element analysed	Target isotope	Formed isotope	F_a
Ce	Ce-136	Ce-137m	20.4
	Ce-136	Ce-137	0.5
	Ce-138	Ce-139m	10.9
	Ce-142	Ce-143	1.6
Pr	Pr-141	Pr-142	1.9
Nd	Nd-148	Nd-149	5.5
	Nd-148	Pm-149	5.5
	Nd-150	Nd-151	10.1
	Nd-150	Pm-151	10.1
Sm	Sm-152	Sm-153	10.7
	Sm-154	Sm-155	4.8
Eu	Eu-151	Eu-152m	1.5
	Eu-152	Eu-152m2	1.4
Gd	Gd-158	Gd-159	15.4
	Gd-160	Gd-161	4.4
Dy	Dy-164	Dy-165	0.2
	Dy-164	Dy-165m	0.3
Ho	Ho-165	Ho-166	9.1
Er	Er-170	Er-171	4.9
	Er-166	Er-167m	5.2
Yb	Yb-176	Yb-177	3.0
	Yb-176	Yb-177m	3.0
Lu	Lu-175	Lu-176m	16.2
Hf	Hf-178	Hf-179m	11.6
	Hf-179	Hf-180m	10.8
Ta	Ta-181	Ta-182m	15.9
W	W-186	W-187	10.5
	W-182	W-183m	15.1
Re	Re-187	Re-188	4.7
	Re-187	Re-188m	4.9
Os	Os-192	Os-193	2.8
	Os-190	Os-191m	2.5
Ir	Ir-193	Ir-194	10.1
	Ir-191	Ir-192m	3.9
Pt	Pt-198	Pt-199m	12.1
	Pt-198	Pt-199	12.1
	Pt-196	Pt-197m	7.7
	Pt-196	Pt-197	9.2
Au	Au-197	Au-198	11.2

TABLE 7. IMPROVEMENT FACTORS FOR ENAA USING SHORT HALF-LIFE RADIONUCLIDES with f = 20 and α = − 0.02 (Cont.)

Element analysed	Target isotope	Formed isotope	F_a
Hg	Hg-196	Hg-197	0.6
	Hg-196	Hg-197m	0.6
	Hg-204	Hg-205	2.4
	Hg-198	Hg-199m	21.3
Pb	Pb-206	Pb-207m	4.4
Th	Th-232	Th-233	9.6
U	U-238	U-239	21.1
	U-238	Np-239	21.1

5.6 DELAYED NEUTRON COUNTING

Measuring delayed neutrons instead of (or in addition to) gamma or beta radiation can further extend a laboratory's capabilities. Delayed neutron emitting nuclides are only produced by the thermal neutron induced fission of ^{233}U, ^{235}U and ^{239}Pu, the fast neutron induced fission of ^{238}U and ^{232}Th and the fast neutron induced (n,p) reaction of ^{17}O. In the case of oxygen, a single delayed neutron precursor is produced (^{17}N, 4.17 s half-life) while in the case of the U, Th and Pu the measurable delayed neutrons are emitted by a variety of short-life fission products. Systems intended to be used for measurement of oxygen require minimal delay from end of irradiation to commencement of counting, however systems where only fission products are measured can suffice with transfer times of 10 to 20 seconds.

As is the case with NAA combined with beta counting, only total neutrons counts are measured in delayed neutron counting (DNC) systems and no energy discrimination of the detected neutrons can be employed. However, the different sources of delayed neutrons can be separated out by various means. When analysing fission products, delaying the measurement for 20 seconds is generally sufficient to allow most of the interfering ^{17}N (from oxygen) to decay. In irradiation facilities with relatively high levels of fast neutrons, the fission products may be originating from both U and Th. The two can be quantified separately if two irradiations and measurements are conducted, one with a bare target (fission induced by both fast and thermal neutrons) and another using a thermal neutron filter as for ENAA, where only fission by fast neutrons takes place [50]. The ability to mathematically differentiate between U and Pu (not typically required for natural samples but is important when analysing special nuclear materials), which both fission by thermal neutrons, has also been demonstrated [51, 52].

The most common usage of DNC is for the rapid analysis of uranium at a range of levels from ultra-trace to concentrates. Measuring U by DNC has some advantages over the more common gamma measurement of ^{239}U or ^{239}Np. Higher measurement sensitivity is achievable with some facilities able to detect picogram levels of ^{235}U. The half-lives of the emitters are shorter, so overall analysis is faster (typically one minute irradiation followed by one minute of counting is used). More significantly, in conventional NAA gamma measurement sensitivity is highly dependent upon what else is present in the matrix – even moderate levels of other gamma emitters will raise overall count rates and negatively affect detection limits. The 74.7 keV gamma emitted by ^{239}U is also susceptible to interference by lead X rays (produced in the detector shielding), and due to its relatively low energy is also somewhat sensitive to differences in density between sample and standard. The detection of neutrons in a well-designed system, however, will not be affected by even high rates of gamma emission, and so delayed neutron counting is largely impervious to such interferences.

Delayed neutron counting can also be combined with gamma spectrometry, either simultaneously [53] or sequentially. Not only does this enable the measurement of multiple elements but can also be used to independently measure ^{235}U (by DNC) and ^{238}U (by NAA) isotopes in a sample if isotopically certified U standards are used. Care needs to be taken when selecting U standards for delayed neutron counting as some reference material suppliers use depleted rather than natural uranium feedstock, which has less of an effect when measuring ^{238}U, but can significantly skew results obtained by DNC which rely on the fission of ^{235}U.

5.7 SUMMARY

The combination of irradiation, decay and counting time is much more crucial when measuring short half-life radionuclides in NAA and will need to be thought over more carefully than as commonly is done when performing NAA using long-half-life radionuclides. The choice will always need to be a compromise. There is an optimum decay time where potential interferences and background have sufficiently decayed, and the activity of the relevant nuclide is still adequate.

As an example, if in an analysis protocol only Al has to be determined, a measurement can be carried out as soon as possible after irradiation. Usually, a high induced activity of ^{28}Al and its high gamma ray energy result in a high Compton background, thus decreasing the sensitivities for other radionuclides considerably. The ^{28}Al has to decay for 10 to 20 minutes for much better opportunities to measure the radionuclides produced from e.g., V, Ti, Mg, Mn or Dy. The situation is similar to the measurement of medium half-life radionuclides, requiring a decay time of one or more days to reduce the major activity from ^{56}Mn and ^{24}Na as their high energy gamma rays also lead to a high Compton background in the gamma ray spectrum.

The sensitivity in NAA using short half-life radionuclides is usually less than when using the long half-life radionuclides from the same elements, as shown in Table 6, for a specific protocol of irradiation, decay and counting time. At the same time, it needs to be considered that:

— A number of elements can only be determined by using their short half-life radionuclides: Li, Be, B, O, F, Mg, Al, Si, S, Cl, Ar, Ca, Ti, V, Mn, Nb, Rh, I, and Pb;
— A number of elements can be measured by their short half-life radionuclide at equal or even better sensitivity than by their long half-life radionuclide (see Table 6);
— A number of elements can be measured at the ng level (or, for test items of 1 g, at $\mu g.kg^{-1}$ level) by their short half-life radionuclides (see Table 5).

The Compton background caused by high energy photons from ^{28}Al and ^{56}Mn (and to some extent also from ^{24}Na) will, in general, lead to higher detection limits for those elements measured on the basis of radionuclides with gamma rays at such Compton background; possibly for such elements, measurement by their long half-life activation products may result in better detection limits. As such, a complete panoramic analysis using short half-life radionuclides needs to be complemented by medium and long half-life radionuclides.

6. SELECTIVITY

Selectivity is defined in the International Vocabulary of Metrology – Basic and General Concepts and Associated Terms [23] as the property of a measuring system, used with a specified measurement procedure, whereby it provides measured quantity values for one or more measurands such that the values of each measurand is independent of other measurands or other quantities in the phenomenon, body or substance being investigated. According to Eurachem [24], analytical selectivity relates to "the extent to which the method can be used to determine particular analytes in mixtures or matrices without interferences from other components of similar behaviour".

In INAA it is usually assumed that each radioisotope detected is produced by the (n,γ) reaction on a stable isotope of the same element. However, in many irradiation sites, there is a significant component of fast neutrons that may produce the radioisotope of interest by fast neutron induced reactions on heavier elements, through threshold reactions or second order reactions. Fission of ^{235}U by thermal neutrons will also induce an interference when the sample contains amounts of uranium. Corrections will have to be made for spectral interferences, for the background of the detector system and for blanks due to, e.g., contaminants in the irradiation vial or contamination during the sample preparation protocol.

6.1 THRESHOLD INTERFERENCE REACTIONS

The calculation of the mass of an element in NAA is usually based on the main reaction under thermal neutrons $^{n}X(n,\gamma)^{n+1}X$ where X is the element to be determined and ^{n+1}X the measured nuclide. But with epithermal and fast neutrons, the reactions $^{n+1}Y(n,p)^{n+1}X$, and $^{n+4}Y(n,\alpha)^{n+1}X$ can also take place, with Y being another element present in the sample. The consequence of this interference is that the apparent elemental mass of element X is based on the sum of activities of the radionuclide ^{n+1}X, obtained by all three reactions, and that corrections are needed in order to calculate the true mass and the mass of element X.

Fast neutron based interferences are considerably more likely at research reactors if the inner irradiation channels of the reactor are used with a relatively higher component of fast neutrons. Neutron reaction interferences require correction factors. Usually these correction factors are determined experimentally using experimentally determined reaction rates. They can also be calculated for the (n,p) and (n,α) reactions for the most commonly observed radionuclides in INAA (see Section 6.3). The relative size of this interference correction depends upon the mass of the target and interfering isotope, the fast neutron flux and the cross-section of the nuclear reactions involved. The most important nuclear threshold reactions for NAA using short half-life radionuclides are listed in Table 8.

TABLE 8. MOST COMMON THRESHOLD INTERFERENCE REACTIONS

Element analysed	Interfering element	Reaction	$t_{1/2}$	Eγ (keV)
F	Na	^{23}Na(n,α)^{20}F	11.07 s	1633.6
Na	Mg	^{24}Mg(n,p)^{24}Na	14.96 h	1368.6; 2754
	Al	^{27}Al(n,α)^{24}Na	14.96 h	1368.6; 2754
Mg	Al	^{27}Al(n,p)^{27}Mg	9.46 min	843.8; 1014.4
	Si	^{30}Si(n,α)^{27}Mg	9.46 min	843.8; 1014.4
Al	Si	^{28}Si(n,p)^{28}Al	2.25 min	1779.0
	P	^{31}P(n,α)^{28}Al	2.25 min	1779.0
Ti	V	^{51}V(n,p)^{51}Ti	5.76 min	320.1
V	Cr	^{52}Cr(n,p)^{52}V	3.74 min	1434.1
	Mn	^{55}Mn(n,α)^{52}V	3.74 min	1434.1
Mn	Fe	^{56}Fe(n,p)^{56}Mn	2.579 h	846.8; 1810.7; 2113.1
	Co	^{59}Co(n,α)^{56}Mn	2.579 h	846.8; 1810.7; 2113.1
Cu	Zn	^{66}Zn(n,p)^{66}Cu	5.12 min	1039.2
		^{64}Zn(n,p)^{64}Cu	12.7 h	1345.8
Ni	Cu	^{65}Cu(n,p)^{65}Ni	2.52 h	1481.8
	Zn	^{68}Zn(n,α)^{65}Ni	2.52 h	1481.8
Rb	Sr	^{88}Sr(n,p)^{88}Rb	17.77 min	898; 1836

The interference by the threshold reactions depends on the elements of interest and the associated elements from which interfering nuclear reactions may occur. As an example, in metallic alloys, the Mn measurement on the basis of ^{56}Mn may be interfered by the ^{56}Fe(n,p)^{56}Mn reaction. Whereas in F containing materials, the F measurement on the basis of ^{19}F(n,γ)^{20}F may be interfered by the ^{23}Na(n,α)^{20}F reaction.

In biological samples, some of the important threshold reactions are ^{24}Mg(n,p)^{24}Na, ^{27}Al(n,p)^{27}Mg, ^{31}P(n,α)^{28}Al, and ^{28}Si(n,p)^{28}Al for the measurements of Na, Al, and Mg. Similarly, in geological samples the reactions ^{28}Si(n,p)^{28}Al and ^{27}Al (n, p)^{27}Mg are important in view of the measurement of Al and Mg. On the other hand, the availability of a large fast neutron component in the inner channels can be advantageous in the determination of some elements that are difficult to evaluate by the (n,γ) reaction, e.g. for the determination of Si (via the ^{29}Si(n,p)^{29}Al reaction) or of P (via the ^{31}P(n,α)^{28}Al reaction).

6.2 THRESHOLD INTERFERENCE REACTIONS BY THE RELATIVE METHOD

It is often erroneously assumed that the correction for the production of the radionuclides by fast neutron reactions such as for ^{28}Al and ^{27}Mg is 'automatically' covered in the relative method, if reference materials are used as standards. This misconception can be explained by looking at the basic equations used in the relative method. Eq. 1 can be simplified to Eq. 4:

$$N_{p,x} = m_x . \frac{\mathrm{N_{Av}} \theta_x I_{\gamma,x}}{M_x} . R_x . (SDC)_x . \varepsilon . t_c \qquad (4)$$

In the relative method samples and standards are irradiated simultaneously (or under identical conditions, as for short half-lives samples and standards are often irradiated consecutively)

which means that, e.g. for the element K on the basis of ^{42}K, Eq. 4 can be rewritten as Eqs. 5 and 6:

$$N_{p,K,s} = m_{K,s}.\frac{\mathrm{N_{Av}}\theta_K I_\gamma}{M_K}.R_{K,s}.(SDC)_{K,s}.\varepsilon.t_c \quad (5)$$

and

$$N_{p,K,r} = m_{K,r}.\frac{\mathrm{N_{Av}}\theta_K I_\gamma}{M_K}.R_{K,r}.(SDC)_{K,r}.\varepsilon.t_c \quad (6)$$

Where *s* and *r* denote the sample and the reference material, respectively. We obtain the simplified Eq. 7 for the relative method (as reaction rates for sample and standard are equal for simultaneous irradiations):

$$m_{x,s} = m_{x,r}\frac{N_{p,x,s}}{N_{p,x,r}}\frac{(DC)_{x,r}}{(DC)_{x,s}} \quad (7)$$

In case of contributions by fast neutron activation, this leads to an increase in the number of counts of the net peaks area due to the threshold reactions, but in a different amount for the samples and the standards. E.g. for ^{28}Al, apart from the ^{27}Al(n,γ)^{28}Al reaction, there will also be contributions due to the ^{31}P(n,α)^{28}Al and ^{28}Si(n,p)^{28}Al reactions.

As such, $N_{p,\mathrm{s}}$ and $N_{p,r}$ are proportional to contributions from all three nuclear reactions (see also Eq. 4) as in Eq. 8:

$$N_{p,\mathrm{Al}} \propto m_{\mathrm{Al}}.R_{27\mathrm{Al}}.(SDC)_{28\mathrm{Al}} + m_{\mathrm{Si}}R_{28\mathrm{Si}}(SDC)_{28\mathrm{Al}} + m_P.R_{31\mathrm{P}}(SDC)_{28\mathrm{Al}} \quad (8)$$

Saturation decay counting (SDC) factors account for the decay of the induced activity during irradiation, cooling and measurement.

In this case m_{Al} requires knowledge of the contributions from production of ^{28}Al from Si and P in both the sample and reference material. This requires not only information on the masses of Si and P in both the sample and the reference material, but also about the respective reactions rates. The masses of Si and P can be obtained from other analytical techniques, from the certificate of an equivalent reference material, from a first well educated guess or, in case of Si, by measurement of Si using the ^{29}Si(n,p)^{29}Al reaction and co-irradiation of a pure silicon standard.

The reaction rate *R* can be estimated by analysis of standards (pure elements or pure compounds of known stoichiometry) of P, Si, Al, Mg and Na. The peak area of the relevant radionuclide has to be corrected for the absolute gamma ray abundance, the detector's photopeak efficiency, the SDC-factor and the mass of the pure element resulting in the activity of the radionuclide in Bq/g/second irradiation time at the end of the irradiation in the specific irradiation facility. Note that such resulting values have to be re-evaluated once changes have been made in the reactor core assembly.

6.2.1 Worked example

Assume irradiations of a sample of pure SiO_2, a sample of pure Al, a sample of pure MgO and a sample of pure P_2O_5, each under optimal conditions for NAA. In each sample the ^{28}Al and

^{27}Mg activity is counted after irradiation with a spectrometer equipped with a dead-time correction module, and the net peak area of the 1779.0 keV and 843.8 keV peaks is corrected for decay towards t=0 (end of irradiation time) and photopeak efficiency. Thus, it is found, e.g.:

— 660 Bq ^{28}Al/mg Si per second irradiation (^{28}Si(n,p)^{28}Al);
— 3.3 Bq ^{27}Mg/mg Si per second irradiation (^{30}Si(n,α)^{27}Mg);
— 272000 Bq ^{28}Al/mg Al per second irradiation (^{27}Al(n,γ)^{28}Al);
— 109 Bq ^{27}Mg/mg Al per second irradiation (^{27}Al(n,p)^{27}Mg);
— 1290 Bq ^{27}Mg/mg Mg per second irradiation (^{26}Mg(n,γ)^{27}Mg);
— 190 Bq ^{28}Al/mg P per second irradiation (^{31}P(n,α)^{28}Al).

Now insight in the relative reaction rates (ratio of activities for threshold and analytical reactions) is obtained:

— 1 g of Si results in a 1779.0 keV peak area similar as from 660/272000 g = 0.0024 g or 2.4 mg Al;
— 1 g of Si results in a 843.8 keV peak area similar as from 3.3/1290 g = 0.0026 g or 2.6 mg Mg;
— 1 g of Al results in a 843.8 keV peak area similar as from 109/1290 = 0.0845 g or 84.5 mg Mg;
— 1 g of P results in a 1779.0 keV peak area similar as from 190/272000 g = 0.0007 g or 0.7 mg Al.

For the Si-P-Al interference this transfers Eq. 8 into Eq. 9:

$$N_p \propto (m_{Al} + 0.0024\ m_{Si} + 0.0007\ m_P).R_{27Al}(SDC)_{28Al} \quad (9)$$

The ratio of the net peak areas of the corresponding peaks of ^{28}Al in the sample and the standard is given by Eq. 10:

$$N_{p,s}/N_{p,r} = (m_{s,Al} + 0.0024.m_{s,Si} + 0.0007.m_{s,P})/ (m_{r,Al} + 0.0024.m_{r,Si} + 0.0007.m_{r,P}) \quad (10)$$

From which the amount (mass) of Al in the sample is obtained (Eq. 11):

$$m_{s,Al} = \left[\frac{N_{p,s}}{N_{p,r}}\left(m_{r,Al} + 0.0024m_{r,Si} + 0.0007m_{r,P}\right)\right] - \left(0.0024m_{s,Si} + 0.0007m_{s,P}\right) \quad (11)$$

Likewise, this yields for the Si-Al-Mg interference (Eq. 12):

$$m_{s,Mg} = \left[\frac{N_{p,s}}{N_{p,r}}\left(m_{r,Mg} + 0.0026m_{r,Al} + 0.0038m_{r,Si}\right)\right] - \left(0.0026m_{s,Al} + 0.0038m_{s,Si}\right) \quad (12)$$

6.2.2 Analysis of a real sample by the relative method

Assume the certificate of the reference material provides certified mass fractions of 35% for Si, 12% for Al, 3% for Mg and 10% P, and that 200 mg (both reference material and sample) is irradiated. So, the irradiated elemental masses are $m_{r,Al}$ = 0.024 g; $m_{r,Si}$ = 0.070 g; $m_{r,P}$ = 0.020 g; $m_{r,Mg}$ = 0.006 g.

Assume the analysis of the sample results in 15% Si via calibration and measurement using the

^{29}Al peak (1272 keV), by direct comparison of the peak areas (corrected for differences in decay and in counting time); $N_{p,s}/N_{p,r} = 0.9$ for the 1779.0 keV peak, so Al (not interference corrected) = 10.80%; $N_{p,s}/N_{p,r} = 1.5$ for the 843.8 keV peak, so Mg (observed, not interference corrected) = 4.5%.

In addition, the first estimate is 0.1% P on the basis of indications from literature for the type of material analysed.

Then it follows from the above Eqs. 11 and 12:

— True mass Al: 0.0217 g or 10.85% mass fraction;
— True mass Mg: 0.0105 g or 5.25% mass fraction.

Note that:

— The interference corrected values are different and could even be completely different from the values that are obtained without correction — it all depends on the differences in ratios between the interfering elements and the element to be quantified;
— The interference corrected values are higher because the reference material has a higher Si and P content than the real sample;
— Even if the first estimate for P was wrong by one order of magnitude and the true P mass fraction is e.g. 1%. the true mass for Al is not impacted, so there is no need to revise the P value or to go for an independent analysis of P.

6.3 THRESHOLD INTERFERENCE REACTIONS BY THE k_0 METHOD

In the k_0-NAA method knowledge of the fast neutron spectrum averaged cross-section data and fast flux φ_f is needed for the calculations. Correction factors can be calculated by using the experimentally determined thermal, epithermal and fast neutron flux and epithermal neutron flux shape factor and nuclear data from the literature using the Høgdahl convention. Using the Høgdahl convention [30] and notations from k_0 standardization, the net counts $N_{p,x}$ calculated on the basis of a given target isotope for a given gamma ray energy (not taking into account thermal, epithermal neutron self shielding and coincidence correction factors), Eq. 1 can be rewritten as Eq. 13:

$$N_{p,x} = m_x . \frac{N_{Av}\theta_x I_{\gamma,x}}{M_x} . \varphi_{epi.}\sigma_{th,x}\left(f + Q_{0,x(\alpha)}\right).(SDC)_x . \varepsilon . t_c \qquad (13)$$

where $f = j_{th}/j_{epi}$ thermal to epithermal neutron fluence rate ratio, α the deviation of the epithermal neutron fluence rate distribution from the 1/E shape, approximated by a $1/E^{1+\alpha}$ dependence, $Q_{0(\alpha)} = I_{0(\alpha)}/\sigma_{th}$. The counts $N_{p,y}$ in the same gamma ray peak based upon the threshold reaction are given by Eq. 14 [54]:

$$N_{p,y} = m_y . \frac{N_{Av}\theta_y I_{\gamma,y}}{M_y} . \left(\varphi_f \overline{\sigma_y}\right).(SDC)_y . \varepsilon . t_c \qquad (14)$$

where $\overline{\sigma_y}$ is the fast neutron spectrum averaged cross-section and j_f is the fast neutron flux. In a uranium fuelled nuclear reactor, the 0.1–10 MeV fast component of the neutron flux is commonly known as the ^{235}U fission neutron spectrum.

The expression for interference corrections in general can be written in Eq. 15 as:

$$m_x = m_{x+y} - F_{x,y}.m_y \tag{15}$$

Where:

- m_x is the true mass based upon a certain gamma ray line for element x corrected for interference;
- m_{x+y} is the observed mass in the same gamma ray line from the target element x and the interfering element y through threshold interference contribution. For correction, the mass of the interfering element in the sample needs to be known;
- m_y is the mass of the interfering element;
- $F_{x,y}$ is a correction factor expressed as a dimensionless ratio of the apparent mass of x (usually expressed in µg) generated per mass of y (in g). This factor is channel specific and usually experimentally determined through irradiation of a reference standard with mass of the (interfering) element m_{std} and low neglible x content. $F_{x,std} = m_{x(apparent)}/m_{std}$ ($m_{x(apparent)}$ is the apparent mass of x generated through the irradiation of the standard std).

From Eqs. 13, 14 and 15 the correction factor $F_{x,y}$ can be obtained (Eq. 16), expressed as a dimensionless ratio of the apparent mass of x (usually expressed in µg) generated per mass of y (usually expressed in g):

$$F_{x,y} = \frac{m_x}{m_y} = \frac{M_x}{M_y}.\frac{\theta_y}{\theta_x}.\frac{\varphi_f}{\varphi_{th}}.\frac{\overline{\sigma_y}}{\sigma_{0,x}}.\frac{f}{f + Q_{0(\alpha)}} \tag{16}$$

$\frac{\varphi_f}{\varphi_{th}}$ can be determined from e.g. the Al-0.1%Au IRMM 530 monitor using the $^{197}Au(n,\gamma)^{198}Au$ and the $^{27}Al(n,p)^{27}Mg$ reaction) or using an Fe-standard using the $^{58}Fe(n,\gamma)^{59}Fe$ and the $^{54}Fe(n,p)^{54}Mn$ reaction.

Correction factors have been calculated for (n,p) and (n,α) reactions for the most commonly observed short half-life radionuclides used in NAA (see Table 9). Calculations were made with a thermal neutron flux 10^{12} (cm^{-2} s^{-1}), $\frac{\varphi_f}{\varphi_{th}} = 5$, f = 20, and α = − 0.02 which are typical values for a MNSR or SLOWPOKE research reactor (data for most $\overline{\sigma_y}$ from Calamand [55]).

Except for the $^{87}Rb(n,\gamma)^{88}Rb$ reaction, all other (n,γ) reactions have a low Q_0 value which would indicate that, if relevant, two irradiations one bare and one Cd covered would be a perfect indicator to check if the calculated interference corrections can be validated.

For the previous example in the relative method where we assume 15% Si and 0.1% P; we now obtain:

- Observed Al: 10.92% mass fraction - apparent Al due to Si: 0.07% and due to P: 0.0001%;
- True Al: 10.85% mass fraction;
- Observed Mg: 7.18% mass fraction - apparent Mg due to Al: 1.93% and due to Si: 0.002%;
- True Mg: 5.25% mass fraction.

The impact of the correction factors given in Table 9 was calculated for two very different materials, a clay sample and a plant sample, used in the IAEA proficiency test by interlaboratory comparison PTNATIAEA20 [56]. The results are given in Table 10. Calculations were made

with a thermal neutron flux 10^{12} (cm^{-2} s^{-1}), $\frac{\varphi_f}{\varphi_{th}} = 5$, f = 20, and α = − 0.02. The clay sample was composed essentially of Si (20%), Ca (13%), Al (5.5%), K (2%), Fe (2.5%) and Mg (1%) (mainly as oxides). The plant sample was mainly composed of C (48%), Ca (1.5%), K (1.1%), Mg (0.2%) and P (0.2%). It clearly shows that the threshold interference reaction correction for the determination of Mg is critical in the clay sample, whereas in the plant sample it is critical in the Al determination.

6.4 FISSION INTERFERENCES REACTIONS

When a sample contains uranium, fission of ^{235}U will induce a fission-interference reaction. The phenomenon is especially important in the determination of lanthanides in geological materials. Fission interference corrections are mainly relevant in NAA using LHL radionuclides, but the determination of Ba, La and Ce may also be impacted in NAA using SHL radionuclides.

Whereas the correction for the ^{235}U interference can be performed experimentally (by co-irradiating a known standard mass of uranium together with the sample), the equivalent way to correct for fission is through calculation using of published fission correction factors published by Landsberger [57] for the relative method or k_0 fission factors for the k_0-NAA method [58, 59].

TABLE 9. CORRECTION FACTORS FOR SOME RELEVANT (n,p) AND (n,α) REACTIONS

Element analysed	Interfering element	Reaction	$\overline{\sigma_y}$ (mb)	Source	Calculated $F_{x,y}$ (µg/g)
F	Na	$^{23}Na(n,\alpha)^{20}F$	0.67	JENDL	1.09E+04
Na	Mg	$^{24}Mg(n,p)^{24}Na$	1.53	Calamand	4.33E+02
	Al	$^{27}Al(n,\alpha)^{24}Na$	0.69	JENDL	2.22E+02
Mg	Al	$^{27}Al(n,p)^{27}Mg$	4.28	JENDL	1.78E+05
	Si	$^{30}Si(n,\alpha)^{27}Mg$	0.13	JENDL	1.62E+02
Al	Si	^{28}Si (n,p) ^{28}Al	5.92	JENDL	4.47E+03
	P	$^{31}P(n,\alpha)^{28}Al$	1.9	Calamand	1.41E+03
Ti	V	$^{51}V(n,p)^{51}Ti$	0.87	Calamand	1.74E+04
V	Cr	$^{52}Cr(n,p)^{52}V$	1.09	Calamand	3.64E+01
	Mn	$^{55}Mn(n,\alpha)^{52}V$	0.11	Calamand	4.15E+00
Mn	Fe	$^{56}Fe(n,p)^{56}Mn$	1.07	JENDL	1.37E+01
	Co	$^{59}Co(n,\alpha)^{56}Mn$	0.16	Calamand	2.08E+00
Cu	Zn	$^{66}Zn(n,p)^{66}Cu$	0.62	Calamand	5.18E+01
		$^{64}Zn(n,p)^{64}Cu$	31	Calamand	8.49E+02
Ni	Cu	$^{65}Cu(n,p)^{65}Ni$	0.48	Calamand	1.81E+03
	Zn	$^{68}Zn(n,\alpha)^{65}Ni$	0.05	Calamand	1.12E+02
Rb	Sr	$^{88}Sr(n,p)^{88}Rb$	0.15	Calamand	3.51E+02

TABLE 10. ESTIMATED IMPACT OF THRESHOLD CORRECTION FACTORS FOR TWO VERY DIFFERENT MATERIALS USED IN PTNATIAEA20

Element	Interference reaction	Clay sample% correction for apparent mass	Plant sample% correction for apparent mass
Al	^{28}Si (n.p) ^{28}Al	2.3%	(1.6 mg/kg)*
Al	^{31}P (n.α) ^{28}Al	0.0%	(4.5 mg/kg)*
Cu	^{66}Zn (n.p) ^{66}Cu	0.04%	0.05%
Mg	^{27}Al (n.p) ^{27}Mg	50.3%	0.16%
Mg	^{30}Si (n.α) ^{27}Mg	0.5%	0.00%
Mn	^{56}Fe (n.p) ^{56}Mn	0.05%	0.01%
Mn	^{59}Co (n.α) ^{56}Mn	0.00%	0.00%
Ni	^{65}Cu (n.p) ^{65}Ni	0.4%	1.7%
Ni	^{68}Zn (n.α) ^{65}Ni	0.19%	1.1%
Rb	^{88}Sr (n.p) ^{88}Rb	0.07%	0.14%
Ti	^{51}V (n.p) ^{51}Ti	0.04%	0.02%
V	^{52}Cr (n.p) ^{52}V	0.012%	0.02%
V	^{55}Mn (n.α) ^{52}V	0.005%	0.00%
Na	^{24}Mg(n.p) ^{24}Na	0.08%	10.6%
Na	^{27}Al(n.α) ^{24}Na	0.24%	0.05%
Cu	^{64}Zn(n.p) ^{64}Cu	0.6%	0.9%

* For Al only the apparent mass fraction is given.

In the k_0-NAA method the apparent mass fraction of an element in g per g of uranium can be calculated in the Høgdahl convention [30] (Eq. 17):

$$F_{x,\mathrm{U}} = \frac{k_{0,x}^{fiss}}{k_{0,x}} \cdot \frac{f + Q_{0,fiss(\alpha)}}{f + Q_{0,x(\alpha)}} \tag{17}$$

The impact of these correction factors was calculated for two very different materials in SHL radionuclide mode of NAA in the materials from PTNATIAEA20. For the Clay sample the impact on Ba (^{235}U(n,f)^{139}Ba) and La (^{235}U(n,f)^{140}La) for short decays is negligible and for Ce (^{235}U(n,f)^{143}Ce) corrections are in the order of a few % depending on the reactor channel. For the plant sample, no fission interferences need to be calculated as most of the lanthanides were not detectable by NAA.

6.5 SPECTRAL INTERFERENCES

When analysing a specific energy for each radionuclide, the related peak of interest can be spectrally interfered by gamma rays emitted by other radionuclides and can overlap with the peak of interest. In general, spectral interferences are easily solved by analysing another peak of the interfering nuclide. As an example, if the relative amounts of Mn and Mg are causing a multiplet at approximately 843.8 to 846.8 keV and if the peaks are difficult to be resolved due to insufficient energy resolution of the detector, identification and quantification on the basis of other peaks (e.g. 1810.7 keV for ^{56}Mn and 1014.4 keV for ^{27}Mg) could be considered. From known gamma ray emission probabilities γ and the corresponding detection efficiency ε of the gamma-lines, it is possible to subtract them from the peak area of the radionuclide of interest using a correction. If the gamma ray peak of interest is denoted by x, and the interfering one by

y, and if the radionuclide giving rise to gamma ray peak *y* has another gamma ray peak *z* in the spectrum which is free of interferences (or can be corrected for) and neglecting coincidence factors, one obtains the correction for interference from Eq. 18:

$$N_{p,x} = N_{p,x+y} - N_{p,z}.F_{y,z} \text{ with } F_{y,z} = \frac{\gamma_y.\varepsilon_{p,y}}{\gamma_z.\varepsilon_{p,z}} \quad (18)$$

If the monitored and interfering radionuclides differ significantly in terms of half-lives, then cooling and re-measurement of the sample until either nuclide has significantly decayed is probably the easiest solution. As an example, ^{27}Mg can be measured a few minutes after irradiation (and correcting for the ^{56}Mn contribution) and ^{56}Mn can be measured after about 2 hours when the ^{27}Mg has decayed.

However, by using a Ge detector with an energy resolution of about 1.8 keV (at 1332.5 keV) many interferences will be reduced or will even be negligible when using a good peak fitting software. This poses hardly a problem for any of the gamma ray lines mentioned in Table 3 as most codes use peak recognition windows in the order of 0.5 to maximum 0.7 keV. No spectral interferences were noted for short half-life radionuclides in the plant material from PTNATIAEA20. In both materials the gamma ray peaks at 843.8 keV from ^{27}Mg and at 846.8 keV from ^{56}Mn were very well separated in the Ge detector gamma ray spectra.

An overview of most common spectral interferences one could encounter in measuring short half-life radionuclides in NAA is given in Table 11.

TABLE 11. MOST COMMON SPECTRAL INTERFERENCES FOR SHORT HALF-LIFE-NAA

Element	Formed radionuclide	$t_{1/2}$	$E\gamma$ (keV)	Interfering $E\gamma$ (keV)
Mg	Mg-27	9.46 min	843.8	846.8 (Mn-56)
Mg	Mg-27	9.46 min	1014.4	1012.4 (Mo-101)
Si	Al-29	6.56 min	1273.4	1268.0 (Al-28 SE)
Ti	Ti-51	5.76 min	320.1	320.1 (Cr-51)
Mn	Mn-56	2.579 h	846.8	843.8 (Mg-27)
Mo	Mo-101	14.61 min	1012.4	1014.5 (Mg-27)
Rh	Rh-104	42.3 s	555.8	554.3 (Br-82)
In	In-116m1	54.29 min	1293.6	1293.6 (Ar-41)

In the special case of samples containing high levels of uranium, some short-lived fission products may spectrally interfere with nuclides to be measured, not to be confused with the fission interference described in Section 6.4. One example is the short-lived fission product ^{134}I (53 min half-life) which emits a gamma ray of 847.0 keV, close to the 846.8 keV gamma of ^{56}Mn. Similarly, ^{142}Ba (231.6 keV gamma) may interfere with ^{85m}Sr (231.9 keV gamma), ^{138}Cs (1435.8 keV gamma) may interfere with ^{52}V and ^{138}Xe (434.6 keV) may interfere with ^{108}Ag. Common NAA software packages will likely misidentify these fission products as the activation products which share the same energies.

In other cases, it is more advantageous to measure the SHL radionuclides versus the LHL equivalent. This applies to, e.g., Se (^{77m}Se rather than ^{75}Se which is severely interfered for most

of its gamma rays), Sm (^{155}Sm rather than ^{153}Sm at 103.2 keV) and to Zn (^{69m}Zn rather than the 1115.5 keV of ^{65}Zn which could be in the tail of the 1120.5 keV peak of ^{46}Sc).

6.6 IMPACT ON THE MEASUREMENT UNCERTAINTY

Except for the traditional uncertainties in INAA or k_0-NAA [60, 61], special attention has to be paid to uncertainties due to timing effects in measuring short half-life radionuclides. Also, the uncertainty resulting from pulse pile-up effects may be significant as count rates may often be high and, more importantly, count rates change during measurements. This will be elaborated on in Section 9.2.

Using a spectrometer equipped with dead-time correction module based on LFC or ZDT, (see Section 9.3) the standard uncertainty of high count rates can be estimated using the double source approach (e.g. by using a fixed ^{60}Co source and a ^{137}Cs source moved to obtain from very low to very high count rates) and can be estimated by a plot of the residuals versus the value at low count rates for the ^{137}Cs source. The uncertainty estimated from the residual plot is usually in the order of 0.5% up to 60 or even 70% dead time values. For systems not using a dead-time correction module it is recommended to limit the dead time to 30%, but even in this case extra uncertainty contributions will need to be accounted for in the range of 0.5 to 1% for fast decaying radionuclides during the measurement.

Mainly the decay and saturation factors (see Eq. 1) are impacted by inaccuracies in the timing. Accurate knowledge of the time at which the irradiations ends is required for calculating the decay factor. The precise moment of start of the irradiation is also required in k_0-NAA for calculating the saturation factor S. In terms of timing, mainly the saturation and decay factor will be impacted. The counting factor is determined by the spectrum acquisition software in the computer and can be assumed to be accurate to a few ms; as such, its contribution to the combined standard uncertainty will be negligible.

The saturation factor will suffer from insufficient knowledge on the exact irradiation time. A distinct difference between the time given by the irradiation timers (usually through photoelectric sensors) and the true irradiation time in the irradiation rig may occur in many irradiation facilities. This affects the travel time from the sensor to the start of the irradiation in the irradiation position. As for the travel time back from the irradiation position to the sensor, an adjustment factor has to be taken into account: $t_{irr} = t_{app} + t_{adj}$, where t_{app} is the irradiation time reported by the control system and t_{adj} is an adjustment time [62]. In most reactors this t_{adj} is not well known and is in the range of several hundreds of ms to even tens of seconds. In one research reactor with long transport times where one has to rely on irradiation timers at some distance from the irradiation position, t_{adj} was found to be 7.8 s with an uncertainty in the order of 0.3 s [63]. In a fast transfer facility where the exact arrival time of the irradiation vial in the irradiation position can be detected by acoustic sensors, the transport time was estimated to be 200 ms with an uncertainty of 14 ms [63].

Irradiation times are very short when using ultra short half-life radionuclides in NAA, since the saturation level will be reached quickly and long measurements are not relevant as they would lead to a significant increase in the background due to long lived radionuclides.

The decay factor will suffer both from an uncertainty in the precise moment of the end of the irradiation as discussed above and from timing synchronization issues between the operating system for the transfer system and the counting system of the Ge detector as both are normally running on separate electronic circuits with separate timing modules. If both are well

synchronized, a standard uncertainty in the order of ms can be assumed. If not, experience shows that this could run up to several seconds. Several sensors are needed in order to make the appropriate corrections to irradiation and decay time. Both the transportation of the irradiation vial to and from the irradiation position have to be measured. This time depends e.g. on the pressure of the propellant (air, nitrogen, etc.) that is used, but also e.g. on the weight of the (loaded) irradiation container.

A Kragten spreadsheet uncertainty approach [64] was made to assess the impact of these uncertainties on S and D and is presented in Table 12. A first simulation was made assuming a worst case scenario where no adjustment or no synchronization is made and whereby an uncertainty of 5 s is assumed for t_{irr} and for t_d. The impact on radionuclides with half-lives of less than 100 s (ultra short half-life radionuclides) is quite large and in many cases the NAA results might be mainly of interest for screening purposes in which the uncertainty is of less relevance. For other short half-life radionuclides the impact of timing will still be a significant contribution to the combined uncertainty of measurement. The impact is negligible for radionuclides with half-lives of an hour or more.

A second simulation was made where the laboratory adjusts the timing on the basis of a first rough estimation and where the laboratory synchronizes its clocks manually whereby an uncertainty of 1 s is taken for t_{irr} and for t_d. For ultra short half-life radionuclides measurements still have to be made in relative mode, in order to keep the uncertainties reasonable. Absolute NAA can be performed using the short half-life, but an extra uncertainty of a few % has to be taken into account. The impact is negligible for radionuclides with half-lives of an hour or more.

A third simulation was made where adjustments are made accurately and all clocks are synchronized, with an uncertainty of 0.3 s taken for t_{irr} and for t_d. For this set-up, both relative and absolute NAA can be performed starting from half-lives of a few seconds, but an extra uncertainty of a few % has to be taken into account.

The last simulation was made where the uncertainty on t_{irr} and t_d are about 10 ms. For this set-up the contribution of timing on the overall result in negligible (starting at half-lives above 10 s) and the main contribution to the SDC factor is due to the uncertainty on the half-life.

TABLE 12. CALCULATED CONTRIBUTION TO THE UNCERTAINTY OF THE SDC-FACTOR FOR NAA USING SHORT HALF-LIFE RADIONUCLIDES

t_{irr}-unc.	**t_d unc.**	**F-20 ($t_{1/2}$ = 11.07 s) t_{irr} = 10 s, t_d = 1 s**	**Al-28 ($t_{1/2}$ = 2.25 m) t_{irr} = 60 s, t_d = 60 s**	**Mg-27 ($t_{1/2}$ = 9.46 m) t_{irr} = 60 s, t_d = 60 s**	**Mn-56 ($t_{1/2}$ = 2.579 h) t_{irr} = 5 min, t_d = 1 h**
± 5 s	± 5 s	Uncertainty about 50%, both on S and D	Uncertainty about 10%, mainly on S	Uncertainty about 10%, mainly on S	Uncertainty about 2%, mainly on S
± 1 s	± 1 s	Uncertainty about 10%, both on S and D	Uncertainty about 2%, mainly on S	Uncertainty about 2%, mainly on S	Uncertainty about 0.4%, mainly on S
± 0.3 s	± 0.3 s	Uncertainty about 3% , both on S and D	Uncertainty about 0.5%, mainly on S	Uncertainty about 0.5%, mainly on S	Uncertainty about 0.1%, mainly on S
± 10 ms	± 10 ms	Uncertainty about 0.1%, both on S and D	Uncertainty < 0.1% mainly due to uncertainty on the half-life of Al-28	Uncertainty < 0.1% mainly due to uncertainty on the half-life of Mg-27	Uncertainty < 0.1% mainly due to uncertainty on the half-life of Mn-56

The uncertainty of the half-life value itself is usually in the order of 0.1 to 1%. The impact of this uncertainty on the value of the SDC-factor is about 0.05 to 0.5%. For any radionuclide with a half-life of more than an hour, the effect of the uncertainty on the half-life will be the most predominant “timing” effect on the SDC factor.

The quantitative calibration in relative NAA and k_0-NAA is usually based on the assumption that the standard or flux monitor and the sample receive an equal neutron dose. This, however, is not always the case as samples and standards are often irradiated separately in NAA using short half-life radionuclides. Preferably, standard and sample need to be irradiated for exactly the same length of time while the reactor flux is kept constant. If relevant, this factor will also need to be integrated in the uncertainty budget.

6.7 SUMMARY

There are, in general, fewer problems due to spectral interferences in NAA using short half-life radionuclides than in NAA using long half-life radionuclides. As an example, Se and Hg can be measured by their short half-life activation products ^{77m}Se and ^{197m}Hg without interference, in contrast with the spectral problems that arise when measuring their long half-life radionuclides ^{75}Se and ^{203}Hg. Similar considerations apply to the measurement of the elements Sm/Gd/Th/U.

Additionally, fission product interferences are much less dominant with respect to the measurement of the various short half-life radionuclides in many samples. On the other hand, threshold reactions may result in significant interferences for NAA using SHL radionuclides.

7. SAFETY

Nuclear safety needs be understood and effectively applied by all the people involved in NAA activities at research reactors. This includes the experimentalists, users, operation and maintenance staff and other staff from the research reactor operating organization. This Section addresses aspects of safety and radiation protection which are specific to the conduct of NAA using short half-life radionuclides. The objective is to raise the reader's awareness regarding safety aspects when implementing NAA at research reactors using short half-life radionuclides.

It is noted that this overview does not aim to be comprehensive, and a graded approach ought to be applied to the risk evaluation, which also needs to be tailored when accelerators or isotopic neutron sources are used. The IAEA Safety Standards Series No. SSR-3 "Safety of Research Reactors" (2016) [65] establishes requirements for all the areas important to safety for research reactors. The IAEA Safety Standards Series No. SSG-24 "Safety in the Utilization and Modification of Research Reactors" (2012) [66] provides recommendations on meeting the requirements on the safety related aspects of the utilization and modification of research reactors.

7.1 RADIATION DOSE

The sample irradiation time needs to be adjusted according to the expected activity. Samples coming out of the reactor needs to be monitored for their radioactivity in which the beta radiation cannot be neglected [67]. Sample vials often need to be quickly removed from the irradiation container, sometimes (as in protocols for measurements of the ultra short radionuclides) within seconds. It introduces an elevated radiation risk and ample precautions need to be taken for minimization of the radiation dose. Safety analysis prior to operating the pneumatic system needs to be performed and radiation protection needs to be optimized to provide the highest level of safety. A passive whole-body personal dosimeter, an electronic personal dosimeter and an extremity dosimeter are suggested. Staff opening irradiation containers need to be alert to the radiation from ^{41}Ar produced in the air inside the container. Ventilation and dismantling the sample in a fume-hood with sufficient personal protection (e.g. lead glass) is therefore suggested.

Care needs to be taken for not over-irradiating samples. Additionally, in the case of elements which produce short half-life radionuclides, maximum attainable activities will be reached quickly (saturation) while others which produce longer-lived ones will continue to grow, potentially reducing the signal-to-noise ratio in gamma spectra. For example, if measuring fluorine using ^{20}F ($t_{1/2}$ = 11 s), the activation rate becomes significantly lower after approximately 30 seconds of irradiation and the activity practically becomes constant after 60 seconds. Irradiating beyond saturation will only increase the activity of other, potentially the interfering nuclides, such as ^{28}Al and ^{24}Na, ultimately negatively affecting the radiation risk.

7.2 IRRADIATION SAFETY

Chemical effects may always occur during exposure to intense neutron and gamma ray fields. It may result in radiolysis of compounds (e.g. proteins, hydrate water, nitrates. etc.) leading to volatile substances with risk of damage to the sample vial and irradiation containers. The risk of such damages is significantly smaller in short irradiations of seconds to minutes compared to irradiations of several hours. Optimizing a protocol for measuring the short half-life radionuclide of an element rather than its more common long half-life radionuclide may

therefore be considered if the materials being analysed are prone to decompose during irradiation.

7.3 ARGON IMPURITY IN PROPELLANT GAS

Propellants other than air need to be analysed for their argon volume percentage. Certificates by producers cannot always be trusted as they often do not measure the argon volume fraction and provide the purity of the gas as 100% minus those fractions measured, e.g. H_2O or CO_2.

As an example, the fast pneumatic transfer systems for NAA using short half-life radionuclides at the Reactor Institute Delft uses 'high purity' nitrogen gas as propellant. As both systems are inside the reactor's confinement, the exhaust of the systems is connected to the confinement's ventilation, which eventually is released to the environment. During an incident, monitors in the ventilation shaft were suddenly triggered by an excessive amount of ^{41}Ar activity, resulting in a reactor shutdown.

The ^{41}Ar release could be traced to an irradiation in the fast pneumatic system. Since repetitions occurred, it was noticed that the high ^{41}Ar only occurred after the system had not been in use for a while. An air leak was suspected but could not be demonstrated. Eventually, the quality of the nitrogen propellant came into focus. Gas was sampled from the cylinder and used with the fast pneumatic transfer system and from other nitrogen gas cylinders –from the same manufacturer- in use at the Reactor Institute. The samples were sent for analysis by mass spectrometry.

The results did show that the nitrogen gas from the cylinder in use with the fast pneumatic transfer system contained about 800 µg/g argon, whereas there was about 160–180 µg/g argon impurity in the nitrogen gas in the other cylinders. It was estimated that, assuming the transfer tube filled with nitrogen gas from such bottles with argon impurities between 160–800 mg/g, a 3 hours exposure over a tube length of 30 cm (and diameter 1.5 cm) at a thermal neutron flux between 10^{12}–10^{13} $cm^{-2}s^{-1}$, about 0.3–1.7 MBq ^{41}Ar would be produced whereas after 6 hours approximately 0.45-2.2 MBq ^{41}Ar would be inside the tube system. Such amounts would be released as a 'plug flow' upon the first time an irradiation container would be sent for irradiation. Since no alternative propellants were available, a practical solution was found by connecting the exhaust of the systems to an ^{41}Ar decay tank for a sufficient period of decay prior to release to the environment.

Unacceptable effects of ^{41}Ar can also be mitigated by either closing the sample container in an inert atmosphere, although even nitrogen gas from cylinders still may contain argon; or by opening the sample container in a fume hood either for removal of the ^{41}Ar only, or for transferring the irradiated sample to a new, not irradiated capsule prior to counting.

The lesson learned in this case is that manufacturers from 'high purity' gas propellants may not explicitly test for the argon content. It may be valuable to ask for an estimate of the amount of argon based on specific measurement so as to evaluate the risk of ^{41}Ar production and release.

8. IRRADIATION FACILITIES

8.1 INTRODUCTION

The range of opportunities of NAA using short half-life radionuclides depends on how quickly the sample can be measured after completing the irradiation. The period between the end of irradiation and start of measurement depends on the transfer time of the sample from the irradiation position to a position that allows for safe handling (t_{tr}) and the handling time needed to transfer the sample to the counting facility. This period can be further split-up in the time needed to remove the sample container from the irradiation container (t_{unl}) and the time needed to bring the sample into the counting facility (t_{cf}).

The total time $t_d = t_{tr} + t_{unl} + t_{cf}$ needed for these actions is the minimum decay time achievable. It may vary from (much) less than a minute to several minutes. This affects the radionuclides with short half-lives ($t_{1/2}$) that can effectively and meaningfully be measured for NAA. As a first indication, one might consider radionuclides with $t_{1/2} < 0.5\ t_d$ as the ones still suitable, although the remaining induced activity will already have reduced by at least a factor of 4. Thus, if t_{tr} = 10 s, t_{unl} = 15 s and t_{cf} = 10 s (total; decay time t_d = 35 s), this would imply that the NAA opportunities are on the basis of radionuclides with half-lives of 17 s or more.

An example of how the minimum decay time affects the elements to be measured is given in Table 13, complementary to the analysis protocols presented in Table 4.

TABLE 13. EXAMPLE OF ACHIEVABLY MEASURABLE ELEMENTS RELATIVE TO TOTAL DECAY TIME. NUCLIDES SHOWN IN **BOLD** ARE PRODUCTS OF FAST NEUTRON (THRESHOLD) REACTIONS

Minimum t_d (s)	**Potentially measurable elements (and radionuclides)**
300	Ag (^{108}Ag), Al (^{28}Al), Ba (^{139}Ba), Br (^{80}Br), Ca (^{49}Ca), Cd (^{111m}Cd, ^{117}In, Cl (^{38}Cl), Co (^{60m}Co), Cs (^{134m}Cs), Cu (^{64}Cu, ^{66}Cu), Dy (^{165}Dy), Ga (^{70}Ga, ^{72}Ga), Gd (^{159}Gd, ^{161}Gd), Ge (^{75}Ge), K (^{42}K), I (^{128}I), In (^{116m1}In,), Ir (^{194}Ir), Lu (^{176m}Lu), Mg (^{27}Mg), Mn (^{56}Mn), Mo (^{101}Mo, ^{101}Tc), Na (^{24}Na), Nb (^{94m}Nb), Nd (^{149}Nd, ^{151}Nd), Ni (^{65}Ni), Pd (^{109m}Pd, ^{109}Pd, ^{109m}Ag), Re (^{188m}Re), Rh (^{104m}Rh), Rb (^{88}Rb), Ru (^{105}Ru, ^{105}Rh), S (^{37}S), Sb (^{122m}Sb), Si (**^{28}Al**, **^{29}Al**, ^{31}Si), Sm (^{155}Sm), Sn (^{123m}Sn, ^{125m}Sn), Sr (^{85m}Sr), Ti (^{51}Ti), U (^{239}U), V (^{52}V), W (^{187}W), Y (^{90m}Y), Zn (^{69m}Zn, ^{71}Zn)
30	+ Ce (^{139m}Ce), Dy (^{165m}Dy), F (**^{19}O**), Ge (^{75m}Ge, ^{77m}Ge), Hf (^{179m1}Hf), In (^{114}In,^{116}In), Ir (^{192m2}Ir), Pd (^{107m}Pd), Rb (^{86m}Rb), Sb (^{124m1}Sb), Sc (^{46m}Sc), Se (^{77m}Se, ^{83m}Se), Y (**^{89m}Y**)
10	+ F (^{20}F), O (**^{16}N**), Pt (^{199m}Pt), U/Pu/**Th** (Fission Product neutron counting), W (^{183m}W), Yb (^{177m}Yb)
1	+ Cl (^{38m}Cl), Er (^{167m}Er), Ge (**^{73m}Ge**), In (^{116m2}In), Pb (**^{207m}Pb**), Zr (^{90m}Zr)

As was explained in Section 6, multiple radionuclides including ones with long half-lives may be produced from the same element; these are not shown here. In such cases there is often a trade-off such that while utilizing a shorter-lived radionuclide can drastically reduce the turnaround time of analysis, measuring a longer-lived radionuclide can improve counting statistics and/or improve detection limits, at the expense of longer turnaround times. For example, cadmium in sufficient quantities and in an ideal matrix such as plastic may be measurable using the short half-life radionuclides, however this is generally not achievable for trace levels in soil. On the other hand, there are no long-half-life radionuclide alternatives for elements such as fluorine and oxygen. Note that some of these nuclides, even with the correct

equipment, may only be detectable in the most ideal of conditions (pure samples) and not in many commonly analysed samples.

8.2 TRANSFER TIME

The shortest time between end of irradiation and start of measurement can be achieved by activation in a neutron beam and, with leaving the sample still in its irradiation position, a measurement immediately after shutting off the neutron beam ($t_d \sim 0$ s). This allows, in principle, for measurement of radionuclides with half-lives as short as a fraction of a second. Such in-beam NAA (not to be confused with prompt gamma analysis) has been explored [68, 69]. The relatively low thermal neutron flux (10^6–10^9 $cm^{-2}s^{-1}$) of such an in-beam neutron activation facility limits, obviously, the activation rate and thus the sensitivity, whereas also the background radiation due to the induced activity in the construction materials of the facility may be a problem. There have been specific applications reported for such a form of NAA with short half-life radionuclides [70].

In most cases, the irradiation is performed by bringing the sample closest to the core of a nuclear research reactor, or to another neutron source such as the target of a neutron generator, particle accelerator, sub-critical facility or isotopic neutron source to be exposed to the highest optimal neutron flux. Pneumatic transfer systems and sometimes hydraulic transfer systems are used. However, also facilities in which the sample is manually loaded and hoisted allow, in principle, for NAA with short-half-life radionuclides. Hydraulic systems are mainly intended to ensure cooling of the irradiation container and the sending and receiving stations are often in shielded boxes or hot cells. This makes them less suitable, though not impossible, for use in NAA with short half-life radionuclides.

Transfer times t_{tr} in pneumatic systems in research reactor facilities typically vary from a few seconds to tens of seconds depending on the design of their system and distance between the reactor and the sending/receiving station. Receiving irradiated samples from manually loaded facilities takes more time, typically in the order of minutes. Pneumatic irradiation facilities dedicated to NAA using short half-life radionuclides have been developed at several research reactors and 14 MeV neutron generators, and transfer times t_{tr} of less than a second to even as short as 30 ms have been reported [71–74]. Several of these facilities have also made for delayed neutron counting optional [75–80].

Irradiation systems at other neutron sources are often simpler in design, with relatively shorter distances between the irradiation position and the sending/receiving station than reactor based systems and are often easy to modify if this improves the opportunities of NAA using short half-life radionuclides [81–83]. Transfer times can be therefore also much shorter, typically less than 10 seconds. Dual pneumatic tube systems have been used with neutron generators in which the sample and the standard are irradiated via two parallel tubes connected to a device allowing for 1 or 2 directional rotation of both capsules during the irradiation, to compensate for the strong flux gradients near the generator's target. (Figure 3) Each tube system is connected to its own counting station [84, 85].

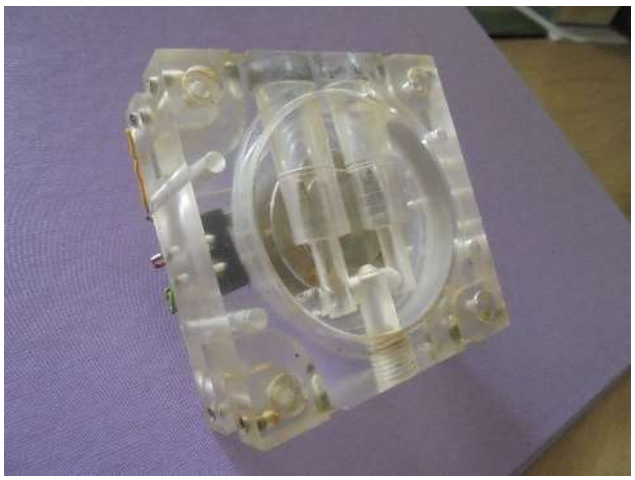

FIG. 3. Example of 1 direction rotation assembly with dual tube system connection, for use with 14 MeV neutron generator (courtesy of P. Bode, TU Delft).

8.3 HANDLING TIME

Pneumatic transfer irradiation facilities, delivered as integral part of the research reactor upon its first commissioning, are usually not designed for NAA on the basis of short half-life radionuclides. The handling time in such facilities depends on:

- The design of the sending/receiving station and the ease of access to the irradiated container. These stations are often surrounded by lead shielding, requiring removal of the container before a count can commence (even if this could be done with the sample container still inside). In some facilities, the irradiated container returns to a shielded glove box. Even the opening of these stations may be time consuming due to radiological safety precautions set by the organizational entity. The design of these stations is therefore the first hindrance towards NAA by radionuclides with half-lives in the range of e.g. a few seconds to 1 minute;
- The need of removing the sample container from the irradiation container. This can be necessary because of:
  - Contamination of the irradiation container resulting from scraped-off activated (and/or corroded) metal particles (Al, Fe, Co, Zn) in bends of the (metal) transfer tubes and in particular in the part of the tubing closest to the reactor core;
  - Induced activity in the construction material of the irradiation container and in the air inside the irradiation container. Opening an irradiated container may have to be performed under the radiological safety regime of the organizational entity, possibly preferably in a fume hood (amongst others because of the radioactive gas, mainly ^{41}Ar, in the container). All such precautions are time consuming and thus limit the measurement of radionuclides with half-lives in the second-minutes range.
- Some laboratories may choose to transfer the irradiated sample itself into a non-irradiated container to eliminate interference from elements inside the sample container. This adds even more handling time and potentially introduces more handling hazards, particularly in the case of granular materials;
- The distances between the sending/receiving station, the unpacking facility and the counting room. The time needed for the related movements can also cause a considerable delay before measurements can be started, unless the three parts are located close to each other inside the same laboratory.

It can be derived from the above that the handling time after the irradiation may sometimes be longer than the transfer time in the irradiation facility and may vary from several tens of seconds to a few minutes. This impacts the radionuclides to be measured. Still, many (conventional) irradiation facilities are suitable for NAA based on measurement of radionuclides with a half-life of at least 1–2 minutes. NAA practitioners have developed dedicated irradiation facilities for measurement of radionuclides with shorter half-lives. Examples of typical design considerations for a self-to-be-made facility for NAA are further elaborated upon below.

8.4 IRRADIATION DURATION

The shorter the half-life of the radionuclide, the higher the requirement on the accuracy of the timing in the NAA procedure. Whereas the live time can be measured with a very high degree of trueness and almost negligible uncertainty, the accurate measurement of the duration of the irradiation, t_{irr} and the decay time t_d is less trivial. Both depend on the accuracy of the moment of arrival of the container in the irradiation position and of its departure. In NAA with short half-life radionuclides, 'every second counts' and, differently from NAA with long half-life radionuclides, uncertainties in the duration of irradiation, decay and measurement may have a significant contribution to the uncertainty in the analysis result.

Accurate measurement of the moment of arrival of the container in the irradiation position is not straightforward. Many existing pneumatic irradiation facilities are equipped with photo sensors, typically at an easily accessible position outside the reactor (or accelerator) radiation zone. In research reactors, this is typically outside the biological shield since the sensors will be damaged by the intense radiation dose in the irradiation position, typically in the order of 100 kGy or more. The moment of arrival in the irradiation position is then estimated on the basis of the 'flight time' once the photocell has detected the passing-by. This flight time might vary from tens of milliseconds (e.g. if the irradiation system is positioned in a radial beam tube) to even a few seconds. Moreover, it cannot be assumed that the flight time is constant as it may depend on the mass of the container and pressure in the system. Confirmatory measurement of the flight time has been demonstrated using self-contained logging accelerometers placed inside irradiation containers [62]. In addition, a light beam reflected in the irradiation position back to an external positioned sensor has been used [86]. At accelerators and isotopic neutron sources, light guides can be used to prevent the sensor being exposed to high radiation levels [71].

The arrival of the container in the irradiation position may provide an acoustic signal that can be detected using a microphone connected to the wall of the metal pneumatic tubing system [63, 73]. Sound travels fast in metal, e.g. in Al or stainless steel at ca. 6000 m/s, so a microphone at a distance of 15 m from the irradiation position can pick up the arrival signal within ca. 2.5 milliseconds.

A small change in the pressure of a pneumatic system upon arrival in the irradiation position may occur if the irradiation container fits tightly inside the transfer tube [73]. Measurement of a pressure shock wave is used in one of the dedicated pneumatic systems for NAA with short half-life radionuclides at the Reactor Institute Delft. A narrow aluminium tube connects the irradiation position with a pressure gauge outside the reactor's biological shield (Figure 4). The timing of the arrival in the irradiation position has been estimated to be as precise as within 0.1 s.

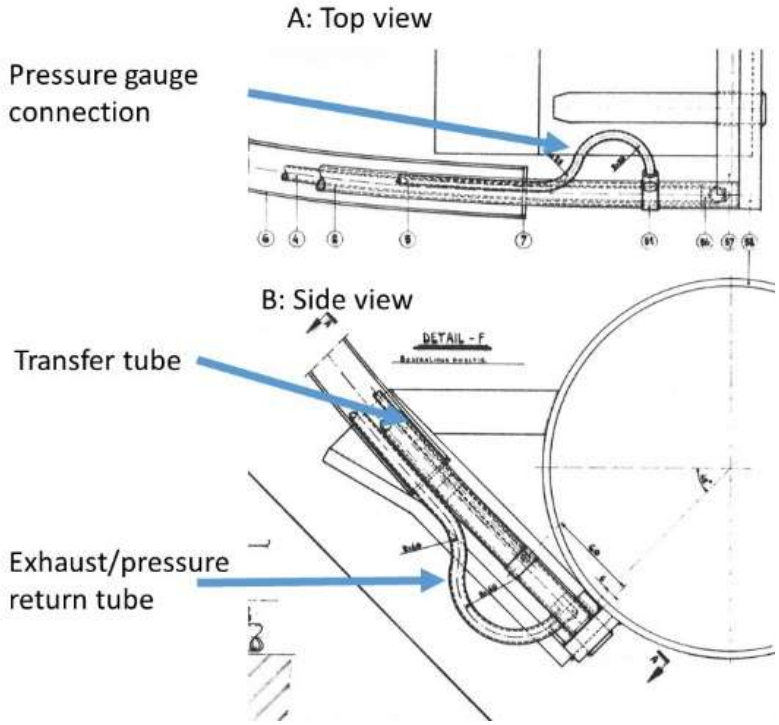

FIG. 4. Irradiation position of fast pneumatic irradiation facility at Reactor Institute Delft, showing transfer tube, pressure exhaust/return tube and tube connecting to the pressure gauge (courtesy of P. Bode, TU Delft).

Co-irradiating a standard or neutron flux monitor is an alternative for estimating the duration of the irradiation.

8.5 CONTAMINATION

The irradiation facilities at research reactors, or at least the part inside the reactor pool or inside a neutron beam tube, are almost always constructed from aluminium alloys or stainless steel. The tubing is often bent, both as part of the shielding against reactor radiation scattered through the tubing and for practical considerations. The irradiation container may scrape off metal particles during its flight and in the irradiation position, resulting in contamination of its exterior with activation products of the metal/alloy tubing such as ^{28}Al, ^{27}Mg, ^{56}Mn, ^{65}Zn and many others. Removal of the sample container prior to counting is therefore necessary.

A carbon–carbon composite material has been used as irradiation end in one of the dedicated pneumatic irradiation facilities for NAA using short half-life radionuclide in Delft, the Netherlands [87, 88]. The irradiation end is inside a radial beam tube (Figures 5 to 7).

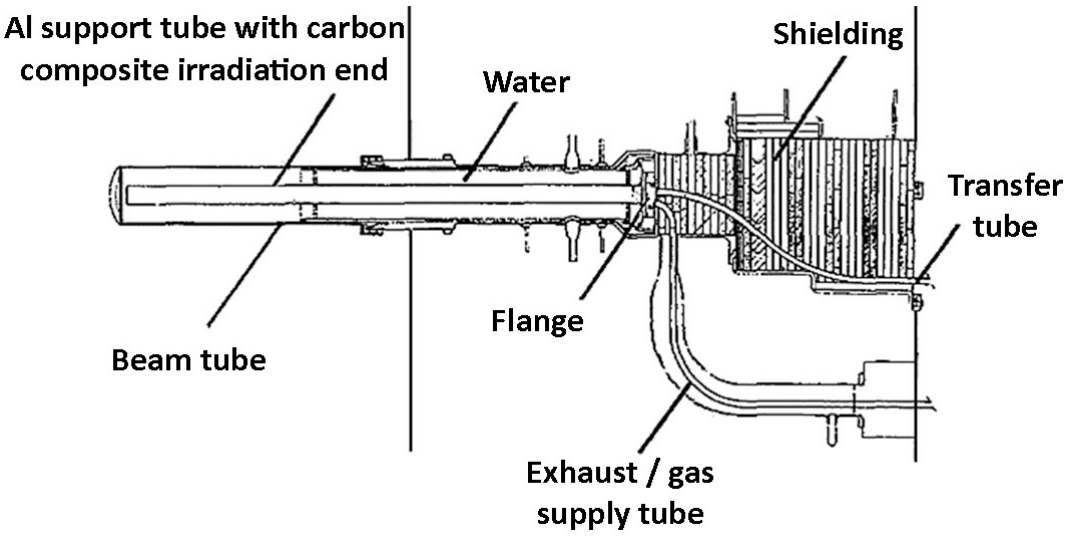

FIG. 5. Examples of S-shaped bending in shielding of radial beam port irradiation system (Reactor Institute Delft) (courtesy of P. Bode, TU Delft).

This facility has no metal parts in the tubing system; the carbon–carbon composite part is connected approximately 2.5 m away to plastic tubing. The bending, required for shielding is in the plastic tubing surrounded by stacked shielding composed of borated polyethylene and alternating, stainless steel and polyethylene. No radioactive contamination of the irradiation container could be detected (see Figure 7). This allows measurement of the activated sample without unloading the irradiation container. It is important to note the difference between carbon fibre and carbon–carbon composite material: Carbon–carbon composite consist of a carbon matrix, densified by carbon vapour deposition. Carbon fibre usually consists of a carbon matrix, densified by resin impregnation, and this organic component is not resistant against reactor radiation.

Automatic separation of sample container from the irradiation container has been reported too [63, 71, 74]. Pneumatic irradiation facilities with other neutron sources (isotopic, accelerator based) do not require metal tubing as, if necessary, the part closest to the source can easily be renewed if radiation damage necessitates.

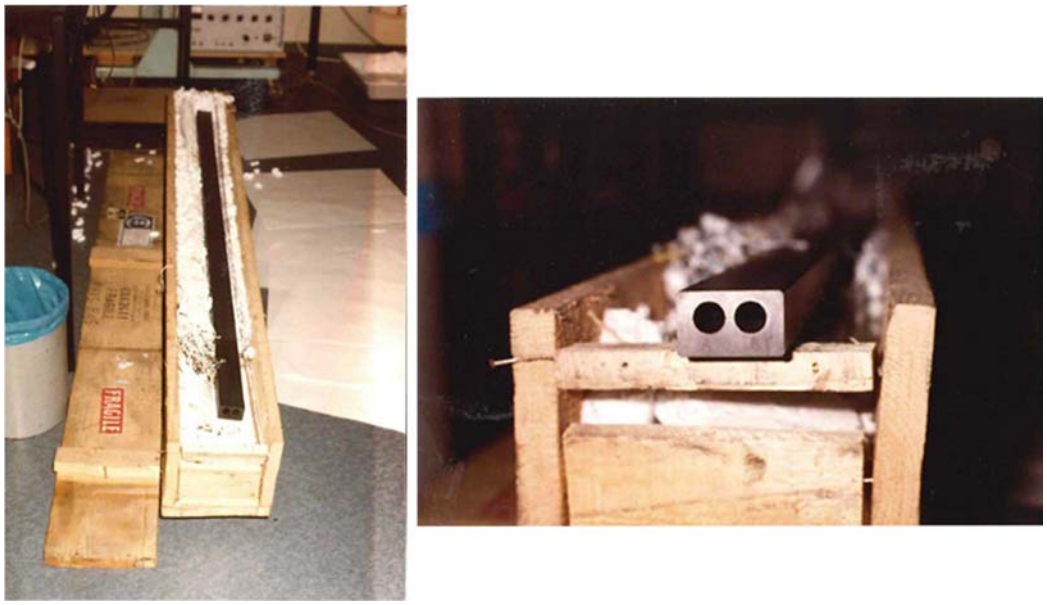

FIG. 6. Carbon–carbon irradiation end prior installation in a radial beam tube at Reactor Institute Delft (courtesy of P. Bode, TU Delft).

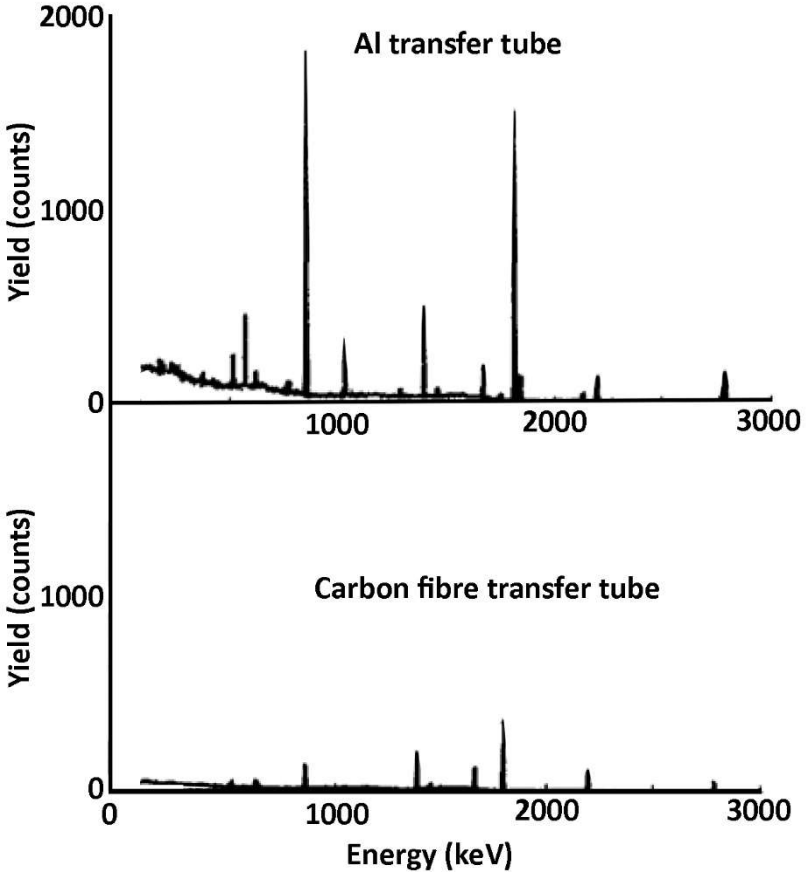

FIG. 7. Gamma-ray spectra of irradiation container in aluminium transfer tube and in carbon–carbon composite irradiation end. Remaining peaks are from impurities in the polyethylene (courtesy of P. Bode, TU Delft).

8.6 IRRADIATION AND SAMPLE CONTAINER

Irradiation containers[1] and sample containers are usually made of plastic for short irradiations in NAA with thermal neutrons, with mostly polyethylene but also polyamide being used [63]. Unlike the metals usually used for long irradiations (often Al), high purity plastics do not significantly activate and so minimize unwanted dose rates to operators, facilitating the rapid post-irradiation handling required for NAA with short half-life radionuclides. As the irradiation dose on the irradiation container is limited, many laboratories permit them to be re-used for multiple irradiations, reducing operating costs. Size and shape of the irradiation container are often specified by the designer/manufacturer of the pneumatic tube system; the NAA laboratory may select the sample container (or other type of encapsulation) suitable for the intended purpose.

Cylindrical containers are most common, sometimes with screw-top lids and also snap-shut types, while rectangular containers have also been used, both in rectangular and in cylindrical transfer tubes [63, 74].

Samples are usually irradiated one at a time for NAA with short half-life radionuclides, and a sample of (one or two) flux monitors or standards may be added. The sample and flux monitor container have to be positioned close to one another and for most applications in NAA the flux

[1] Irradiation containers for pneumatic transfer systems are commonly denoted as ‘rabbits’ in nuclear technology applications, as ‘bunnies’ or ‘carriers’ in other technological or office applications. The term ‘rabbit’ is here avoided as it may lead to unwanted, wrong interpretations.

gradient over two closely packed containers may be acceptable in view of the required accuracy of the analysis. If a very high accuracy is needed, it may also be necessary to sandwich the sample in between flux monitors for precise estimation of the flux gradient. Impurities in the plastic containers vary from brand to brand. The impact of their activation products to the measurement of short half-life radionuclides may be significant, especially if the impurities are of the same elements intended to be measured in the samples. Examples of such impurities in polyethylene are Al, Mn, Ti and/or Zn. Empty containers need to have their impurities measured in order to facilitate blank subtraction of elements which exist in both the sample and the container(s) they're measured in. The frequency at which this is done varies from laboratory to laboratory. Some include blanks with every irradiation batch while others only measure blanks when a new shipment or manufacturing lot is received.

Irradiation containers have also been made of high purity graphite [89]. The low induced activity in the graphite container itself allows for measurement of the sample's activity while still inside the irradiation container. An irradiation container made from graphite is used at the High Flux Reactor of Oak Ridge National Laboratory, USA [90]. This is a small capsule (approximately 3 cm length and 1.5 cm diameter) with a screw cap, in which small sample containers can be inserted. The Heinz Maier-Leibnitz Zentrum uses different irradiation capsules: a polyethylene capsule in their pneumatic irradiation system for SHL and an Al rabbit for the hydraulic capsule irradiation system for LHL [91].

For epithermal activation a neutron absorber is included between the sample and the irradiation container (except where the absorber is integrated into the irradiation facility itself, as described in Section 8.8.4.2), typically cadmium or boron. Cadmium metal is frequently used even though it has some drawbacks, namely that it is a toxic heavy metal which has to be handled carefully and usually becomes more radioactive than the sample itself and as such significantly adds to the radiological hazard. Boron, while not quite as effective as cadmium in terms of neutron filtration, is not toxic to handle and does not emit remnant radioactivity after irradiation. However, during irradiation it becomes a significant heat source, which can lead to melting of the irradiation and/or sample container. Careful safety assessments have to be carried out to ascertain the suitability of either of these neutron filters for purposes of epithermal activation. An alternative is to surround the in-pile irradiation position itself with the neutron absorber.

Metal irradiation containers have been used in 14 MeV NAA for the determination of oxygen using 14 MeV neutrons and measurement of the 6 MeV gammas emitted by ^{16}N with half-life of 7 s. Metals with low traces of oxygen have to be selected. High purity aluminium, copper, molybdenum, nickel or niobium have been used for this [27]. Also, a flow-through sample container has been described in which the propellant nitrogen gas eliminates the presence of exterior oxygen. It has been used for the certification of a standard reference steel for oxygen [92].

8.7 IMPROVEMENT OF EXPERIMENTAL CONDITIONS RELATED TO IRRADIATION AND SAMPLE HANDLING

The transfer time in existing irradiation systems cannot always be shortened, but improvements may be achievable in the time needed for handling the irradiation and sample container after the irradiation.

The sending/receiving station may be repositioned closer to the counting room by extending the existing tubing system; or the gamma ray spectrometer may be positioned very close to the sending-receiving station.

The logistics of handling the irradiation container may be optimized too, such as the ease of opening the station, and/or removal of the irradiation container from the sample container. The receiving station may thus be redesigned that the irradiation container returns in a position near the detector for measurements without unpacking the irradiation container; notwithstanding the constraints mentioned in the above (radioactive contamination, ^{41}Ar background, etc). All such measures might be needed to achieve the capability of NAA using radionuclides with half-lives of less than one minute.

Systems in which the irradiation container does not have to be opened after irradiation facilitate cyclic activation or, if the transfer time is short enough, e.g., 30 s or less, delayed neutron counting. However, if flux monitors are used for estimation of the irradiation duration, it implies that the activity induced in the flux monitor is measured simultaneously with the activity of the sample. The flux monitor has thus to be chosen such that the activity of its radionuclide, and the emitted gamma radiation produced does not interfere with the gamma ray spectrum of the radionuclides produced in the sample. This may vary case by case. A suitable radionuclide to be considered for this purpose might be ^{134m}Cs.

8.8 DESIGN CONSIDERATIONS FOR NEW IRRADIATION FACILITIES

8.8.1 Introduction

Designing a new pneumatic irradiation system starts by solving or optimizing a specification matrix:

- The minimum half-life of the radionuclide to be measured;
- The maximum transfer time from irradiation position to receiving position;
- The access to the neutron source;
- The type of neutrons needed: thermal, thermal plus epithermal plus fast, or selectable;
- The distance from the irradiation position to the nearest location for positioning the counting facility;
- The type of radiation to be measured: gamma rays, delayed neutrons or (high-energy) betas;
- The need for cyclic activation;
- The type and size of the available irradiation container, potential induced activity;
- The need for rotation during irradiation if an accelerator-based neutron source is used;
- Unpacking issues;
- The need for automatic sample changing and/or counting;
- Maximum allowable propellant pressure;
- Type of propellant allowed;
- Temperature inside the irradiation position;
- Maximum acceptable weight;
- Safety issues.

The design will include the sending/receiving station, and its integration with the detector system may be optional.

8.8.2 Tubing

The basic components of a pneumatic transfer system include the tube assembly consisting of the transfer tube and a pressure/exhaust tube. Most irradiation facilities have been designed for

cylindrical samples, but rectangular systems have also been used [63, 74]. The tubing assembly may be entirely separate, e.g. parallel tubes or concentric tubes (see Figure 8).

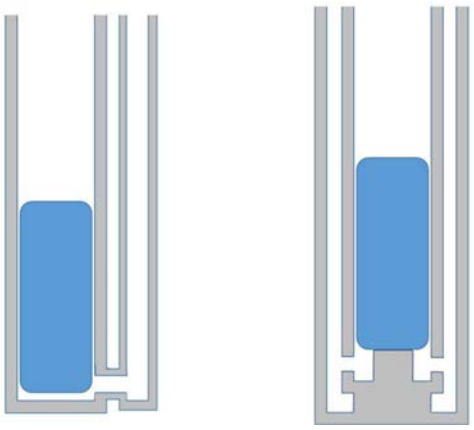

FIG. 8. Examples of irradiation end of pneumatic tube system with irradiation container shown and different tubing assemblies: left, parallel tubing; right: concentric tubing (courtesy of P. Bode, TU Delft).

The tubing system can be made from metal, e.g. aluminium alloy, ceramics or carbon composite (as described in Section 8.5). Plastic tubing can be applied at reactors for the part outside the direct radiation zone and for systems with accelerators or isotopic neutron sources as, differently from reactor systems, the tube can easily be replaced in case of radiation damage. Plastic tubing may have the disadvantage that it is not as cylindrically symmetrical as metal tubing and may become oval with time, which hinders (or even blocks) the passing of the irradiation container. This happens often with soft polyvinyl chloride hoses and polyethylene tubing. The problem can be solved by inserting such a hose into a metal tube, thus forcing it to maintain the cylindrical shape.

The irradiation container needs to fit tightly inside the transfer tubes, both beam port and in-pool pneumatic irradiation systems to attain the highest speed and consequently the shortest transfer time of the container. The tight fitting is, however, also an enhanced risk factor if the container cannot be returned at the end of the irradiation due to e.g. electrical failure, loss of propellant or because of excessive mass. In the worst case, if this malfunction cannot quickly be mitigated, radiation and thermal damage may cause deformation of the container and it may get stuck inside the tube.

Assessment of the thermal and radiation heating in the irradiation position and the maximum weight of the irradiation container by which it can be lifted by the propellant are essential for setting the boundary conditions for use of the facility. In addition, a safety system may be required to be designed. The valves accommodating the return of the irradiation container (propellant pressure and exhaust) have to open once electrical power is switched off. Similarly, an auxiliary pressurized vessel can be automatically emptied sending the irradiation container back once monitors indicate loss of the prime propellant during irradiation.

Attention needs to be paid to the physical location of the tubing in addition to minimising lengths and hence transfer times, as they are ultimately conveying radioactive items tubing and thus ideally are not positioned near to where people are located (ALARA). Furthermore, care needs to be taken to ensure adequate distance or shielding is maintained between detection systems (integrated or otherwise) and conveying tubes. Active samples passing over detectors currently in use measuring other samples will be subject to interference by the passing sample, so tubing needs to be laid out to avoid this situation.

8.8.3 Propellant

Pressurized air, nitrogen gas or CO_2 are used as propellant. Of these, air is not common at reactor-based systems due to the production of ^{41}Ar, but it can be used in systems with accelerators (neutron generators) or at isotopic neutron sources. The production of nitrogen radicals has been reported as a disadvantage of the use of nitrogen gas [63].

Vacuum, or at least under pressure, is used in many pneumatic transfer systems too. The irradiation container is sucked through the transfer tube either way. Ideally, such a system needs to be connected to a pressurized gas tank, filled with nitrogen or CO_2.

8.8.4 Location of irradiation facility

At reactors, pneumatic transfer systems both in-pool and in beam tubes have been developed. A pneumatic tubing system inside a radial-or tangential- beam tube can provide the shortest distance to its receiving station or the counting facility; systems in radial beam ports are most common.

8.8.4.1 In beam tube facilities at research reactors

The drawback of a horizontal irradiation facility in a beam tube are: (i) the neutron flux is often lower than can be achieved with a facility mounted in-pool near the reactor core; (ii) there is a significant longitudinal neutron flux gradient in the irradiation container if the irradiation container is directed perpendicular to the reactor core (see Figure 9 and ref. [88]) and (iii) the pneumatics have to be adjusted to prevent bouncing of the irradiation container. The longitudinal flux gradient can be cancelled by re-irradiating the sample after a 180 degrees end-for-end inversion [93]. Obviously, such systems can only be installed if the reactor core can be moved away from the beam tube.

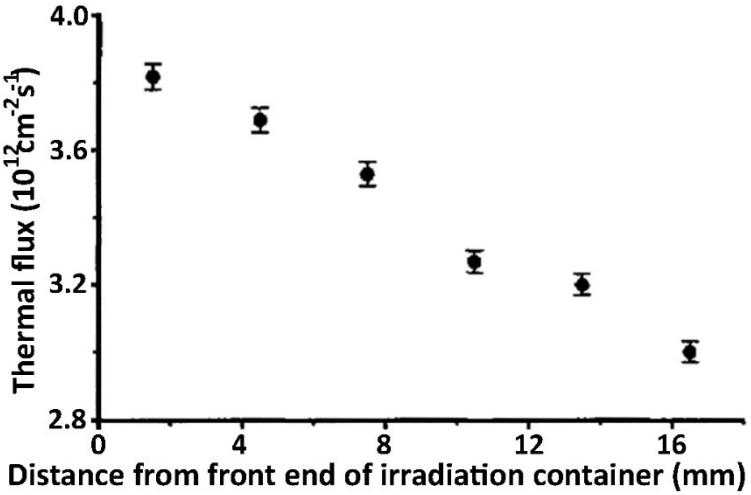

FIG. 9. Thermal neutron flux gradient in irradiation container in radial beam tube, perpendicular view to reactor core (courtesy of P. Bode, TU Delft).

S-shaped bending, needed to reduce the streaming of reactor radiation (both neutrons and gamma rays) outwards through the transfer tube can be made in the part where the metal or carbon irradiation end is connected by plastic tubing. This contributes to minimizing the contamination of the irradiation container by abrasion in the bends during its flight.

A pneumatic system for NAA using short half-life radionuclides in a tangential beam tube had been used in the DR-1 reactor (now decommissioned) in Risø, Denmark [94]. Such a system may be considered if radial beam ports are fully occupied. An advantage of such a facility is that the irradiation container, in its irradiation position, is typically near the centre of the reactor's surface, and neutron flux gradients may be almost negligible. Two options exist for such a facility: the irradiation container enters and leaves the tube at the same side of the tube, similar as in a radial beam tube; or a hole-through facility is used, in which the irradiation container enters the system on one side and leaves on the other side. This requires only one tube for both propellant and exhaust. The challenge, however, lies with designing a controllable stopper at the centre of the transfer tube.

Obviously, there will be safety requirements to pneumatic transfer systems in beam tubes, but they may be easier to accommodate than for systems to be inserted inside reactor pools.

8.8.4.2 In-pool facilities at research reactors

A pneumatic irradiation system to be inserted in the reactor pool may have to satisfy higher safety requirements than a beam tube facility, depending on its configuration, positioning inside the reactor's reflector, and especially if an in-core facility is considered. Special attention may have to be given to leak tightness as propellant gas bubbles may enter the reactor core, especially in reactors with a forced cooling system. S-shaped bends (Figure 10) will be needed in the parts inside the pool, with enhanced risk of contamination of the irradiation container by abrasion of metal parts.

As described in Section 8.5, the use of carbon–carbon composite for the irradiation end of the facility is an option that may be considered; such a part may be connected at sufficient distance from the core to plastic tubing.

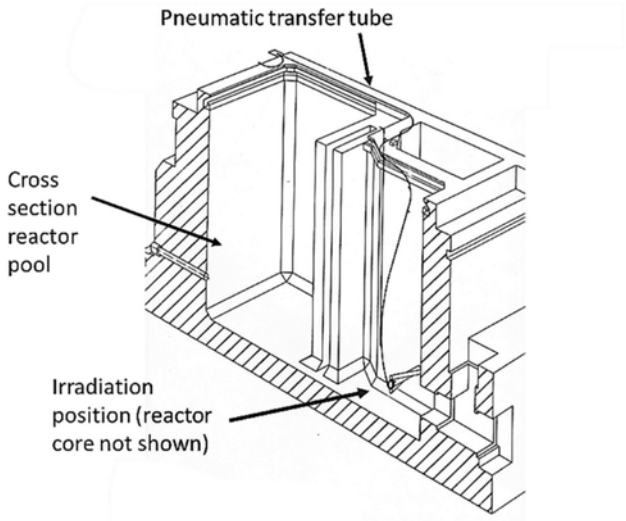

FIG. 10. Example of pneumatic transfer system with S-shaped bend in in-pool part at reactor Institute Delft (courtesy of P. Bode, TU Delft).

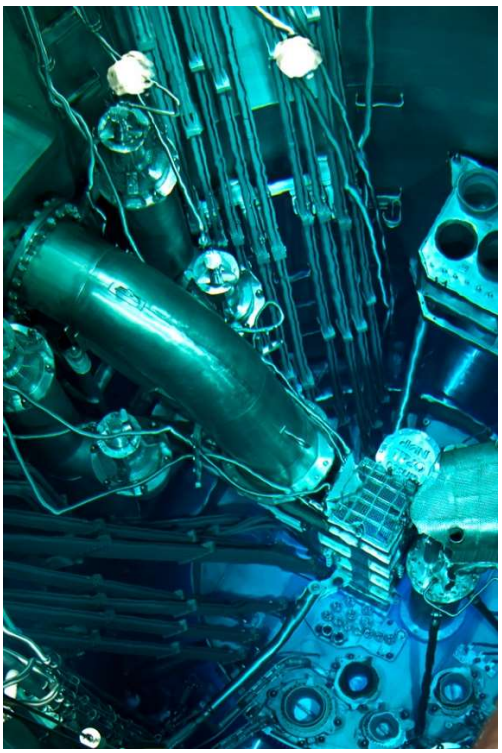

FIG. 11. OPAL-reactor showing the pneumatic tubes going into the reactor (courtesy of A. Stopic, ANSTO).

Neutron flux gradients may be less than in beam tube facilities if the irradiation position is vertical parallel to the fuel elements. The magnitude of the neutron flux also needs to be considered. In higher power research reactors (above 10 MW), the temptation exists to install a dedicated irradiation facility for NAA using short half-life radionuclides in a location where the neutron flux is high, but this is not necessarily desirable as excessive activation of targets and/or gamma ray heating can be a problematic issue. To obtain optimal counting rates at the detector systems, lower neutron fluxes can be compensated for, to a certain degree, by increasing sample sizes and irradiation durations, but in the case of excessively high neutron fluxes, reducing sample sizes and irradiation durations can become problematic and may negatively affect measurement accuracy. Very small sub-samples of granular materials may be inhomogeneous and not representative of the whole sample, while attaining highly accurate and reproducible irradiation durations of the order of seconds is challenging. Ideally, the thermal neutron flux of NAA irradiation facilities does not much exceed 10^{13} $cm^{-2}s^{-1}$. An additional benefit of selecting a lower flux position in a higher power research reactor, generally achieved by increasing the distance between the reactor core and the irradiation position, is a reduction in the relative proportion of fast and epithermal neutrons, reducing, if not eliminating, threshold reaction corrections.

In-pool pneumatic irradiation facilities may be equipped with a fixed or retractable cadmium sleeve around the irradiation position to facilitate epithermal activation without having to include cadmium (or other neutron absorbing material) in the irradiation container itself. Facilities frequently performing epithermal activation would benefit from a well designed system, which is not only more convenient to use but also eliminates the need for operators to frequently handle cadmium, which is not only a toxic heavy metal but adds to the radiation hazard after irradiation. Depending on the flux they are subject to, and on the frequency of reactor operation, such cadmium shields will burn out over time and will need eventual replacement. This is less easy to realize in beam tube facilities since the perpendicular ‘view’ of the irradiation container to the core cannot be fully covered by a retractable sleeve.

In some facilities, the irradiation rig has fixed monitoring equipment for the neutron flux such as self-powered neutron detectors or temperature (thermocouple). While not as accurate as flux monitors, and also slow to respond to flux changes, self-powered neutron detectors can potentially negate the need for flux monitors or standards where the highest level of precision is not necessarily required. Real time temperature monitoring can be integrated into reactor safety systems such that if excessive temperatures are detected, the targets are automatically ejected.

8.8.4.3 Accelerators and isotopic neutron sources

Conventional and radiological safety measures also have to be considered when positioning a pneumatic irradiation system at an accelerator or isotopic neutron sources. As these neutron sources can be switched off or shielded by e.g. shutters, the system can easily be inspected in case of malfunctioning, repair or replacement. As described in the above, plastic tubing is preferred and irradiation ends can be made of plastic tube, eventually equipped with mechanical sensors to detect the arrival of the irradiation container. Single of multiple axis rotators [83, 85, 95, 96] will contribute to the uniformity of the neutron irradiation over the container.

8.9 SENSORS

Pneumatic irradiation facilities have to be equipped with sensors to control its operation, detect not only the arrival of the irradiation container in the irradiation position but also its passing at critical points such as the entry into the reactor pool and along diverters. Photo sensors are most commonly applied. Two sensors positioned within a short distance to each other provide the additional advantage that also the direction of the passing can be monitored, which may be advantageous in systems in which the containers can go either way. For beam tube facilities, the sensor for detection of arrival in the irradiation position can be mounted at the tubing just before it enters the shielding, often not more than 2 to 3 meters from the irradiation position. The wavelength of the light source needs to be carefully selected for the highest contrast in detecting the opaque plastic irradiation container, and near-infrared systems have been applied [63, 96]. This results in a very short delay between the passing of the irradiation container and its actual arrival.

The timing of arrival of the irradiation container in the irradiation position of an in-pool facility may be less accurate than in a beam-port facility due to the longer distance between the photo sensors and the irradiation position. Monitoring the acoustic signal, as explained in Section 8.4, is a good alternative.

8.10 BOUNCING

The high acceleration and speed of the irradiation containers during their flight may introduce problems when they are started and stopped in the irradiation and counting positions. The shock may destroy e.g., samples that have been pelletized to achieve a well-defined geometry during irradiation and counting. Bouncing can be minimized or prevented by smart switching of the pneumatic system e.g., keeping the exhaust valve open once the valve providing the propellant has been switched off or by switching the valves in such a way that an air cushion is realized upon arrival. Ample dry runs of a system to be mounted in a horizontal beam tube need to be performed (in, e.g., a mock-up) before installation, to assess the bouncing of the container upon arrival in the irradiation position and to assess the relation with the container's speed and mass. Bouncing of the irradiation container may also occur in the irradiation end of an in-pool facility

but as these systems are mostly vertical, gravity will ensure that the container eventually ends in its final position.

8.11 DIVERTERS

Pneumatic transfer systems can be equipped outside the radiation zone with diverters to facilitate different destinations for the irradiation container, e.g. either directly to one or more counting systems (either a gamma ray spectrometer or a delayed neutron counter), to an intermediate storage, to an unpacking facility or finally to a waste storage (e.g. at the end of a series of cyclic activation). Examples of systems with one or more diverters [70] are shown in Figure 12, and an example of a diverter is shown in Figure 13 [97].

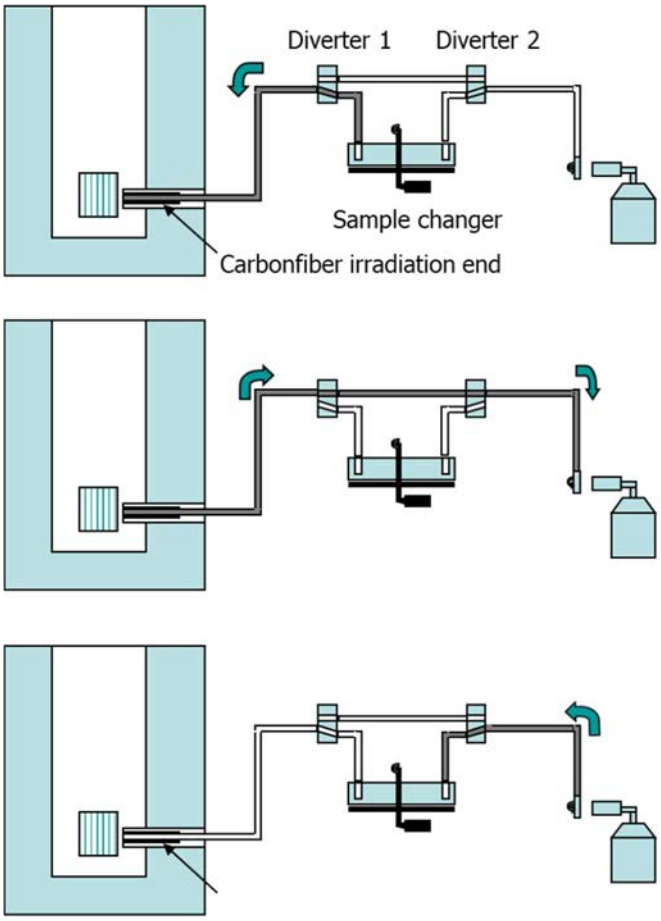

FIG. 12. Pneumatic irradiation system with diverters (at Reactor Institute Delft) (courtesy of P. Bode, TU Delft).

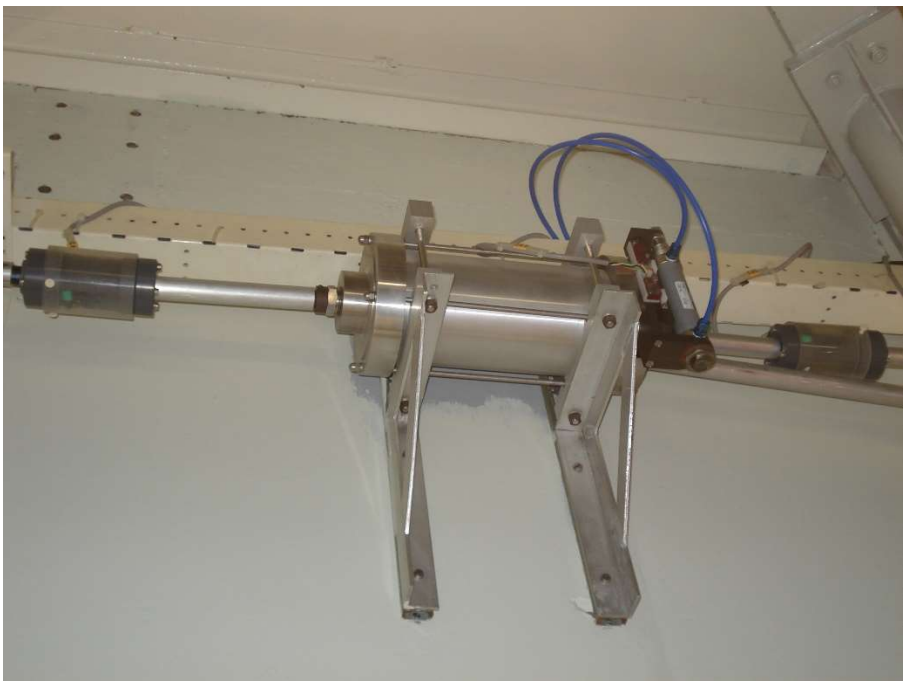

FIG. 13. Example of diverter, pneumatic driven, showing one transfer tube (left connected to two tubes (right) and connections to pneumatic system for moving the diverter. On both sides are also shown the photo-sensors, at Reactor Institute Delft [98] (courtesy of P. Bode, TU Delft).

8.12 SENDING AND RECEIVING STATION

In the most basic systems, often supplied as part of the delivery of a new reactor, a single device serves as both sending and receiving station. More elaborate systems with separate sending and receiving stations (in combination with diverters) are more flexible and facilitate higher order automation. In such cases sending stations often feature multiple-sample loaders. The sending station could be part of a sample changer; the receiving end may be either a simple device from which the irradiation container can be picked up with handling tools, or a device integrated with the radiation detectors. This is a common approach with delayed neutron counting but also with receiving ends may be positioned near e.g. a gamma ray spectrometer if the sample activity can be counted without opening the irradiation container, e.g. for the conduct of cyclic activation analysis (see Section 4). Such a receiving station can be constructed from, e.g. transparent poly(methyl methacrylate), serving as absorber of beta radiation as well, and may, similarly as described in the above for accelerators, allow for continuous rotation of the container during counting.

8.13 FACILITIES WITH AUTOMATIC SEPARATION OF IRRADIATION AND SAMPLE CONTAINER

Automatic separation of sample container and irradiation container upon arrival near the counting station is possible if contamination of the irradiation container cannot be avoided. This has been made with specially designed irradiation containers holding the sample container to be released by centrifugal force in a bend [63, 74]. Also, open end irradiation containers have been used in which the sample container was held by friction. In this case, the irradiation container is sent, by propellant gas, with the closed end forwards to the irradiation position; upon its return, the container is stopped at the receiving end after which the sample container, by its momentum, continues its flight towards the detector [71]. These approaches are not suitable for cyclic activation, require specific machine of irradiation container, and ample testing to assure that the sample container is not unwantedly released during the transfer.

8.14 AUTOMATION OF IRRADIATION FACILITIES

Sending/receiving stations of existing pneumatic irradiation facilities at reactors or other neutron sources can be modified with e.g. stack or disc loaders for consecutive irradiations [80, 98–103]. The irradiated containers then return as a reverse stack in a receiving station for later opening. Such systems are usually designed for unattended irradiations, e.g. outside office hours, because of safety considerations and reducing operator dose, and mainly for inducing radionuclides with relatively long half-lives (see Figures 14 and 15).

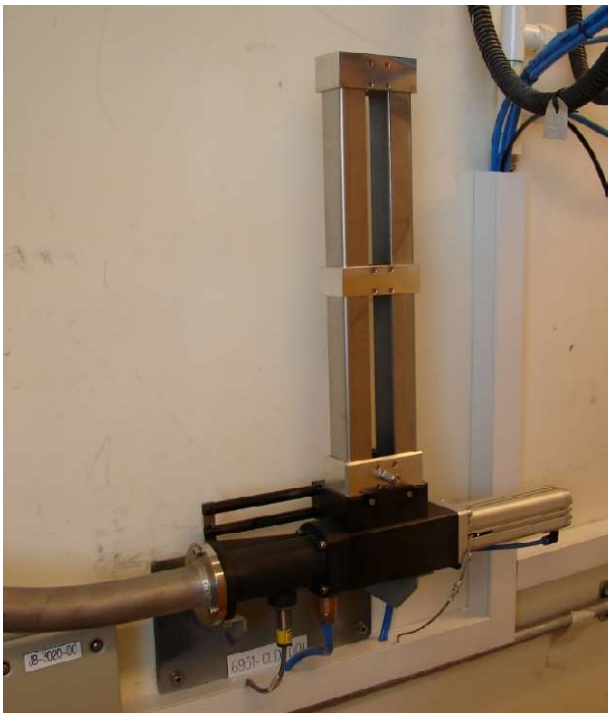

FIG. 14. Example of a vertical stack loader at the OPAL reactor (courtesy of A. Stopic, ANSTO).

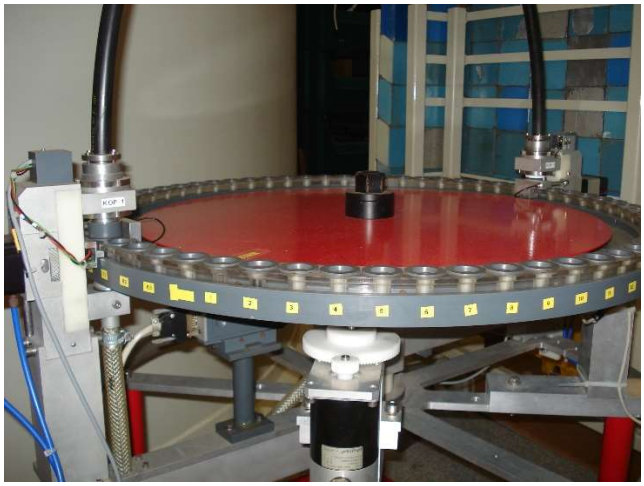

FIG. 15. Example of a rotation disc loader at a fast rabbit system at the Delft research reactor (courtesy of P. Bode, TU Delft).

In principle, this approach can also be applied for NAA using short half-life radionuclides. A diverter in the transfer tube facilitates returning the irradiation container directly to the counting position or to a temporary storage facility for intermediate decay [77, 80, 98, 101, 102]. In such an automated system, the sample is counted still in the irradiation container, under the assumption that contamination of the sample container induced activity in the container

material and presence of ^{41}Ar in the container does not interfere the measurement of the induced activity in the sample.

Automation of existing facilities may also require entire modification or replacement of the pneumatics (valves, switches) and controls (sensors), whereas the transfer system and irradiation containers may still not be optimal for NAA with short half-life radionuclides. It is questionable whether all such efforts outweigh the benefits and if design of a dedicated (automated) system wouldn't be a preferred solution.

8.15 CONTROL OF IRRADIATION FACILITIES

Pneumatic irradiation facilities, with or without diverters and automation, are relatively simple mechanical assemblies requiring opening and closure of valves, stepping motors and registration of signals from sensors. They can be operated with state-of-the-art controllers, such as (currently) programmable logic controllers. Universal software modules are suitable for creating the user interface. In some cases the control systems are a subset of the reactor control system, potentially reducing the number of architectures needing to be supported.

The developments in such controllers and software modules are so fast, that any further description, discussion and evaluation will be rapidly outdated. Synchronization of the controller with the counting system is crucial for USHL and SHL. Examples of controllers of recently developed irradiation systems for NAA with short half-life radionuclides can be found in the literature [63, 80, 100, 103, 104].

9. COUNTING SYSTEMS

Gamma ray detectors and neutron detectors are mostly used for measuring the induced activity of short half-life radionuclides, but detection of (high energy) beta radiation also provides opportunities in NAA using short half-life radionuclides.

9.1 MEASUREMENT OF GAMMA RAYS

Gamma ray spectrometry in NAA is performed both with semiconductor detectors and scintillation detectors, depending on the complexity of the gamma ray spectrum. In principle similar gamma ray spectrometers can be used as in other types of NAA. HPGe semiconductor detectors are most commonly used due to their superior energy resolution. There are a few short half-life radionuclides emitting gamma ray energies above 3 MeV, such as ^{49}Ca (3084.4 keV), ^{37}S (3103.4 keV) and ^{16}N (6130 keV). There may be applications in which measurement of ^{16}N could be of interest; it can be produced by (n,g), (n,a) and (n,p) reactions on N, F and O, respectively. The latter reaction is one of the main applications of NAA with 14 MeV neutron generators, used for measurement of oxygen in metals.

9.1.1 Germanium detector size

There is no straightforward recommendation that can be given for the preferred detector specifications for NAA with short half-life radionuclides. It all depends on the radionuclides to be measured, gamma rays of interest and attainable induced activities. In general, most HPGe detectors have a resolution of less than 2 keV (defined at 1332 keV), which is sufficient to separate the 843.8 keV and 846.8 keV peaks of ^{27}Mg and ^{56}Mn, respectively. However, the higher the efficiency the higher the cost and usually the lower the resolution. As an example, a detector with a low relative efficiency (e.g. 10%) may share this with a very good energy resolution (< 1.7 keV for ^{60}Co 1332.5 keV) which provides an superb resolution of the 843.8-846.8 keV doublet of ^{27}Mg and ^{56}Mn, or the 1267-1272 keV doublet of ^{28}Al (single escape peak) and ^{29}Al. On the other hand, a high efficiency detector (relative efficiency 40-80% or more) may be needed if activation is performed in a low neutron flux, where it also contributes to a better sensitivity for the short half-life radionuclides emitting gamma rays above 1 MeV such as ^{38}Cl, ^{28}Al, ^{52}V, ^{49}Ca or ^{37}S. A high efficiency detector offers more flexibility since higher induced activities can be counted at larger source to detector distance and lower induced activities at a short distance.

The lowest energies mentioned in Table 5 are about 50 to 60 keV (^{192m}Ir, ^{60m}Co and ^{104m}Rh). These can be measured by a typical p-type HPGe detector, provided the efficiency calibration in the low energy range is accurate, and taking into account that there may be interfering X rays. Unlike n-type detectors, p-types have a thick outer dead layer with a typical thickness of several hundreds of microns.

In addition to the summing of gamma rays, other radiation, especially X rays, can be in true coincidence with the gamma rays of interest in NAA. X rays in cascade with gamma rays can originate from electron capture, positron decay, or internal conversion. The summing effects with most of the X rays can be ignored for the p-type Ge detectors because of the thick dead layer. On the contrary, the detectors with a thin entrance window, e.g. n-type detectors and extended range p-type detectors, can experience severe summing of X rays and gamma rays which are to be avoided as much as possible in NAA.

9.1.2 Ge detector cryostat configuration

Similarly, there is no constraint in NAA with short half-life radionuclides that would require a specific cryostat geometry. Counting at horizontal (side-looking) cryostats has the advantage that sample containers can be rotated along their longitudinal axis during counting, and that shielding can be more compact, although this is also achievable with vertical U-type cryostats. The choice of cryostat geometry strongly depends further on the shape and positioning of the counting station.

Well-type Ge detectors are an option if the induced activity is very low, e.g. if the activation is performed in a low neutron flux, such as with isotopic neutron sources or accelerators/neutron generators. The comparator method can be considered to account for the well-known summation effect within these detectors. Otherwise, additional calibration factors can be measured, which is usually not be an extreme effort since the number of short half-life radionuclides measured routinely is rather small.

9.1.3 Scintillation detectors

Semiconductor detectors are the workhorses in NAA, but there may be still quite a few cases in which scintillation detectors may be preferred. Examples are (typically but not exclusive) with NAA using neutron generators or isotopic neutron sources; and/or/if e.g. only one radionuclide has to be measured at a higher detection efficiency, if the experimental set-up complicates the use of semiconductor detectors or for economic reasons.

Scintillation detectors are preferred for measuring the 6 MeV gamma ray of ^{16}N for Oxygen assessment in 14 MeV NAA. For the N-16 measurement, detectors with sizes of 4" or more can be used, and the receiving end of the transfer system can be positioned in between two such detectors facing each other. A 1 cm plastic, e.g. poly(methyl methacrylate), shield can be used to reduce the effect of beta radiation. Large well-type scintillation detectors can be considered. Scintillation detectors are more susceptible to count rate variation than semiconductor detectors, which may result in gain instability. Some detectors nowadays available are equipped with a built-in gain stabilization for an ^{241}Am source which produces not only the 59.5 keV in the spectrum but also a peak due to scintillations caused by the alpha particles at a gamma ray equivalent of 3 MeV. These two peaks can serve as virtual pulsers (dead time correction) and for gain stabilization. The nuisance of gain instability and distortion/broadening of the peaks in the spectrum can also be circumvented in the ^{16}N measurement by an integral count of the events above a threshold energy value e.g. at 4 MeV.

9.2 PULSE PROCESSING

Counting systems for use with short half-life radionuclides, have to operate at very high and rapidly changing counting rates due to the significant decay during the counting time. A prerequisite is that the pulse processing electronics during this period need to operate with a minimum of counting losses. Transistor feedback preamplifiers are preferred for Ge detectors in NAA with short half-life radionuclides as they perform best under high and rapidly varying count rates; besides, these preamplifiers also lead to a better energy resolution at high count rates in comparison to resistor feedback preamplifiers.

Both traditional analogue pulse processing methods can be used: spectroscopy amplifier and analogue to digital converter (ADC) connected to the multichannel analyser or associated software emulation thereof. Wilkinson-type ADCs are usually preferred because they have

much better linearity than successive approximation ADCs. In conventional pulse height analysis, dead time corrections are in place by increasing in a fixed way the true data acquisition time as it occurs in the live-time mode. In NAA using short half-life radionuclides this compensation is usually insufficient.

The spectroscopy amplifier needs to have an active pile-up rejector because of the often high count rates when measuring short half-life radionuclides.

A digital (signal processing) spectrometer (DSP) is the alternative approach. These systems replace the entire analogue chain up to the multichannel pulse height analyser; the DSP unit communicates with the multichannel analyser emulation software. The fast algorithms used in the digital pulse processing provides a higher throughput without significant resolution degradation if count rates increase, and a higher energy stability than in analogue signal processing. DSPs are also equipped with a pile-up rejection and dead time correction (see next paragraph). Some systems can be used not only for pulse height analysis but also for multi-channel scaling which could be of interest for the earlier mentioned approach of ^{8}Li measurement by Cerenkov counting (see Section 9.6).

Both analogue systems and digital spectrometers are available with inputs and outputs for sample changer control and synchronization.

As the developments in DSP are fast and new modules with more features are launched regularly, a further description of these electronics may be quickly outdated, and details on current capabilities can be sought with the manufacturers of these systems.

Scintillation detectors are also available with integrated high voltage supply, preamplifier and digital pulse processor/multichannel analyser directly connected to the photomultiplier base. However, scintillation detectors of which the preamplifier output signal can be connected to a separated DSP, similar as in use for Ge spectrometry, may be preferred for NAA using short half-life radionuclide applications because of dead time correction option (see below).

9.3 DEAD TIME VARIATION AND CORRECTION

Counting systems for use with short half-life radionuclides have to operate at very high and rapidly changing counting rates due to the significant decay during the counting time. A prerequisite is that the multichannel analyser during this period needs to operate with a minimum of counting losses. In conventional pulse height analysis, dead time corrections are placed by increasing the true data acquisition time as it occurs in the live-time mode in a fixed way. This compensation is usually insufficient for NAA using short half-life radionuclides.

The dead time variation during counting can be corrected for by calculus and by hardware. The calculus is a first approximation that can be used if the dead time variation is caused by only one decaying radionuclide in the sample. The ratio of the correct number of counts and the measured number of counts is calculated using Eq. 19 [105]:

$$\frac{c_{\text{correct}}}{c_{\text{measured}}} = \frac{e^{\lambda(CT-LT)} - 1}{\lambda(CT - LT)} \tag{19}$$

in which c_{correct} is the count rate corrected for the variable dead time c_{measured} is the count rate as measured during the clock time CT; LT is the live time; and l is the decay constant of the short half-life radionuclide.

A different approach is needed if the dead time variation is caused by more than one decaying radionuclide. Dead time stabilizers have been developed [16–18, 106] in which the dead time was kept at the high level at the start of the measurement, thus reducing the detector efficiency. Another solution was found by moving the sample to the detector as a function of its changing activity [107]. The breakthrough came by the pioneering work of G. Westphal et al. on LFC and the virtual pulse generator [108, 109] who perfected the original work on the differential dead time correction by J. Harms [15].

Loss free counting modules have been implemented in several NAA laboratories for accurate measurements of short half-life radionuclides. In this mode, the multichannel analyser employs a virtual pulse generator whereby real-time corrections of system counting losses are made, taking into account both dead time and pile-up losses each time within millisecond periods of time. As such, the pulses lost because of the finite resolving time of the system are added in real time to the acquired data in the same way they were initially lost. These corrections are then added to the channels addressed by the ADC in real-time. This method has been shown to be operate at counting rates up to several hundred thousand counts per seconds. Nowadays, suppliers of electronics for gamma ray spectrometry offer digital DSPs with a dead-time correction module standard build-in. The term ‘Zero Dead Time (ZDT) counting’ was introduced by a supplier since the estimate of the instantaneous dead time was different than in Westphal’s LFC method [110].

It is important to bear in mind that counting statistics are disturbed by an artificial increase of the number of counts in the channels when in LFC mode [111]. In this dual channel LFC mode, both an artificial “corrected” spectrum is collected in one memory group that will be used for the mass fraction calculations and the “uncorrected” spectrum is collected in another memory group that will be used for calculation of the counting statistics (as this holds the true counts). There is ample experimental evidence that this correction of the variable dead time is sufficiently accurate for NAA [110, 112, 113] up to initial dead times of 60% with an extra standard uncertainty of only 1–2%. Dead time correction modules are indispensable for accurate NAA using short half-life radionuclides.

9.4 COMPTON SUPPRESSION SYSTEMS FOR NAA USING SHORT HALF-LIFE RADIONUCLIDES

Compton suppression systems have been used for improving the detection limits in NAA using short half-life radionuclides [114–116]. The systems are less suitable for measuring radionuclides with half-lives in the order of (several) seconds given the time needed for positioning the sample in such a system, although sample transfer systems can be incorporated into the design with some compromise on performance [115]. There are no specific constraints for measuring short half-life radionuclides with Compton suppression systems other than those for the normal use of such systems. The count rate needs to be kept low (e.g. dead time < 10%) to achieve the highest suppression factor, but still an ADC with LFC or ZDT correction will be needed as explained in Section 9.3.

.

9.5 SHIELDING

Common (graded) lead shields can be used for gamma ray detectors in NAA using short half-life radionuclides. However, if the spectrometer is located within the reactor containment building, the ambient air may contain ^{41}Ar. Conventional lead shields will not help to reduce this as the main problem is by the ^{41}Ar in the air directly surrounding the detector's endcap. The reduction of its contribution to the background radiation can best be achieved by continuous flushing of the cavity in the shield with fresh air or inert gas such as nitrogen. In addition, the detector's endcap may be surrounded by e.g. 10 cm of low-Z material (to minimize an increase of the backscatter peak in the spectrum) such as polystyrene or polyurethane. Also, the main space in the cavity can be filled with this, thereby leaving for the sample container to be counted only a small volume in front of the detector's window to be flushed. An example of such a design is shown in Figure 16.

The gamma-radiation background inside reactor confinements/containments may also include the gamma rays of various activation products in reactor components, components of neutron beam instruments and stowed radioactive materials like handling tools. Typically, one can expect the presence of the gamma rays of ^{60}Co, ^{65}Zn, ^{124}Sb; in some cases even the high energy gamma rays of ^{16}N formed in the pool water can be measured.

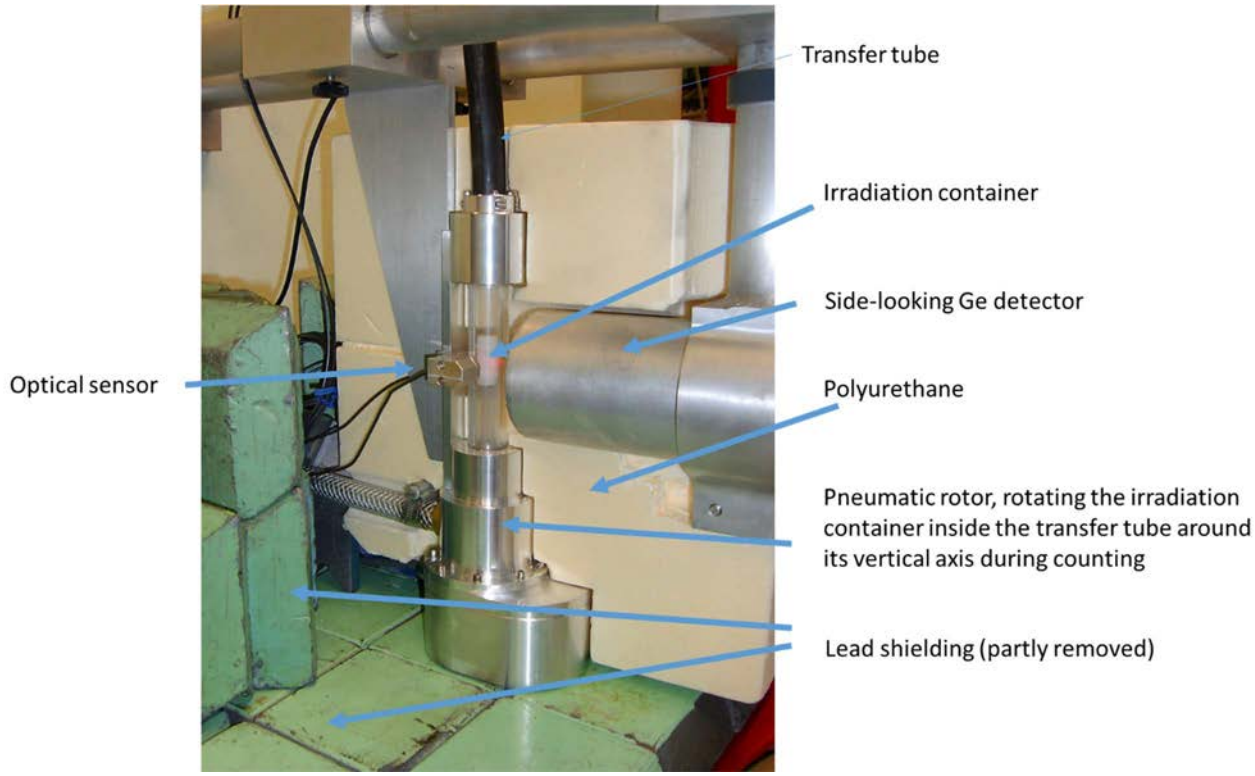

FIG. 16. Inside of shielding cavity at counting station of automatic fast irradiation system at Reactor Institute Delft, showing the low-Z-material filling the cavity in the shielding for Ar-41 background reduction (courtesy of P. Bode, TU Delft).

9.6 RECEIVING STATIONS SERVING AS BETA DETECTOR

High energy beta radiation can be measured with a Cerenkov counter which consists of a radiator optically coupled to a suitable photomultiplier tube. The receiving station of the pneumatic transfer system can serve as radiator; a poly(methyl methacrylate) block will suffice. Multiple photomultipliers can be surrounded by such a block thus mimicking a well-type detector. The entire assembly needs to be light tight. Such Cerenkov counting has been applied

for measurement of lithium by the 0.84 s ^{8}Li which decays under emission of 13 MeV beta radiation [94, 117–119]. The counts are collected in the multichannel scaling mode during the few seconds decay of the radionuclide. The qualitative analysis, verification that the counts are indeed from ^{8}Li, is made by evaluating the decay constant from the channel contents, whereas the integral counts over the measurement duration (e.g., 10 s) provides the basis for the quantitation. It cannot be excluded that, eventually, silicon photomultiplier devices can be used too for this purpose, which would allow for a compact detection system.

9.7 MEASUREMENT OF DELAYED NEUTRONS

To enable delayed neutron counting, a dedicated neutron counting array has to be integrated with the sample transfer system. Detection is achieved using multiple gas-filled neutron proportional counters arranged around the sample. Typically, ^{3}He or BF_3 filled detector tubes are used. Higher efficiencies can be achieved using ^{3}He compared to BF_3 of similar specifications, but BF_3 detectors rely on a higher energy pulse which is better able to discriminate against interference from gamma rays. Because of this, systems using ^{3}He usually include a lead (or other heavy material) shield between the sample and detectors to attenuate the gammas. Sensitivity of such detectors to neutrons increases with decreasing neutron energy. As delayed neutrons are emitted with keV to MeV energies, the detectors are surrounded by neutron moderating material, commonly paraffin or polyethylene, to maximise detection efficiency. Often a layer of cadmium surrounds the array for both radiological protection and to eliminate background neutron counts. Lead shielding also needs to be included to minimise radiological dose to personnel from the samples, which emit far higher gamma radiation than neutron.

The number of detectors used vary depending on the sensitivity required by the user. For example, facilities only interested in measuring U in ores and concentrates with gram-sized samples may find five detectors sufficient. On the other hand, facilities wanting to measure very low levels of fissionable material from small samples such as filter smears would employ many more detector tubes, possibly arranged in more than one circle around the sample.

The outputs of the multiple detectors are generally connected in parallel to the amplifier(s) and single channel analyser, the window of the latter set to pass the characteristic peak produced by neutron interaction with the converter used in the detector (0.765 MeV for ^{3}He, 2.31 MeV for ^{10}B). The single channel analyser output is then connected to a counter. Multichannel scalers are useful for more detailed analysis of the neutron counts over time, such as if attempting to differentiate the source of the delayed neutrons (e.g. O, U, Pu). Some facilities using a large number of detectors use multiple amplifiers, single channel analysers and even high voltage power supplies, combining the outputs of the single channel analysers into a single counter rather than combining all of the (pre-conditioned) detector outputs.

9.8 DETECTOR DAMAGE BY DELAYED NEUTRONS

Irradiating uranium results not only in the well-measurable 74.7 keV of ^{239}U (half-life 23.45 min) and its daughter ^{239}Np, but also in short half-life fission products, some of which emit delayed neutrons. The latter is the basis of delayed neutron counting. However, if samples with significant uranium mass fractions have to be analysed routinely, one needs to anticipate potential neutron damage of the Ge detector by the short half-life uranium fission products. Since the longest half-life of neutron emitting fission products is in the order of 1 min (^{87}Br), a decay of 5-10 min will be sufficient to minimize the risk of radiation damage. As an alternative, a ^{6}Li container absorber could be placed between sample and detector, and an n-type HPGe

detector is to be preferred over a p-type detector, as it is more resistant to neutron damage. All such measures need to be weighed against the risk, which also depends on the number of such analyses that have to be performed.

Nonetheless, and even if sufficient decay time is applied, the gamma ray spectrum of samples containing uranium may be difficult to interpret due to the gamma ray lines of short half-life fission products that are not always completely covered by gamma ray catalogues, nor within the Table of Isotopes [120] or the Nuclear Data Tables [121].

10. CONCLUSIONS

NAA using such short half-life radionuclides can be a valuable extension of NAA using medium and long half-life radionuclides because:

— Additional elements can be measured since their neutron activation products only have short half-lives;
— Several radionuclides with short half-lives can be measured with less spectral interference than the radionuclides with longer half-lives, produced by activation of the same element;
— Some elements can be quantified with a better sensitivity by measuring their short half-life activation products rather than the longer half-life ones.

An analysis with short half-life radionuclides requires a very short irradiation time (often in the order of seconds to a minutes), an equally short waiting time prior to a measurement during typically seconds to minutes of the induced activity. This facilitates completing the entire analysis by NAA within one working day (or even less), from sample receipt to reporting. Several tens of samples can thus be processed, depending on the elements to be measured and the related protocols. Automation of the entire facility might even increase such a throughput. It may provide a competitive opportunity for NAA laboratories for its own research projects, participation in projects of others and services to stakeholders. A summary of the conclusions in this document is given in Table 14.

TABLE 14: REFERENCE GUIDE OF ANALYTICAL ASPECTS OF NAA USING SHORT HALF-LIFE RADIONUCLIDES

Singleness	Al, Ar, B, Be, Cl, F, I, Li, Mg, Nb, O, Pb, Rh, S, Ti and V are elements that can only be measured with NAA by short half-life radionuclides. Mn and Si can be determined in combination SHL/MHL, but not in LHL
Speed	Except for Fe, Tb and Tm there are many elements that can be determined by short half-life radionuclides. These elements that can be reported within one working day, but often at the cost of a somewhat lower sensitivity.
Sensitivity	There are a number of elements where measurement of the short half-life radionuclide has good theoretical sensitivity in the 1 to 100 ng level e.g. Na, Al, Ar, Sc, V, Mn, Co, Cu, Ga, As, Se, Br, Sr, Mo, Ru, Rh, Pd, Ag, In, Sb, I, Cs, La, Nd, Sm, Eu, Gd, Dy, Ho, Er, Yb, Lu, Hf, W, Re, Ir, Au and U. This is however a theoretical factor and the sample specific Compton background due to high energy photons from short half-life ^{28}Al, ^{24}Na and/or ^{56}Mn will be decisive if the associated detection limit is acceptable.
Selectivity	Short half-life radionuclides can, in general, be measured with less spectral interference than their longer half-life radionuclides produced from activation of the same element (such as Se, Sm). The same is true for fission interference. Radionuclide production by threshold reactions causes more interferences in measuring short half-life radionuclides than with long half-life radionuclides.
Working range	High induced activities resulting in high count rates and dead time issues could limit the upper part of the working range.
Background	In principle, SHL NAA is less dependent on the detector background as higher count rates generally apply.

TABLE 14: REFERENCE GUIDE OF ANALYTICAL ASPECTS OF NAA USING SHORT HALF-LIFE RADIONUCLIDES (Cont.)

Uncertainty	The neutron dose of samples and standards may be different if they are irradiated separately. This affects the accuracy of the analysis. Obviously, the irradiation duration needs to be the same and the neutron flux needs to be kept constant. Contributions of uncertainty due to this effect, but also uncertainties in timing and the relatively higher Compton background contribute to a (slightly) higher combined uncertainty of measurement than in LHL NAA.
Hardware: timing issues	A fast transfer system for transporting samples between the irradiation and the counting facilities is needed. A pneumatic transfer system is commonly used. Irradiation times can be kept very short since the saturation level will be reached quickly. Transfer time, irradiation time and decay time have to be precisely timed (e.g. using sensors) and need to be reproducible. Transfer times may vary from several 100 milliseconds to seconds with a reproducibility up to one to several %. This time needs to be as short as possible, preferably not exceeding the half-life of the radionuclide of interest. Automation with minimum need for user intervention during measurement contribute to optimizing throughput capacity and reducing radiation dose to workers is needed. The automation facility needs to allow for measuring both short half-life and long half-life activation products. In SHL NAA optimisation in terms of the irradiation/decay/counting protocol is much more essential than in LHL NAA, especially if the short half-life radionuclide of interest has to be measured in the presence of interfering short half-life radionuclide. Depending on this protocol the design/capacity of the irradiation container this could lead to a higher analysis cost than for LHL NAA.
Sample size	High count rates can be avoided by using samples smaller in size than in LHL NAA.
Safety	Short irradiations imply higher radiological safety risks if the irradiation container needs to be opened before counting. The risk of radiolysis of e.g. organic compounds, decomposition and pressure built-up is much smaller than in NAA on the basis of long half-life radionuclides due to the short irradiation and much lower radiation dose from the neutron source.

REFERENCES

[1] CHAI Z., et al., Vocabulary of radioanalytical methods (IUPAC Recommendations 2020), Pure and Applied Chemistry **93** (2021) 69–111, https://doi.org/10.1515/pac-2019-0302

[2] ALBERT, P., CARON, M., CHAUDRON G., Analyse des traces de sodium, de cuivre et de terres rares dans l'aluminium de haute pureté par la méthode d'activation à la pile, Compt. Rend. **233** (1951) 1108–1109.

[3] ALBERT, P., CARON, M., CHAUDRON G., Analyse des impuretés métalliques dans le fer de haute pureté par la méthode d'activation à la pile., Compt. Rend. **236** (1953) 1030–1031.

[4] MEINKE, W.W., Review of fundamental developments in analysis: Nucleonics, Anal. Chem. **28** (1956) 736–756, https://doi.org/10.1021/ac60112a025

[5] BROOKSBANK JR. W.A., LEDDICOTTE, G.W., REYNOLDS, S.A., Determination of Trace Elements in Titanium by Neutron Activation Analysis, Anal. Chem. **28** (1956) 1033–1035, https://doi.org/10.1021/ac60114a031

[6] ATCHINSON, G.J., BEAMER W.H., Neutron activation analysis with the van de Graaff accelerator; Application to the Halogens, Anal. Chem. **28** (1956) 237–243, https://doi.org/10.1021/ac60110a028

[7] LEVEQUE, P., GOENVEE, H., Determination of elements by induced radioactivity of short life, Bull. Soc. Chim. France (1955) 1213–1216.

[8] TURNER, S.E., Fast neutron activation analysis: silicon and aluminium, Anal. Chem. **28** (1956) 1457–1459, https://doi.org/10.1021/ac60117a031

[9] AMIEL, S., PEISACH, M., Oxygen 18 determination by counting delayed neutrons of nitrogen-17, Anal. Chem. **35** (1963) 323–327, https://doi.org/10.1021/ac60196a016

[10] AMIEL, S., WELWART, Y., Lithium and lithium-6 analysis by counting delayed neutrons, Anal. Chem. **35** (1963) 566–570, https://doi.org/10.1021/ac60197a008

[11] AMIEL, S., Analytical applications of delayed neutron emission in fissionable elements. Anal. Chem. **34** (1962) 1683–1692, https://doi.org/10.1021/ac60193a010

[12] GIVENS, W.W., MILLS, W.R., CALDWELL, R.L., Cyclic Activation Analysis, Nucl. Instr. Meth. **80** (1970) 95–103, https://doi.org/10.1016/0029-554X(70)90302-2

[13] EGAN, A., KERR, S.A., MINSKI, M.J., Determination of selenium in biological materials using Se-77m (T=17.5 sec) and cyclic activation analysis, Radiochem. Radioanal. Lett. **28** (1977) 369–378.

[14] JAMIESON, J.M., EICHHOLZ, G.G., Analysis of Fissile Material by Cyclic Activation of Delayed Neutrons, Trans. Am. Nucl. Soc. **23** (1976) 96, https://doi.org/10.13182/NT78-A17011

[15] HARMS, J., Automatic dead time correction for multichannel pulse height analyzers at variable counting rates, Nucl. Instr. Meth. **53** (1967) 192–196, https://doi.org/10.1016/0029-554X(67)91356-0

[16] GÖRNER, W., HÖHNEL G., An automatic lifetime correction in multichannel counting of short half-life nuclides, Nucl. Instr. Meth. **88** (1970) 193–195, https://doi.org/10.1016/0029-554X(70)90494-5

[17] BARTOSEK, J., ADAMS, F., HOSTE, J., A dead time correction system for gamma ray spectrometers of short half-life isotopes, Nucl. Instr. Meth. **103** (1972) 45–47, https://doi.org/10.1016/0029-554X(72)90456-9

[18] DE BRUIN, M., THEN, S.S., BODE, P., KORTHOVEN, P.J.M., A simple dead time stabilizer for gamma ray spectrometers, Nucl. Instr. Meth. **121** (1974) 611–613, https://doi.org/10.1016/0029-554X(74)90222-5

[19] WESTPHAL, G.P., Loss-free counting, A concept for real-time compensation of dead time and pile-up losses in nuclear pulse spectroscopy, Nucl. Instr. Meth. **146** (1977) 605–606, https://doi.org/10.1016/0029-554X(77)90220-8
[20] INTERNATIONAL ATOMIC ENERGY AGENCY, Applications of Short Half-Life Activation Products in Neutron Activation Analysis of Bio-Environmental Specimens, IAEA/RL/141, IAEA, Vienna, Austria (1987).
[21] INTERNATIONAL ATOMIC ENERGY AGENCY, Live Chart of Nuclides nuclear structure and decay data https://www-nds.iaea.org/relnsd/vcharthtml/VChartHTML.html
[22] INTERNATIONAL ATOMIC ENERGY AGENCY, Practical Aspects of Operating a Neutron Activation Analysis Laboratory, IAEA-TECDOC-564, Vienna, Austria (1990).
[23] INTERNATIONAL BUREAU OF WEIGHTS AND MEASURES, International Vocabulary of Metrology – Basic and General Concepts and Associated Terms (VIM), JCGM 200:2012 (2012), www.bipm.org.
[24] EURACHEM, The Fitness for Purpose of Analytical Methods: A Laboratory Guide to Method Validation and Related Topics, MAGNUSSON, N., ÖRNEMARK, U. (eds), 2nd edn, (2014), www.eurachem.org
[25] GREENBERG, R.R., BODE,P., DE NADAI FERNANDES, E.A., Neutron activation analysis: a primary method of measurement, Spectrochim. Acta B **66** (2011) 193–241, https://doi.org/10.1016/j.sab.2010.12.011
[26] NARGOLWALLA, S.S., NIEWODNICZANSKI, J., SUDDUETH, J.E., Experimental sensitivities for 3 MeV neutron activation analysis, J. Radioanal. Chem. **5** (1970) 403–423, https://doi.org/10.1007/BF02513858
[27] NARGOLWALLA, S. S., PRZYBYLOWICZ, E. P., Activation with Neutron generators, Wiley, New York (1973).
[28] PEPELNIK, R., Sensitivities of high-flux 14 MeV neutron activation analysis, Nucl. Instr. Meth. Phys. B **40–41** (1989) 1205–1207, https://doi.org/10.1016/0168-583X(89)90619-8
[29] DIPRETE, D.P., DIPRETE, C.C., SIGG, R.A., Neutron activation analysis applications at the Savannah River Site using an isotopic neutron source, J. Radioanal. Nucl. Chem. **277** (2008) 43–47, https://doi.org/10.1007/s10967-008-0707-6
[30] HØGDAHL, O.T., Neutron Absorption in Pile Neutron Activation Analysis, MMPP-226-1 University of Michigan (1962).
[31] ROTH, S., GRASS, F., DE CORTE, F., MOENS, L., BUCHTELA, K., Determination of k_0- and Q_0-factors of short-lived nuclides, J. Radioanal. Nucl. Chem. **169** (1993) 159–175, https://doi.org/10.1007/BF02046791
[32] VAN LIERDE, S., DE CORTE, F., BOSSUS, D., VAN SLUIJS, R., POMME, S. Determination of k_0 and related nuclear data for short-lived radionuclides to be used in KAYZERO-NAA at DSM research, Nucl. Instrum. Methods Phys. Res. A **422**(1999) 874–879, https://doi.org/10.1016/S0168-9002(98)01033-X
[33] SZENTMIKLÓSI, L., RÉVAY, ZS., BELGYA, T., Measurement of partial gamma-ray production cross-sections and k_0-factors for radionuclides with chopped-beam PGAA—Part II, Nucl. Instrum. Methods Phys. Res. A **622** (2010) 468-472, https://doi.org/10.1016/j.nima.2009.12.077
[34] ARBOCCÒ, F., et al., Experimental determination of k0, Q0 factors, effective resonance energies and neutron cross-sections for 37 isotopes of interest in NAA, J. Radioanal. Nucl. Chem. **302** (2014) 655–672, https://doi.org/10.1007/s10967-014-3281-0
[35] K0-INTERNATIONAL SCIENTIFIC COMMITTEE NUCLEAR DATA SUB-COMMITTEE, k_0 database, https://www.kayzero.com/k0naa/k0naaorg/Nuclear_Data_SC/Nuclear_Data_SC.html

[36] DE CORTE, F., SIMONITS, A., Recommended nuclear data for use in the k0 standardization of neutron activation analysis, Atomic Data and Nuclear Data Tables, **85** (2003) 47-67, https://doi.org/10.1016/S0092-640X(03)00036-6
[37] SPYROU, N.M., Cyclic Activation Analysis, A Review, J. Radioanal. Chem. **61** (1981) 211–242, https://doi.org/10.1007/BF02517411
[38] SPYROU, N.M., ADESANMI, C., KIDD, M., Usefulness of Thermal and Epithermal Cyclic Activation Analysis with Reactor System, J. Radioanal. Chem. **72** (1982) 155–182, https://doi.org/10.1007/BF02516782
[39] DESILVA K.N., CHATT A., A Method to Improve Precision and Detection Limits for Measuring Trace Elements Through Short half-life Nuclides, J. Trace Microprobe Technol. **1** (1982–1983) 307–337.
[40] CHATT A., et al., Cyclic Neutron Activation Analysis of Biological and Metallurgical Samples, Can. J. Chem. **59** (1981) 1660–1664, https://doi.org/10.1139/v81-246
[41] HOU, X., "Cyclic activation analysis", Encyclopaedia of analytical chemistry. Applications, theory and instrumentation, MEYERS, R. A. (Ed), Wiley, (2000) 12447–12459.
[42] NONIE, S.E., RADNLE, K., The multielement potential of fast neutron cyclic activation analysis, J. Radioanal. Nucl. Chem. Articles **185** (1994) 35–44, https://doi.org/10.1007/BF02042950
[43] CHATTOPADHYAY A., DESILVA K.N, Pseudo-Cyclic Neutron Activation analysis of Ag, F, Rb, Sc and Se in Biological Samples, Trans. Am. Nucl. Soc. **32** (1979) 185–186.
[44] BRUNE, D., JIRLOW, J., Optimization in Activation Analysis by Means of Epithermal Neutrons. Determination of Molybdenum in Steel, Nukleonik **6** (1964) 242–244.
[45] STEINNES E., "Epithermal Neutron Activation Analysis of Geological Material", Activation Analysis in Geochemistry and Cosmochemistry 113, BRUNFELT, A. O. STEINNES, E. (Eds), Universitetsforlaget, Oslo (1971).
[46] SPYROU, N.M., KERR, S., Cyclic activation: The measurement of short half-life isotopes in the analysis of biological and environmental samples, J. Radioanal. Nucl. Chem. **48** (1979) 169–183, https://doi.org/10.1007/BF02519783
[47] PARRY S.J., Epithermal Neutron Activation Analysis of Short half-life Nuclides in Geological Material, J. Radioanal. Chem. **72** (1982) 195–207, https://doi.org/10.1007/BF02516784
[48] LANDSBERGER, S., BIEGALSKI, S. R., O'KELLY, B. J., BASUNIA, M. S., Use of coincident and non-coincident gamma rays in Compton suppression neutron activation analysis, J. Radioanal. Nucl. Chem. **263** (2005) 817–821, https://doi.org/10.1007/s10967-005-0664-2
[49] ZHANG W., CHATT A., Epithermal instrumental neutron activation analysis in conjunction with anti-coincidence gamma ray spectrometry for investigating iodine levels in Canadian foods, J Radioanal. Nucl. Chem. **296** (2013) 495-501, https://doi.org/10.1007/s10967-012-2064-8
[50] AMIEL, S, Analytical applications of delayed neutron emission in fissionable elements, Anal. Chem. **34** (1962) 1683–1692, https://doi.org/10.1021/ac60193a010
[51] GLASGOW, D., Delayed neutron activation analysis for safeguards, J. Radioanal. Nucl. Chem. **276** (2008) 207–211, https://doi.org/10.1007/s10967-007-0434-4
[52] XIAO, C., et al., Application of delayed neutron counting at CIAE, J. Radioanal. Nucl. Chem. **312** (2017) 711–715, https://doi.org/10.1007/s10967-017-5215-0
[53] ANDREWS, M.T., CORCORAN, E.C., GOORLEY, J.T., KELLY, D.G., A system for the measurement of delayed neutrons and gammas from special nuclear materials, J. Radioanal. Nucl. Chem. **303** (2015) 2431–2437, https://doi.org/10.1007/s10967-014-3786-6

[54] WASIM, M., Interferences in instrumental neutron activation analysis by threshold reactions and uranium fission for miniature neutron source reactor, Radiochim. Acta **101** (2013) 601–606, https://doi.org/10.1524/ract.2013.2064
[55] CALAMAND, A., "Cross-sections for fission neutron spectrum induced reactions", Handbook of Neutron Activation Cross-Sections, IAEA Technical Report Series No. 156, IAEA, Vienna, (1974) 273–310.
[56] INTERNATIONAL ATOMIC ENERGY AGENCY, Worldwide open proficiency test for nuclear and related analytical technique laboratories, PTNATIAEA 20, IAEA, Vienna (2022).
[57] LANDSBERGER. S., Spectral interferences from uranium fission in neutron activation analysis, Chemical Geology **57** (1986) 415–421, https://doi.org/10.1016/0009-2541(86)90061-6
[58] DE CORTE, F., VAN LIERDE, S., Determination and evaluation of fission k0-factors for correction of the 235U(n,f) interference in k_0-NAA, J. Radioanal. Nucl. Chem. **248** (2001) 97–101, https://doi.org/10.1023/A:1010634326208
[59] ARBOCCÒ, F., et al., Experimental k_0 and k_0-fission factors for the determination of the $n(^{235}U)/n(^{238}U)$ enrichment levels and correction for ^{235}U fission interferences in samples containing uranium, J. Radioanal. Nucl. Chem. **302** (2014) 721–735, https://doi.org/10.1007/s10967-014-3275-y
[60] INTERNATIONAL ATOMIC ENERGY AGENCY, Quantifying Uncertainty in Nuclear Analytical Measurements, IAEA-TECDOC-1401, IAEA, Vienna (2004).
[61] ROBOUCH, P., ARANA, G., EGUSKIZA, M., POMMÉ, S., ETXEBARRIA, N., Uncertainty Budget for k_0 NAA, J. Radioanal. Nucl. Chem. **245** (2000) 195–197, https://doi.org/10.1023/A:1006703431541
[62] STOPIC, A., BENNETT, J., Irradiation pneumatic system fine-tuning using accelerometers, J Radioanal Nucl Chem **309** (2016) 145–148, https://doi.org/10.1007/s10967-015-4685-1
[63] LI, X., HENKELMANN, R., BAUMGÄRTNER, F., An automated fast transfer system at the research reactor Munich, Nucl. Instrum. Methods Phys. Res. A **522** (2004) 470–476, https://doi.org/10.1016/j.nima.2003.12.011
[64] KRAGTEN, J., Tutorial review. Calculating standard deviations and confidence intervals with a universally applicable spreadsheet technique, Analyst **119** (1994) 2161–2165, https://doi.org/10.1039/AN9941902161
[65] INTERNATIONAL ATOMIC ENERGY AGENCY, Safety of Research Reactors, IAEA Safety Standards Series No. SSR-3, IAEA, Vienna (2016).
[66] INTERNATIONAL ATOMIC ENERGY AGENCY, Safety in the Utilization and Modification of Research Reactors, IAEA Safety Standards Series No. SSG-24, IAEA, Vienna (2012).
[67] BELANDI, T.J., LANDSBERGER, S., Beta Exposure in a neutron activation analysis laboratory, J. Radioanal. Nucl. Chem. **269** (2006) 297–302, https://doi.org/10.1007/s10967-006-0382-4
[68] RÉVAY, Z., KUDĚJOVÁ, P., KLESZCZ, K., SÖLLRADL, S., GENREITH, C., In-beam activation analysis facility at MLZ, Garching, Nucl. Instrum. Methods Phys. Res. A **799** (2015) 114–123, https://doi.org/10.1016/j.nima.2015.07.063
[69] TURKOGLU, D., CHEN-MAYER, H., Chopped Cold Neutron Beam Activation, Analysis IEEE transact. Nucl. Sci. **68** (2021) 1505–1510, https://doi.org/10.1109/TNS.2021.3080682
[70] JIN, X. et al., Application of In-beam Activation Analysis in Elemental Distribution Analysis, IOP Conf. Ser.: Mater. Sci. Eng. **563** (2019) 022050, https://doi.org/10.1088/1757-899X/563/2/022050

[71] GAWLIK, D., GATSCHKE, W., BEHNE, D., BRÄTTER, P., The NAA system at the reactor BER II clinical analysis of fluorine, calcium, phosphorus and aluminium in bone biopsies, comparison with photon activation analysis and ion sensitive electrode, J. Radioanal. Chem. **61** (1981) 313–322, https://doi.org/10.1007/BF02517417
[72] SALAHI, A., GRASS, F., A rapid transportation facility for irradiation with thermal and fast neutrons, J. Radioanal. Chem. **61** (1981) 63–68, https://doi.org/10.1007/BF02517398
[73] HEYDORN, K., WESTERMANN, J., Fast transportation system evaluation at the Danish Mach 1 irradiation facility, J. Radioanal. Chem. **61** (1981) 69–79, https://doi.org/10.1007/BF02517399
[74] FANGER, H-U., PEPENIK, R., MICHAELIS, W., Fast-neutron activation analysis with short-lived nuclides, J. Radioanal. Chem. **61** (1981) 147–163, https://doi.org/10.1007/BF02517405
[75] SCHLECHTE, P., Fast sensitive analysis of uranium and thorium in natural samples based on delayed neutron counting using an ultrafast conveyor tube system, J. Radioanal. Chem. **61** (1981) 55–61, https://doi.org/10.1007/BF02517397
[76] PAPADOPOULOS, N. N., An inexpensive automatic uranium and short-lived radioisotope analyser, J. Radioanal. Chem. **61** (1981) 81–91, https://doi.org/10.1007/BF02517400
[77] MINOR, M. M., HENSLEY, W. K., DENTON, M. M., GARCIA S. R., An automated activation analysis system, J. Radioanal. Chem. **70** (1982) 459–471, https://doi.org/10.1007/BF02516130
[78] ATTAS, M., CHEN, J. D., HILDEBRANDT, E.A., An automated facility for neutron activation analysis, J. Radioanal. Nucl. Chem. **109** (1987) 55–68, https://doi.org/10.1007/BF02117523
[79] CHUNG, Y.S., et al., New pneumatic transfer systems for neutron activation analysis at the HANARO research reactor, J. Radioanal. Nucl. Chem. **278** (2008) 707–712, https://doi.org/10.1007/s10967-008-1509-6
[80] YONGGANG, Y., et al., Development of INAA automation at CARR, J. Radioanal. Nucl. Chem. **307** (2016) 1651–1656, https://doi.org/10.1007/s10967-015-4557-8
[81] ÇETINER, M.A., DEMIREL, H., DEMIRBAŞ, A., YÜCEL, H., ÇELENK, I., Automation of a pneumatic system by controlling a microcomputer equipped with a custom add on board for neutron activation analysis, Appl. Rad. Isot. **48** (1997) 397–402, https://doi.org/10.1016/S0969-8043(96)00261-8
[82] SHIMIZU, T., et al., An improved pneumatic sample transport system for measurement of activation cross-sections with d-D neutrons in the energy range between 2.1 and 3.1 MeV, Nucl. Instrum. Methods Phys. Res. A **527** (2004) 543–553, https://doi.org/10.1016/j.nima.2004.03.184
[83] SIMPSON, J.D., CHICHESTER, D.L., HILL, J.R., The A-711 high yield neutron generator and automated pneumatic transfer system for fast neutron activation analysis, Nucl. Instrum. Methods Phys. Res. B **241** (2005) 228–231, https://doi.org/10.1016/j.nimb.2005.07.184
[84] MOTT, W.E., ORANGE, J.M., Precision activation analysis with 14-million electron volt neutrons, Anal.Chem. **37** (1965) 1338–1341, https://doi.org/10.1021/ac60230a012
[85] LUNDGREN, F.A., et.al., Use of a dual sample-biaxial rotating assembly with a pneumatic tube transfer system for high precision 14-MeV neutron activation analysis, Anal. Chem. **40** (1968) 672–677, https://doi.org/10.1021/ac60260a017
[86] BRAETTER, P., GATSCHKE, W., GAWLIK, D., MOELLER, J., System for time and fluence measurements at fast pneumatic transfer systems for neutron activation analysis, Kerntechnik **18** (1976) 532–535.

[87] BODE, P., DE BRUIN, M., The use of carbon fibre for the irradiation position of a fast rabbit system, J. Radioanal. Nucl. Chem. **112** (1987) 375–381, https://doi.org/10.1007/BF02132369
[88] BODE P., Instrumental and organizational aspects of a neutron activation analysis laboratory, PhD Thesis, TU Delft, Netherlands (1996).
[89] CHISELA, F., GAWLIK, D., BRÄTTER, P., Evaluation of high purity graphite sample containers for use with rapid instrumental epithermal neutron activation analysis, J. Radioanal. Nucl. Chem. **102** (1986) 347–357, https://doi.org/10.1007/BF02047909
[90] NEUTRON SCIENCES DIRECTORATE, OAK RIDGE NATIONAL LABORATORY, Nuclear Forensics (Neutron Activation Analysis), https://neutrons.ornl.gov/suites/nuclear-forensics
[91] HEINZ MAIER-LEIBNITZ ZENTRUM, Neutron activation analysis (NAA), https://mlz-garching.de/naa
[92] NARGOLWALLA, S. S., PRZYBYLOWICZ, E. P., SUDDUETH, J. E., BIRKHEAD, S. L., Solution of blank problems in 14-Mev. neutron activation analysis for trace oxygen, Anal. Chem. **41** (1969) 168–170, https://doi.org/10.1021/ac60270a050
[93] LINDSTROM, R. M., BECKER, D. A., LANGLAND, J. K., GREENBERG, R. R., The NIST rapid irradiation and counting system, J. Radioanal. Nucl. Chem. **215** (1997) 47–50, https://doi.org/10.1007/BF02109876
[94] HEYDORN, K., SKANBORG, P.Z., GWOZDZ, R., SCHMIDT, J.O., WACKS, M. E., Determination of lithium by instrumental neutron activation analysis, J. Radioanal. Chem. **37** (1977) 155–168, https://doi.org/10.1007/BF02520521
[95] ANDERS, O.U., BRIDEN, D.W., A Rapid, Nondestructive Method of Precision Oxygen Analysis by Neutron Activation, Anal. Chem. **36** (1964) 287–292.
[96] DYER, F.F., BATE, L.C., STRAIN, J.E., Three-Dimensionally Rotating Sample Holder For 14-Million Electron Volt Neutron Irradiations, Anal. Chem. **39** (1967) 1907–1909, https://doi.org/10.1021/ac50157a085
[97] INTERNATIONAL ATOMIC ENERGY AGENCY, Development of an Integrated Approach to Routine Automation of Neutron Activation Analysis, IAEA-TECDOC-1839, IAEA, Vienna (2018).
[98] BODE, P., DE BRUIN, M., An automated system for activation analysis with short half-life radionuclides using a carbonfiber irradiation facility, J.Radioanal. Nucl. Chem. **123** (1988) 365–375, https://doi.org/10.1007/BF02034904
[99] ZIEMAN, J.J., RIGOT, W.L., ROMICK, J.D., QUINN, T.J., KOCHER, C.W., Automated system for neutron activation analysis determination of short lived isotopes at The DOW Chemical Company's TRIGA research reactor, Nucl. Instrum. Methods Phys. Res. A **353** (1994) 389–392, https://doi.org/10.1016/0168-9002(94)91682-9
[100] MONTGOMERY, M.L., YOHO, M.D., BIEGALSKI, S.R., LANDSBERGER, S., WELCH, L., A 14 MeV neutron irradiation facility with an automatic fast cycle pneumatic, J. Radioanal. Nucl. Chem. **309** (2016) 101–106, http://dx.doi.org/10.1007/s10967-016-4725-5
[101] RUPNIK, S., SMODIŠ, B., Automation of a TRIGA-type pneumatic transfer system, J. Radioanal. Nucl. Chem. **309** (2016) 107–113, https://doi.org/10.1007/s10967-016-4763-z
[102] ISMAIL, S. S., A new automated sample transfer system for instrumental neutron activation analysis, J. Automated Meth. Management Chem. **2010** (2010) 389374, https://doi.org/10.1155/2010/389374
[103] ERIKSSON, S.M., et al., Delayed-neutron activation analysis at NIST, J. Radioanal. Nucl. Chem. **298** (2013) 1819–1822, https://doi.org/10.1007/s10967-013-2568-x

[104] HO, V.D., HO, M.D., HA, T.V., TRAN, Q.T., CAO, D.V., The upgrading of the cyclic neutron activation analysis facility at the Dalat research reactor, J. Radioanal. Nucl. Chem. **315** (2018) 703–709, https://doi.org/10.1007/s10967-017-5673-4
[105] DE SOETE, D., GJJBELS, R., HOSTE, J. (Eds), Neutron Activation Analysis, London, New York, Wiley-Interscience (1972).
[106] STERLINSKI, S., HAMMER, W., Automatic stabilization of relative counting losses in gamma ray spectrometry of short-live nuclides, J. Radioanal. Chem. **61** (1981) 93–110, https://doi.org/10.1007/BF02517401
[107] PAPADOPOULOS, N. N., TSAGAS, N. F., Short-lived nuclide radioactive decay compensation by counting geometry variation in NAA, J Radioanal. Nucl. Chem. **198** (1995) 253–260, https://doi.org/10.1007/BF02038263
[108] WESTPHAL, G.P., On the performance of loss-free counting – A method for real-time compensation of dead time and pile-up losses in nuclear pulse spectroscopy, Nucl. Instrum. Methods **163** (1979) 189–196, https://doi.org/10.1016/0029-554X(79)90049-1
[109] WESTPHAL, G.P., LEMMEL, H., The perfection of loss-free counting, J. Radioanal. Nucl. Chem.**276** (2008) 601–607, https://doi.org/10.1007/s10967-008-0606-x
[110] BLAAUW, M., FLEMING, R.F., KEYSER, R., Digital signal processing and zero dead time counting, J. Radioanal. Nucl. Chem. **248** (2001) 309–-313, https://doi.org/10.1023/A:1010603403264
[111] POMMÉ, S., "Dead Time, Pile-Up, and Counting Statistics", ACS Symposium Series 945: Applied Modelling and Computations in Nuclear Science, SEMKOW, T., JEROME, S., POMMÉ, S., STROM, D. (Eds), American Chemical Society, Colombus (2006) 218–232.
[112] POMMÉ, S., KENNEDY, G., Pulse loss and counting statistics with a digital spectrometer, Appl. Radiat. Isot. **52** (2000) 377–380, https://doi.org/10.1016/S0969-8043(99)00181-5
[113] ACHARYA, R., et al., Performance of digital gamma ray spectrometer for loss free counting and its application to NAA using short-lived radionuclides, J. Radioanal. Nucl. Chem. **302** (2014) 1333–1337, https://doi.org/10.1007/s10967-014-3565-4
[114] ANDERSON, D.L., CUNNINGHAM, W.C., Compton suppression spectrometry for analysis of short-lived neutron activation products in food, J. Radioanal. Nucl. Chem **276** (2008) 23–28, https://doi.org/10.1007/s10967-007-0404-x
[115] DAS, H.A., ZONDERHUIS, J., Application of anti-Compton counting in instrumental neutron activation analysis, J. Radioanal. Nucl. Chem **114** (1987) 207–213, https://doi.org/10.1007/BF02039793
[116] NYARKO, B.J.B., AKAHO, E. H. K., FLETCHER, J. J., CHATT, A., Neutron Activation analysis for Dy, Hf, Rb, Sc and Se in some Ghanaian cereals and vegetables using short-lived nuclides and Compton suppression spectrometry, Appl. Radiat. Isotop. **66** (2008) 1067–1072, https://doi.org/10.1016/j.apradiso.2007.10.001
[117] LUKENS, H. R., A neutron activation analysis method for the determination of Be, Li, B, F and Pb, J. Radioanal. Chem. **1** (1968) 349–354, https://doi.org/10.1007/BF02513690
[118] WIERNIK, M., AMIEL, S., Determination of lithium and its isotopic composition by activation analysis and measurement of ^{8}Li and ^{17}N, J. Radioanal. Chem. **5** (1970) 123–131, https://doi.org/10.1007/BF02513706
[119] ERDTMANN, G., KRÖNER, B., Determination of lithium in graphite by neutron activation analysis, J. Radioanal. Nucl. Chem. **113** (1987) 317–326, https://doi.org/10.1007/BF02050503
[120] FIRESTONE, R.B., SHIRLEY, V. S., Table Of Isotopes, Wiley New York (1996).
[121] ELSEVIER, Atomic Data and Nuclear Data Tables https://www.sciencedirect.com/journal/atomic-data-and-nuclear-data-tables

ABBREVIATIONS

ADC	Analogue to digital converter
ALARA	As low as reasonably achievable
DNC	Delayed neutron counting
DSP	Digital signal processing spectrometer
ENAA	Epithermal neutron activation analysis
HPGe	High purity germanium
INAA	Instrumental neutron activation analysis
k_0-NAA	Neutron activation analysis with the k_0 method
LFC	Loss free counting
LHL	Long half-life
MHL	Medium half-life
NAA	Neutron activation analysis
RNAA	Radiochemical neutron activation analysis
SDC	Saturation decay counting
SHL	Short half-life
USHL	Ultra short half-life
ZDT	Zero dead time

CONTRIBUTORS TO DRAFTING AND REVIEW

Bode, P.	NUQAM Consultancy, Netherlands
Frost, R.	Uppsala University, Sweden
Antoine, J.	International Centre for Environmental and Nuclear Sciences, University of the West Indies, Jamaica
Jasan, R.C.	Comisión Nacional de Energía Atómica, Argentina
Kameník, J.	Nuclear Physics Institute, Czech Academy of Sciences, Czech Republic
Pessoa Barradas, N.	International Atomic Energy Agency
Smodiš, B.	Jožef Stefan Institute, Slovenia
Stopic, Attila	Australian Nuclear Science & Technology Organisation, Australia
Sun, K.	International Atomic Energy Agency
Vermaercke, P.	Belgian Nuclear Research Centre, Belgium

Consultants Meetings

Consultancy Meeting on the Development of a Publication on Neutron Activation Analysis with Short Half-Life Radioisotope, Vienna, Austria, 13–15 April 2021

IAEA
International Atomic Energy Agency

No. 26

ORDERING LOCALLY

IAEA priced publications may be purchased from the sources listed below or from major local booksellers.

Orders for unpriced publications should be made directly to the IAEA. The contact details are given at the end of this list.

NORTH AMERICA

Bernan / Rowman & Littlefield

15250 NBN Way, Blue Ridge Summit, PA 17214, USA
Telephone: +1 800 462 6420 • Fax: +1 800 338 4550

Email: orders@rowman.com • Web site: www.rowman.com/bernan

REST OF WORLD

Please contact your preferred local supplier, or our lead distributor:

Eurospan Group

Gray's Inn House
127 Clerkenwell Road
London EC1R 5DB
United Kingdom

Trade orders and enquiries:

Telephone: +44 (0)176 760 4972 • Fax: +44 (0)176 760 1640
Email: eurospan@turpin-distribution.com

Individual orders:

www.eurospanbookstore.com/iaea

For further information:

Telephone: +44 (0)207 240 0856 • Fax: +44 (0)207 379 0609
Email: info@eurospangroup.com • Web site: www.eurospangroup.com

Orders for both priced and unpriced publications may be addressed directly to:

Marketing and Sales Unit
International Atomic Energy Agency
Vienna International Centre, PO Box 100, 1400 Vienna, Austria
Telephone: +43 1 2600 22529 or 22530 • Fax: +43 1 26007 22529
Email: sales.publications@iaea.org • Web site: www.iaea.org/publications

24-01705E

International Atomic Energy Agency
Vienna